IOWA STATE UNIVERSITY
Digital Repository

Retrospective Theses and Dissertations

Iowa State University Capstones, Theses and Dissertations

1984

A kinetic study on the oleaginous yeast, Candida curvata D

Burton Douglas Brown
Iowa State University

Follow this and additional works at: https://lib.dr.iastate.edu/rtd

 Part of the Microbiology Commons

Recommended Citation
Brown, Burton Douglas, "A kinetic study on the oleaginous yeast, Candida curvata D " (1984). *Retrospective Theses and Dissertations*. 8150.
https://lib.dr.iastate.edu/rtd/8150

This Dissertation is brought to you for free and open access by the Iowa State University Capstones, Theses and Dissertations at Iowa State University Digital Repository. It has been accepted for inclusion in Retrospective Theses and Dissertations by an authorized administrator of Iowa State University Digital Repository. For more information, please contact digirep@iastate.edu.

www.manaraa.com

INFORMATION TO USERS

This reproduction was made from a copy of a document sent to us for microfilming. While the most advanced technology has been used to photograph and reproduce this document, the quality of the reproduction is heavily dependent upon the quality of the material submitted.

The following explanation of techniques is provided to help clarify markings or notations which may appear on this reproduction.

1. The sign or "target" for pages apparently lacking from the document photographed is "Missing Page(s)". If it was possible to obtain the missing page(s) or section, they are spliced into the film along with adjacent pages. This may have necessitated cutting through an image and duplicating adjacent pages to assure complete continuity.

2. When an image on the film is obliterated with a round black mark, it is an indication of either blurred copy because of movement during exposure, duplicate copy, or copyrighted materials that should not have been filmed. For blurred pages, a good image of the page can be found in the adjacent frame. If copyrighted materials were deleted, a target note will appear listing the pages in the adjacent frame.

3. When a map, drawing or chart, etc., is part of the material being photographed, a definite method of "sectioning" the material has been followed. It is customary to begin filming at the upper left hand corner of a large sheet and to continue from left to right in equal sections with small overlaps. If necessary, sectioning is continued again—beginning below the first row and continuing on until complete.

4. For illustrations that cannot be satisfactorily reproduced by xerographic means, photographic prints can be purchased at additional cost and inserted into your xerographic copy. These prints are available upon request from the Dissertations Customer Services Department.

5. Some pages in any document may have indistinct print. In all cases the best available copy has been filmed.

University
Microfilms
International

300 N. Zeeb Road
Ann Arbor, MI 48106

8505804

Brown, Burton Douglas

A KINETIC STUDY ON THE OLEAGINOUS YEAST, CANDIDA CURVATA D

Iowa State University PH.D. 1984

University
Microfilms
International 300 N. Zeeb Road, Ann Arbor, MI 48106

A kinetic study on the oleaginous yeast, *Candida curvata* D

by

Burton Douglas Brown

A Dissertation Submitted to the
Graduate Faculty in Partial Fulfillment of the
Requirements for the Degree of
DOCTOR OF PHILOSOPHY

Major: Food Technology

Approved:

Signature was redacted for privacy.

In Charge of Major Work

Signature was redacted for privacy.

For the Major Department

Signature was redacted for privacy.

For the Graduate College

Iowa State University
Ames, Iowa

1984

TABLE OF CONTENTS

NOMENCLATURE

A	inverse of first-order dependence on N_u of μ_1, g·hr/l.
B	saturation parameter for cellular nitrogen accumulation, g/l.
D	dilution rate, 1/hr.
k_i	saturation parameter for determining the asymptotic approach of X_s/N_x to K.
K	maximum value for X_s/N_x, g/g.
K_L	saturation parameter for lactose consumption, g/l.
L	lactose concentration, g/l.
L_1, L_2, L_3	lactose concentration during the first, second and third phase, respectively, of lactose consumption as determined for continuous fermentations, g/l.
L_o	initial lactose concentration, g/l.
n	exponential factor.
N	extracellular nitrogen concentration, g/l.
N_b	nonutilizable N, g/l.
N_u	utilizable N, g/l.
N_{uo}	initial N_u, g/l.
N_x	cellular nitrogen concentration, g/l.
X	total biomass concentration, g/l.
X_c	nonnitrogenous nonlipid biomass concentration, g/l.
X_f	lipid concentation, g/l.

X_s	nonlipid biomass concentration, g/l.
$1/Y_1$	lactose required for nonnitrogenous nonlipid biomass accumulation, g/g.
$1/Y_2$	lactose required for lipid accumulation, g/g.
α	contribution to the nonlipid biomass by the accumulation of cellular nitrogen, g/g.
β	mass to nitrogen ratio for cellular nitrogenous compounds, g/g.
γ	value for X_f/X_s during the initial accumulation of nonlipid biomass, g/g.
μ_{m1}	maximum specific rate of cellular nitrogen accumulation, 1/hr.
μ_{m2}	maximum specific rate of nonnitrogenous nonlipid biomass accumulation, 1/hr.
μ_{m3}	maximum specific rate of lipid accumulation, 1/hr.
μ_1	specific rate of cellular nitrogen accumulation, 1/hr.
$(\mu_1/\mu_{m1})_{max}$	value for μ_1/μ_{m1} at which Equation (16) is maximum.

INTRODUCTION

Lipid accumulation in yeast and mold has been studied for some time. Interest has been spurred by thoughts of producing a fat or oil in times of shortages, producing a high energy food source to ease world food problems, producing a valuable product through waste treatment, producing a substitute for expensive oil or fat, or more recently, biomodifying lipids. Lipids produced by yeast or mold must, nevertheless, compete in the established vegetable oil market. As a result, improving the overall profitability of the fermentation is also highly desirable.

One approach to this is to develop a kinetic model to describe the relationship between growth and lipid accumulation. With such a model, the kinetics of the system could be better understood, facilitating further improvements in the profitability of lipid production by yeast or mold. As of yet, no detailed studies of oleaginous yeast have been conducted to elucidate the kinetics of growth and lipid accumulation. This thesis will present such a study and the resulting kinetic model.

LITERATURE REVIEW

Microbial Lipid Accumulation

Microorganisms

Many species of yeast and mold have been isolated which are capable of accumulating lipid. Ratledge (1978) has listed 20 species of yeast representing the genera of Candida, Cryptococcus, Hansenula, Lipomyces and Rhodotorula. Also listed were 31 species of mold representing the genera of Aspergillus, Chaetomium, Cladosporium, Gibberella, Fusarium, Malbranchea, Mortierella, Mucor, Myrothecium, Penicillium, Pythium, Rhizopus and Stilbella. Table 1 lists some oleaginous yeast reported since 1977.

Nutrients

Successful accumulation of lipid in yeasts grown on a carbohydrate has been shown to require oxygen (Lundin, 1950; Nord, 1939). Recently, however, it has been shown that oxygen required during lipid synthesis is less than that required for growth (Moon et al., 1978).

Enebo et al. (1946) was the first to demonstrate that a yeast could accumulate up to 60% of its biomass when cultivated in a nitrogen-limited broth. Lipid accumulation has since then been reported to result from limiting phosphate in the medium (Fahmy et al., 1962; Floetenmeyer, 1983; Gill et al., 1977). However, a finite level of phosphate seems to be required to promote lipid

Table 1. Some yeasts examined since 1977 as potential fat producers

Organism	Substrate	Fat content (% dry wt)	Fat coefficient (g fat produced/ 100 g substrate utilized)	Reference
Candida curvata D	lactose	57	27	Moon et al., 1978
Candida curvata R	lactose	51	20	Moon et al., 1978
Rhodosporidium toruloides CBS 5490	glucose	25.9[a]	--	Boulton and Ratledge, 1981
Rhodotorula glutinis Y_4	sucrose	42	20.4	Misra et al., 1984
Rhodotorula graminis NCYC 502	glucose	24.2[a]	--	Boulton and Ratledge, 1981
Trichosporon cutaneum 24	lactose	20	9	Moon et al., 1978
Trichosporon cutaneum 40	lactose	45	24	Moon et al., 1978

[a]Cultures were harvested after 48 hours of incubation.

accumulation (Allen et al., 1964; Floetenmeyer, 1983). Lipid accumulation has also been reported to be induced by limiting iron, zinc and inositol (Tomita et al., 1979; Yamauchi et al., 1983).

Steinberg and Ordal (1954) reported that lipid accumulation in Rhodotorula glutinis did not require sodium, calcium or ferric chlorides, or any of the constituents of yeast extract. At a 1% level in the broth, $CaCl_2$, NaCl, or to a lesser extent, KCl actually promoted lipid accumulation in Candida curvata D (Floetenmeyer, 1983). A 2% level of NaCl was however less effective than a 1% level of NaCl in promoting lipid accumulation.

Boulton and Ratledge (1980) observed that citrate synthase obtained from the oleaginous yeast Candida 107 required magnesium ions (Mg^{2+}) for activity under in vitro conditions similar to those thought to exist in vivo during lipid accumulation. In agreement with this, it has been observed that limiting Mg^{2+} and nitrogen simultaneously in the fermentation broth resulted in decreased yields of both lipid and nonlipid biomass of Candida 107, as compared to those yields obtained when only nitrogen was limited in the broth (Gill et al., 1977)

The inorganic compound from which nitrogen is obtained has been shown to affect both growth and lipid accumulation (Chahal et al., 1979; Yoon et al., 1982). The yield of nonlipid biomass from consumption of nitrogen as provided by various inorganic or organic nitrogenous compounds has been shown in batch fermentations to

decrease with nitrogen consumption (Yoon et al., 1982), remain constant with nitrogen consumption (Misra et al., 1984; Moon et al., 1978; Pedersen, 1961), or more commonly, to increase with nitrogen consumption (Allen et al., 1964; Enebo et al., 1946; Hopton and Woodbine, 1960; Moon et al., 1978; Yamauchi et al., 1983).

Fermentation systems

Prior to 1939, it was thought that growing oleaginous yeast on the surface of stationary substrates was the only feasible method for producing microbial lipid (Lundin, 1950). Nord (1939) was the first to demonstrate a successful method of aerating submerged cultures of mold in which the biomass contained about 10% lipid. This marked the beginning of the use of aerated, submerged batch fermentations for cultivating oleaginous yeast.

Oleaginous yeast have been evaluated in batch fermentations by two distinct methods. In the first method, growth and lipid accumulation occurred in the same fermentation vessel (Duncan, 1973; Enebo et al., 1946; Evans and Ratledge, 1983a; Fahmy et al., 1962; Hopton and Woodbine, 1960; Kessel, 1968; Moon et al., 1978; Pedersen, 1961). In the second method, following the completion of cell growth in one vessel, the cells were transferred to a second vessel in which lipid accumulation could be observed (Lundin, 1950; Steinberg and Ordal, 1954; Roy et al., 1978). This gave the added advantage of more easily examining the factors which might affect lipid accumulation.

Fed-batch systems have also been investigated for lipid production. Allen et al. (1964) observed that R. glutinis could accumulate only a limited amount of lipid despite the addition of sugar to the fermentation broth at 24 hr intervals during lipid accumulation. Yamauchi et al. (1983) observed that by continuously feeding a nitrogen source during cell replication, high biomass concentrations of 150 g/l containing up to 50% lipid could be obtained. The authors considered that the high biomass concentrations were possible because a minimum dissolved oxygen concentration was maintained throughout the fermentation.

Continuous systems were considered not profitable by Enebo et al. (1946) due to the low dilution rate required. But Gill et al. (1977) reported that, for Candida 107, a single-stage continuous fermentation system produced lipid as efficiently as a batch system but at five times the productivity of the batch system. Since then, other studies of continuous lipid-accumulating fermentations have been reported with similar efficiencies in lipid formation (Choi et al., 1982; Evans and Ratledge, 1983a; Floetenmeyer, 1983; Ratledge and Hall, 1979).

Hall and Ratledge (1977) concluded that a two-stage continuous fermentation system was not better than a single-stage continuous system. They drew this conclusion after observing a poorer efficiency of conversion of glucose to lipid in the second stage of their system as compared to that obtained in a single-stage system.

A similar study of another two-stage continuous fermentation also showed a poor efficiency however for conversion of sucrose to lipid (Almazan et al., 1981).

Biochemical mechanism of fatty acid synthesis

The presently accepted biochemical pathway for the conversion of glucose to fatty acid is summarized in Figure 1. This pathway is considered to be common for all oleaginous yeast (Boulton and Ratledge, 1981; Evans et al., 1983a). The pathways and the enzymes involved will be discussed further.

The rate of glucose uptake has been observed to be independent of the specific growth rate in oleaginous yeast (Botham and Ratledge, 1978, 1979). Ratledge and Botham (1977) established that both the Embden-Meyerhof and the pentose phosphate pathways were active in vivo, in an approximate molar flux ratio of 1 to 2, respectively, in Candida 107, an oleaginous yeast. Boulton and Ratledge (1980) demonstrated that citrate synthase obtained from Candida 107 was not inhibited in vitro under the conditions which favored lipid accumulation.

Botham and Ratledge (1979) reported that NAD^+:isocitrate dehydrogenase which was obtained from Candida 107 was completely inhibited in vitro under conditions favoring lipid accumulation. But in vitro, inhibition of this particular enzyme obtained from C. utilis, which is not an oleaginous yeast, was only partial. ATP: citrate lyase was found in Candida 107, but not in C. utilis.

Figure 1. Presently accepted biochemical pathway for the conversion of glucose to fatty acid. Glucose-6-phosphatase (1); Embden-Meyeroff pathway (2); pentose phosphate pathway (3); pyruvate dehydrogenase (4); pyruvate carboxylase (5); citrate synthase (6); aconitase (7); NAD^+:isocitrate dehydrogenase (8); ATP:citrate lyase (9); cytosolic NAD^+:malate dehydrogenase (10); L-malate/citrate translocase (11); mitochondrial NAD^+:malate dehydrogenase (12); malic enzyme (13); mitochondrial membrane (14); membrane translocases. (from Evans and Ratledge, 1983b; Evans et al., 1983a; Ratledge and Botham, 1977)

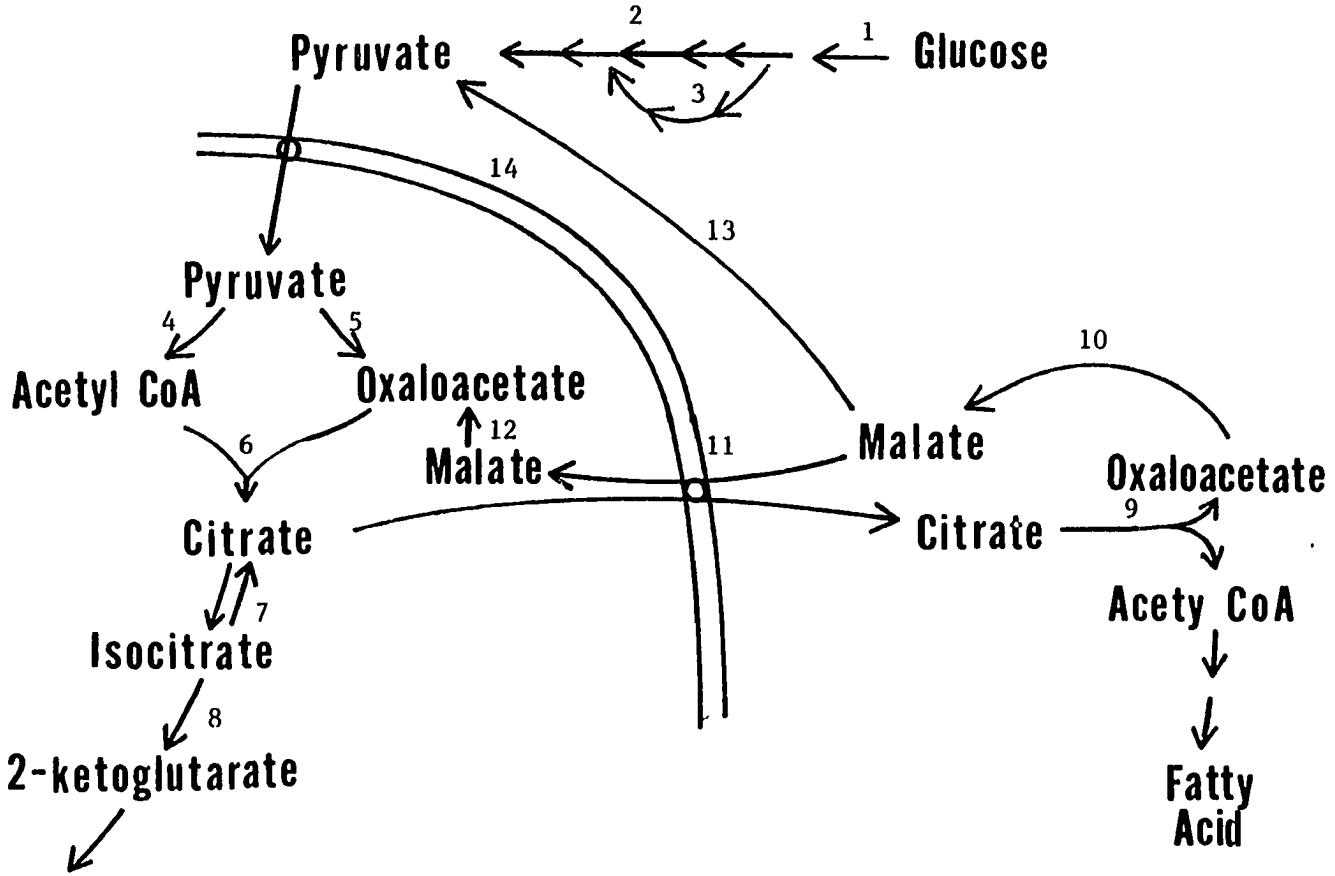
Pyruvate
2
1
Glucose
3
14
13
Pyruvate
4
5
Acetyl CoA
Oxaloacetate
10
12
11
Malate
Malate
Oxaloacetate
6
9
Citrate
Citrate
7
Acety CoA
Isocitrate
8
2-ketoglutarate
Fatty
Acid

Acetyl CoA carboxylase obtained from Candida 107 was activated in vitro by citrate. But when this enzyme was obtained from C. utilis, the enzyme was not observed to be activated in vitro by citrate.

Boulton and Ratledge (1981) demonstrated the ubiquity of ATP: citrate lyase in lipid-accumulating yeast. They proposed that this enzyme controls the rate of fatty acid synthesis in oleaginous yeast. This was proposed as a result of observing that the in vitro activity of this enzyme obtained from Lipomyces starkeyi was of the same order of magnitude as required for the estimated molar rate of fatty acid synthesis for that yeast. Evans and Ratledge (1983b) concluded this enzyme may be controlling the rate of fatty acid synthesis in C. curvata D after observing that the increase in the rate of lipid synthesis corresponded with the increase in the activity of ATP:citrate lyase (Figure 2). In contrast, acetyl CoA carboxylase is considered the rate-limiting enzyme leading to fatty acid synthesis in mammals (Smith et al., 1983). Other enzymes also essential for fatty acid synthesis have also been observed to increase in activity during the transition from growth to lipid accumulation (Evans and Ratledge, 1983b). This has been observed in mammalian tissues as well, and is considered to result from induced synthesis of these enzymes (Smith et al., 1983)

Evans et al. (1983a) reported that the mitochondrial L-malate/citrate translocase was more active in oleaginous yeast than in non-oleaginous yeast. This translocase was observed to be activated by

Figure 2. Changes in the concentrations and enzyme activity during batch fermentation of Candida curvata D. Specific activity of ATP:citrate lyase (▽); concentrations of nonlipid biomass, X_s (○) and lipid, X_f (□), intracellular molarity of citrate (△). (from Evans and Ratledge, 1983b)

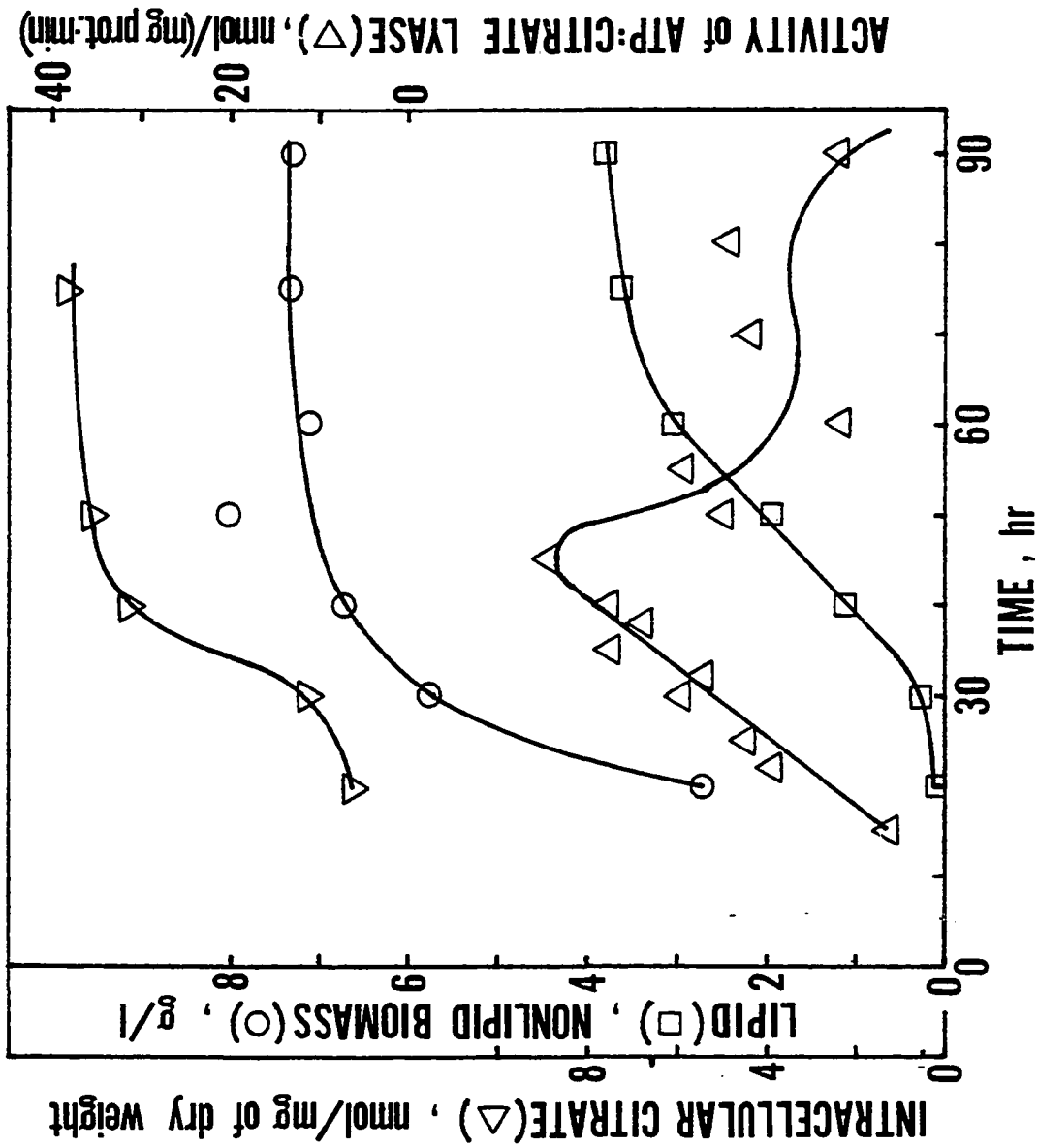
ACTIVITY of ATP:CITRATE LYASE(△), nmol/(mg prot·min)
40
20
0
TIME, hr
0
30
60
90
LIPID(□), NONLIPID BIOMASS(○), g/l
0
2
4
6
8
INTRACELLULAR CITRATE(△), nmol/mg of dry weight
0
4
8

conditions favoring lipid accumulation (Evans et al., 1983b), and inhibited by conditions resulting from the breakdown and utilization of stored triacylglycerides (Evans et al., 1983c).

Botham and Ratledge (1979) observed the effect of a pulse input of [1-^{14}C] acetate into single-stage, steady state continuous cultures of Candida 107 and C. utilis. Roughly 50% and 30% of the radioisotope was incorporated into the lipid of Candida 107 and C. utilis, respectively. The authors concluded that in both these yeasts "lipid turnover either does not occur or occurs at an immeasurably slow rate."

Mathematical Modeling

Barford and Hall (1978) have categorized microbial fermentation models according to the way the microbial kinetics can be described. This is summarized in Table 2.

Microbiological models can also be categorized as empirical or mechanistic (Barford and Hall, 1978). An empirical model can be likened to a black box in which only inputs and outputs are observed. But how this transformation is accomplished is not considered by the model. On the other hand, the mechanistic model is based on hypotheses about how transformations are accomplished. The advantage of the mechanistic model over the empirical model is that the hypotheses about the microbial system can be tested. In general however, the model usefulness is determined by the purpose in developing the

Table 2. Definition of model types based on culture description (from Barford and Hall, 1978)

Model type	Basic culture variable
(A) Stochastic	Individual cell
(B) Deterministic	Cell mass
(i) Distributed or segregated	
(ii) Structured or unstructured	

Areas of application

Stochastic models are applicable to areas where possible fluctuations around a mean value are of importance as well as any phenomena specifically requiring individual differences for explanation of particular phenomenon. Stochastic models may be distributed or segregated (see below).

Deterministic models do not specifically include the effect of quantization or individual differences unless they can be related to some average value.

This refers to whether the cell mass is considered as a separate phase (segregated) or as part of the overall culture medium (distributed). Segregated models are necessary to explain any mass transfer or partition effects between the medium and biomass. Most importantly distributed models describe processes occurring within the cell in terms of external conditions.

This refers to whether changes in cell composition are included in the model (both distributed and segregated models may be structured). Structured models consider the total biomass as the sum of two or more components and the metabolic processes achieved by the cooperation of all components.

model, such as process optimization, data analysis, or process control.

Growth models

Blackman (1905) observed that the rate of assimilation of CO_2 in photosynthesis was influenced by several factors, such as light intensity, carbon dioxide concentration, available water, amount of chlorophyll, and the temperature of the chlorophyll. He observed that when the concentration of carbon dioxide varied, the maximum rate of assimilation of CO_2 was determined by the intensity of the incident light rather than by the CO_2 concentration. He proposed this rate dependence could be described as follows:

$$\nu = \begin{cases} K \cdot S_c & ; \; S_c < \nu_m/K \\ \nu_m & ; \; S_c \geqslant \nu_m/K \end{cases} \qquad (1)$$

where ν is the rate of assimilation of CO_2, mM/hr; ν_m is the maximum rate of assimilation of CO_2 as determined by light intensity, mM/hr; K is the first-order rate parameter for CO_2 assimilation, 1/hr; S_c is the CO_2 concentration, mM. This equation has not been widely accepted, probably because of its discontinuous nature and the nontypical description of continuous data as illustrated by Condrey (1982).

Monod (1942) however proposed that growth of microorganisms when limited by one essential nutrient could be said to be controlled by one slow, enzyme-catalyzed step. As such, the equation

he proposed had the same form as that for an irreversible enzyme-catalyzed reaction using a single substrate (Henri, 1903; Michaelis and Menten, 1913). It is as follows

$$\mu = \frac{1}{X}\frac{dX}{dt} = \mu_m/(1 + K_s/S) \qquad (2)$$

where μ is the specific growth rate, 1/hr; μ_m is the maximum specific rate, 1/hr; K_s is the Michaelis-Menten saturation parameter, g/l; S is the substrate concentration, g/l; and X is the cell concentration, g/l. Monod's equation or modifications of this equation has been used extensively in modeling batch and continuous fermentations (Guthke and Knorre, 1982; Levenspiel, 1980; Tseng and Phillips, 1982).

Dabes et al. (1973) observed a similar dependence to that observed by Blackman (1905) for the rate of photosynthesis of Chlorella ellipsoidea on both carbon dioxide concentration and light intensity. As a result, they proposed to describe such a rate dependence based on an unbranched enzyme-catalyzed reaction pathway, in which all but two reaction steps were considered at equilibrium. The first slow enzyme-catalyzed reaction step was considered reversible and the second was considered irreversible. A 3-parameter model was obtained from the above described reaction pathway by assuming the maximum rates of the first slow enzyme-catalyzed reaction step were fast compared to that of the second step. And thus it took on the following form

$$S_1 = \omega\ (A + B/(\omega_m - \omega)) \qquad (3)$$

where ω is the specific overall rate of the pathway, 1/hr; ω_m is the maximum specific overall rate of the pathway as determined by the second slow reaction step, 1/hr; A is proportional to the Michaelis-Menten saturation parameter of the first slow enzyme-catalyzed reaction step, g•hr/l; B is proportional to the Michaelis-Menten saturation parameter of the second slow enzyme-catalyzed reaction step, g/l; and S_1 is the concentration of that substrate first acted on by the pathway, g/l. The authors demonstrated that both the Monod and the Blackman models represented extremes of this 3-parameter model. This 3-parameter model is also identical to that describing diffusion-limited growth, in which growth is described by the Monod equation (Reiner, 1959).

Bellgardt et al. (1982) proposed modeling aerobic growth of Saccharomyces cerevisiae on glucose as resulting from the interaction of several converging reaction pathways. Based on the observed phenomena that metabolic rates are normally controlled such that internal metabolic intermediates do not accumulate excessively, they proposed that the slowest reaction pathway rate would determine the rate of the other reaction pathways. This corresponded to a generalization of Blackman model extended however to branched, enzyme-catalyzed reaction pathways. Uptake of the nutrients glucose and ethanol was also considered rate-limiting and was described using Monod kinetics. As a result, the authors described their model as "multiple-Monod-Blackman" kinetics.

Moser (1958) proposed a modification of Monod's equation. He proposed that all of the single steps of an enzyme-catalyzed reaction pathway would affect the overall velocity of the system in contrast to Monod's concept of rate-control exercised by a single enzyme-catalyzed reaction. And he also stated that the data available at that time were insufficiently precise to specify any one growth model as better than other proposed growth models. His model took on the form

$$\mu = \mu_m/(1 + \gamma \cdot S^{-\lambda}) \tag{4}$$

where γ is a saturation parameter, $(g/l)^{\lambda}$; and λ is a numerical exponential parameter. This equation has been used occasionally in modeling microbial growth (Chiu et al., 1972).

Contois (1959) modified Monod's equation to reflect the observed effect of cell concentration on the saturation parameter, K_s. He observed that in continuous culture different initial concentrations of limiting substrate did not affect the maximum growth rate, μ_m, but did affect the saturation parameter of Monod's model. This resulted in the following form

$$\mu = \mu_m/(1 + K_{sx} \cdot X/S) \tag{5}$$

where K_{sx} is the saturation parameter reflecting the effect of cell concentration. Monod's (1942) observations were at constant cell concentrations and therefore did not contradict what Contois (1959) observed. This equation has also been widely used in describing

microbial growth (Tsuchiya and Kimura, 1982; Tsuchiya et al., 1980; Bajpai and Reuß, 1980).

Another interesting growth model is known which on integration gives the logistic curve. In this model, the specific growth rate is porportional to the difference between the estimated maximum cell concentration and the observed cell concentration. Such a dependence has been explained as overcrowding of cells (Kendall, 1949), and in terms of a toxin production rate proportional to the growth rate (Bailey and Ollis, 1977). The differential form is as follows

$$\mu = \mu_m(1 - X/\beta) \qquad (6)$$

where β is the maximum cell concentration, g/l. This model has been used in describing growth in batch fermentations, in which the growth-limiting substrate(s) was not known (Constantinides et al., 1970).

The discussion up to this point has been restricted to unstructured growth models, with the exception of the model of Bellgardt et al. (1982). Unstructured growth models have been observed to provide a reasonable description of cell mass production. But for those cases in which growth is accompanied with changing cell composition, Fredrickson et al. (1971) has mathematically proven that the model must be structured in order for growth to be completely described. Because of the increased complexity of these models, their relatively recent popularity can be considered to be a result of the availability of computers.

Williams (1967) proposed structuring a cell into two portions, one portion dedicated to nutrient uptake and cellular synthetic reactions, and the other in determining cell division. As such, the model qualitatively described the relationship between biomass and the number of cells. Aerobic growth of Saccharomyces cerevisiae on glucose has been successfully described by subdividing biomass into two portions similar to that in the Williams (1967) model (Bijkerk and Hall, 1977; Pamment et al., 1978).

Of particular interest for this study is nitrogen-limited growth models. Contois (1959) described ammonia-limited growth of Aerobacter aerogenes using the equation he developed. He observed a constant yield of biomass formed from ingested ammonia.

Nitrogen or phosphate or both were limited for growth of Chlorella vulgaris. This was modeled by allowing a variable yield of biomass from ingested limiting nutrient(s) (Panikov, 1979; Panikov and Pirt, 1978). This variable yield was observed to depend on the specific growth rate.

An adenine-requiring strain of Bacillus subtilis was described in a batch fermentation (Tsuchiya et al., 1980) and in continuous fermentations (Tsuchiya and Kimura, 1982) by modeling the biomass as growing on adenine and dying and releasing adenine back into the broth. This approach satisfactorily described the stationary phase of biomass concentration in the batch fermentation. It also described the higher yield of biomass at lower dilution rates in

single-stage continuous fermentations.

Models of product formation

Gaden (1955, 1956, 1959) classified product formation into three categories. In the first, the main product is formed during the primary energy metabolism, such as in the formation of ethanol, lactic acid, or biomass. In the second type, the main product results indirectly from energy metabolism, such as in citric acid synthesis. In the final type, the biosynthesis of complex molecules, such as antibiotics or vitamins, is not directly related to energy metabolism.

Deindoerfer (1960) proposed however to classify product formation into four different types based on the relationship between nutrient uptake and product formation. In the first type, nutrients are converted to a product in a fixed stoichiometry without intermediates accumulating, such as in the formation of ethanol or lactic acid. In the second type, nutrients are converted to a product in what seems to be variable yields, such as lipid synthesis by oleaginous yeast. In the third type, nutrients are converted to a product with the accumulation of intermediates. This type includes the fermentation of glucose to gluconolactone and then to gluconic acid. In the final type, nutrients are completely converted to the intermediate before conversion to a product. An example of this category includes 5-ketogluconic acid produced from glucose but only after glucose is exhausted.

Luedeking and Piret (1959) developed a model which described lactic acid formation. The rate of formation was observed to be proportional to both the rate of growth and concentration of the biomass. It had the following form

$$\frac{1}{X}\frac{dP}{dt} = \alpha \cdot \mu + \beta \qquad (7)$$

where P is the product concentration, g/l; α is the proportionality parameter between growth and product formation rates; and β is the parameter for the first-order dependence of product formation on cell concentration, 1/hr. This equation has also been shown to describe anaerobic ethanol production (Aiyar and Luedeking, 1966). By taking into account the lag between the beginning of growth and the beginning of citric acid production, citric acid production has also been satisfactorily described using this equation (Roehr et al., 1981).

Shu (1961) introduced a stochastic model to describe product formation. His model is based on three assumptions. First, the population contains cells of varying ages. Second, all cells undergo a natural aging phenomena. And third, the rate of product formation for a particular cell is dependent only on the cell's age. Cell age was described as the sum of one or more exponential decay functions. Using this, he quantitatively described the dependence of the formation of lysine on the time after inoculation at which the precursor, α-ketoadepic acid, was added to a batch fermentation. He also demonstrated that citric acid and penicillin production

could be qualitatively represented with his model.

Antibiotic fermentations have been extensively studied. Antibiotic production is known to be inhibited by excessive substrate concentrations. The mycelium is known to differentiate in the ability to form antibiotics, as well as to show age effects on this ability. The time-lag between the beginning of mycelium growth and antibiotic formation has been modeled in a number of ways. It has been modeled using a simple time delay between the description of growth and that of antibiotic formation (Constantinides et al., 1970; Nestaas and Wang, 1983). It has also been modeled as resulting from the inhibition of antibiotic formation by high substrate concentrations (Bajpai and Reuß, 1980; Guthke and Knorre, 1982). This lag has also been accounted for by modeling a simplified version of the metabolic pathways (Calam et al., 1971). The differentiation in mycelium metabolic activity has been modeled by subdividing the mycelium into that which was growing or dying but not producing antibiotic, and that which was producing antibiotic but not growing (Guthke and Knorre, 1982; Nestaas and Wang, 1983). The antibiotic production rate has in general been modeled as proportional to the concentration of that mycelium actively producing antibiotic (Constantinides et al., 1970; Bajpai and Reuß, 1980; Guthke and Knorre, 1982; Nestaas and Wang, 1983).

Brown and Hsu (1982) introduced a model to describe the lipid accumulation of a batch fermentation of C. curvata R as reported by

Moon et al. (1978). The nonlipid biomass was satisfactorily described using the Monod equation in which the limiting substrate was nitrogen. The rate of lipid formation was described such that as the specific rate of nonlipid biomass accumulation slowed, the specific rate of lipid formation increased. Specific rates were expressed with respect to the nonlipid biomass concentration. The model which best described the accumulation of lipid in the biomass was based on the assumption that two irreversible enzymatic steps in series controlled the rate of lipid synthesis. This resulted in predicting the accumulation of an intermediate when using the parameters which gave the best fit of the fermentation data. Evans and Ratledge (1983b) observed the accumulation of citrate using C. curvata D. The observed maximum concentration of citric acid was however one-hundredth of the concentration of the intermediate predicted by the model of Brown and Hsu (1982).

Enzymes are also an important product of fermentations. The presently accepted mode by which enzyme synthesis occurs, known as the operon model, recognizes inhibition and activation of the rate of transcription of DNA coding for the enzyme, the rate of enzyme synthesis from this template, and other factors as controlling the overall rate of enzyme synthesis (Smith et al., 1983). This concept has been widely used in some variation to describe enzyme production in fermentation systems (Gondo et al., 1978; Imanaka et al., 1972; Toda and Yabe, 1979; Toda et al., 1979).

MATERIALS AND METHODS

Yeast Strain

Candida curvata D which was isolated from a dairy floor drain in the Iowa State University cheese plant (Moon et al., 1978) was used throughout this study. The strain was maintained by weekly transfers on medium in Petri plates and monthly transfers on slants of medium. The medium used contained 15 g/l malt extract (Difco Laboratories, Detroit, MI) and 15 g/l Bacto agar (Difco Laboratories, Detroit, MI).

Fermentations

Media

Media formulations for the fermentations are summarized in Table 3. The medium was sterilized as one unit. Twenty-gallon, autoclavable glass jars containing 10 liters of medium were autoclaved at 121 C for 40 min as suggested by Drew (1981). Twenty-gallon, autoclavable polypropylene bottles (Nalge Company, Rochester, NY) containing 10 liters of medium required 105 min at 121 C. The sterility of the medium was established by holding the container containing the autoclaved medium at room temperature for several days. Microscopic examination of the medium verified its sterility.

Table 3. Media formulation for various fermentations[a]

Component	Batch 1	Batch 2 and Continuous
α-Lactose•H_2O	62 g/l	60 g/l
Yeast extract[b]	3.9	3.8
KH_2PO_4	2.5	2.5
$MgSO_4 \cdot 7H_2O$	1.0	1.0
KHphthalate[c]	3.0	3.0
Antifoam[d]	--	0.2
$FeCl_3 \cdot 6H_2O$	2 mg/l	2 mg/l

[a]Adjusted to pH 5.5 with NaOH before autoclaving.

[b]Difco Laboratories, Detroit, MI.

[c]Potassium hydrogen phthalate, acidimetric standard, Fisher Scientific Co., Pittsburgh, PA.

[d]FG-10 Silicone Antifoam, Dow Corning, Midland, MI.

Equipment

Batch 1 fermentation The batch 1 fermentation was conducted in a MicroFerm-Fermenter System (New Brunswick Scientific Co., Inc., New Brunswick, NJ). The volume of the fermenter was 14 liters. The stirring rate was maintained at 500 revolutions per minute (rpm), except during the period of extensive foaming which occurred between 10 and 25 hr after inoculation. During this period the stirring rate was increased to 800 rpm. The air used for aeration was filtered with glass wool. Air flow rate was maintained at ca. one volume of air per volume of fermentation broth per minute (vvm). Initially, the volume of the broth was 11 liters. Silicone antifoam (Dow Corning, Midland, MI) was diluted to a 1% emulsion and sterilized by heating 20 min at 121 C. Antifoam was added directly to the fermentation broth as needed from a reservoir connected to the fermenter. Temperature of the fermentation broth was maintained at 30±0.5 C.

Fermentation broth was removed from the fermenter for analysis using a sampling line located in the headplate of the fermenter. The volume of the sampling line was ca. 24 ml. The broth was forced out of the fermenter by pressurizing the headspace in the fermenter.

Batch 2 fermentation The batch 2 fermentation was conducted in a 7-liter fermenter (New Brunswick Scientific Co., Inc., New Brunswick, NJ). Air flow was kept at 1 vvm. The volume of the fermentation broth started at 5.7 liters and was at least 3.7 liters at the end of the fermentation. Agitation was maintained at 500 rpm

except during the period between 10 and 25 hr after inoculation. During that period, the agitation was increased to 800 rpm as it was for the batch 1 fermentation.

Air sterilized by passage through a glass wool filter was humidified by bubbling it through 2 glass cylinders containing sterile distilled water before being dispersed into the fermentation broth. Both glass cylinders containing the water and the fermenter were immersed in a water bath whose temperature was maintained to give a fermentation-broth temperature of 30±0.5 C (Figure 3). The glass cylinder held a maximum of 1000 ml of water. Approximately 250 ml of distilled water was replaced per day.

Liquid broth samples were pumped out of the fermenter through a sampling line having a volume of ca. 2 ml.

Continuous fermentations Continuous fermentations were conducted in a 7-liter fermenter which was also used for the batch 2 fermentation. The fermentation set-up is represented in Figure 3. The air used in aerating the culture was filtered and humidified as discussed for the batch 2 fermentation, before being dispersed into the fermentation broth at a flow rate of ca. 1 vvm. The volume of the fermentation broth was maintained constant at a given dilution rate; but it was greater at the higher dilution rates, varying from 3.6 to 3.9 liters. The volume was determined from the height of the liquid in the fermenter when the stirring and aeration were turned off.

Figure 3. Schematic diagram of equipment sep-up for single-stage continuous fermentations. 1, feed reservoir; 2, burette for flow measurement; 3, peristaltic pump heads; 4, water break (Drew, 1981); 5, air break (Drew, 1981); 6, valve; 7, air-flow rotometer; 8, air filter; 9, air humidification columns; 10, sterile water reservoir, 11, 7-liter fermenter; 12, pump; 13, hooded sampling ports (Bailey and Ollis, 1977); 14, effluent reservoir; 15, constant-temperature water bath

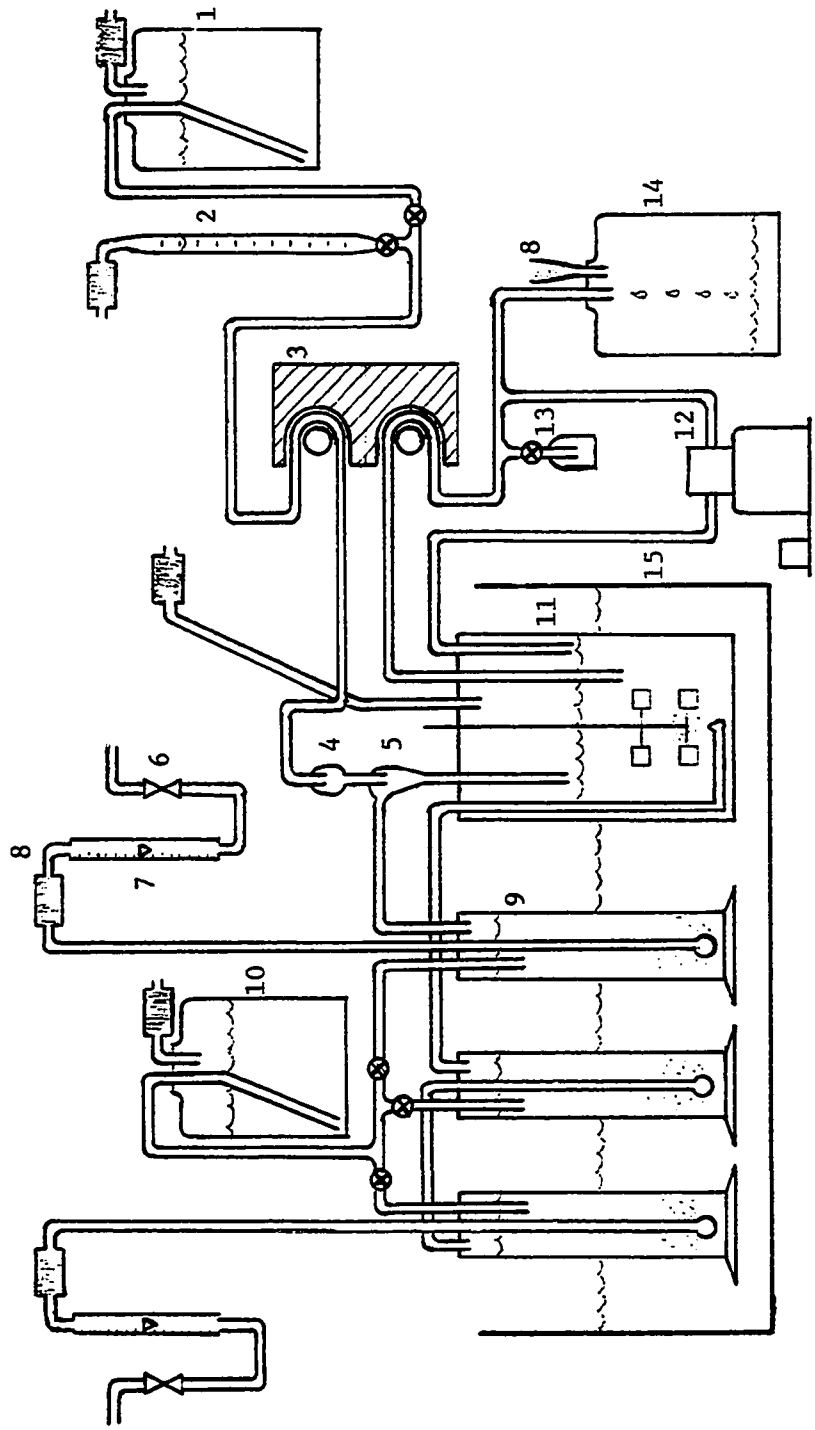
1
2
3
4
5
6
7
8
9
10
11
12
13
14
15

A peristaltic pump (Cole-Parmer Instrument Co., Chicago, IL) was used to meter sterile medium into the fermentation broth. Flow rates were maintained between 1 to 20 ml/min depending on the dilution rate. Connections between amber or black rubber tubing were facilitated with glass tubing. The volumetric flow rate was determined in quadruplicate as the time required to pump between 2 and 8 ml of sterile broth from the 10-ml pipet (Figure 3). The flow rate was checked several times each day and adjusted as needed.

A water break and air break were inserted in the feed line downstream from the peristaltic pump (Figure 3). This was done to prevent back-flow contamination of the feed reservoir by the fermentation vessel (Drew, 1981). The air for the air break was filtered using glass wool and bubbled in a glass cylinder containing sterile distilled water before entering the air break at a pretreatment flow rate of ca. 4 standard liters per minute (Figure 3).

Two liquid withdrawal lines were operated simultaneously. One withdrawal line was submerged below the surface of the liquid in the fermenter. Broth samples were obtained from this line using the hooded sampling port. The other withdrawal line with its opening located at the surface of the liquid in the fermenter was operated at several-fold greater volumetric rate than the feed rate of the sterile broth.

After a steady state was obtained, fermentation broth was removed from the fermenter through a sampling line located in the

headplate of the fermenter immediately after turning off the withdrawal and feed pumps. The volume of the sampling line was ca. 24 ml. The broth was forced out of the fermenter by pressurizing the headspace in the fermenter.

Analysis

Sampling of fermentations

At each sampling time for the batch 1 fermentation, ca. 100 ml of fermentation broth were removed from the fermenter through the sampling line. The first 40 ml collected were discarded. Two equal portions of the remaining ca. 60 ml of fermentation broth were collected directly from the sampling line into two 150-ml sterile dilution bottles, which were then kept in an ice bath.

At each sampling for the batch 2 fermentation, the first 12 ml of fermentation broth collected were discarded. Immediately following this, 40 or 80 ml of broth were collected into a sterile 150-ml dilution bottle, which was then kept in an ice bath.

For each steady state continuous fermentation, the first ca. 150 ml of fermentation broth collected were discarded. Immediately following this, ca. 320 ml of broth were collected in 4 equal portions into 4 sterile 150-ml dilution bottles, which were then kept in an ice bath.

Microscopic cell count and viable cell count followed immediately. The yeast biomass was separated from the broth by

centrifuging at 60 × g for 10 min or filtering with 0.45 μm membrane (Millipore Filter Corp., Bedford, MA) or both. The cells which were isolated for cellular nitrogen determination were first sedimented by centrifuging between 5 and 40 ml of fermentation broth. The pellet obtained by centrifuging the broth was then washed twice with distilled water and resedimented between each washing by centrifuging the cell suspension. The cell-free fermentation broth and supernatant fluid resulting from the washings were combined and analyzed for extracellular nitrogen. If centrifuging did not completely sediment the cells, the supernatant fluid was filtered through a 0.45 μm membrane. The lipid content was determined by assaying the filter cake used for the cell dry weight determination or the pellet obtained from centrifuging the fermentation broth or both. For this assay, the pellet was not washed. If centrifuging did not completely sediment the cells, the supernatant fluid was filtered. The separated cells and cell-free broth were frozen for later analysis of lactose, nitrogen and lipid content. The filter cake used for cell dry weight determination was stored in a desiccator for later analysis.

Steady state determination

The effluent from the continuous fermentations was sampled periodically at a frequency determined by the dilution rate. The broth was diluted to give an absorbance at 540 nm of less than 0.4. The continuous fermentation was considered to be at a steady state

if the absorbance remained constant over ½ fermenter volume replacement.

Viable cell counts

Viable cell counts were conducted only for the batch 1 fermentation and were performed by spread plating serially diluted fermentation broth as described by Koch (1981). The broth was diluted with sterile, distilled water. The yeast were incubated in Petri plates containing the same medium used in maintaining this strain. An incubation period of 2 to 4 days was required for the colonies to become visible.

Microscopic cell counts

Microscopic cell counts were performed on a hemacytometer cell counting slide (American Scientific Products, McGaw Park, IL). The fermentation broth was appropriately diluted to give cell counts of, at most, 3 cells per smallest square. Only whole cells were counted. The counting chamber consisted of 25 large squares each containing 16 of the smallest squares. Cells were counted in 9 of these large squares, and the results were averaged and calculated as

$$\frac{\#\ \text{cells}}{\text{ml}} = \frac{\#\ \text{cells}}{\text{large square}} \quad \frac{2.5\text{x}10^5\ \text{large squares}}{\text{ml}} \qquad (8)$$

The percentage of budding cells was determined as the average of the percentage of budding cells in each of the 9 large squares which had been counted for whole cells.

Nonfilterable dry weight

Between 3 and 40 ml of fermentation broth were filtered through a 0.45 μm membrane (Millipore Filter Corp., Bedford, MA) with the aid of a 1/6-horsepower vacuum pump (General Electric). The filter cake was washed twice with 1.0 ml of distilled water that had been filtered through a 0.22 μm membrane (Millipore Filter Corp., Bedford, MA). The weight of the membrane with and without the filter cake was determined after drying it at 60-70 C at ca. 29" of Hg vacuum for at least 12 hr. The nonfilterable dry weight concentration was determined as the difference between these two weights divided by the volume of fermentation broth filtered.

Lactose

This assay is based on a modification of the colorimetric assay for lactose issued for lactase isolated from Saccharomyces fragilis (Sigma Chemical Co., 1983). The assay is divided into two parts. The first part consists of the hydrolysis of lactose by lactase over a predetermined time interval. In the second part, the oxidation of glucose by glucose oxidase is coupled using peroxidase to the formation of a colored compound from o-dianisidine. The intensity of color formed measured as absorbance at 450 nm is proportional to the glucose concentration.

The assay was modified by including a lactase activator solution, and a higher activity of lactase at 1 unit/ml in the lactose-hydrolysis solution (Kurz and Wallenfels, 1974). Components of the

media excluding lactose and antifoam were added with the lactose standard (Table 4) to account for the effect of the nonlactose media constituents on the activity of lactase. These components are referred to as dilution salts in Tables 4 and 5. The lactose standards were prepared gravimetrically from β-lactose (Sigma Chemical Company, St. Louis, MO) which had been dried at 90-100 C for 3 days at ca. 29" of Hg vacuum.

The formulations of the various reagent solutions used in the lactose hydrolysis step are summarized in Table 5. The procedure for the hydrolysis step is summarized in Table 4. When assaying for lactose, the fermentation broth was diluted 1 to 1, 1 to 3, 1 to 10, or 0.7 to 25 (v/v) depending on the concentration of lactose in the broth. This was done to give a lactose concentration in the hydrolysis solution of 0.75 g/l or less.

Analysis for the glucose released during the hydrolysis of lactose was accomplished by adding 0.1 ml of the final lactose-hydrolysis solution to 3.0 ml of ice-chilled Glucostat (Sigma Chemical Company, St. Louis, MO). The absorbance of the mixture at 450 nm was determined after incubating the mixture 45 to 75 min in a 20 C water bath (Sigma Chemical Co., 1982). The blanks from the hydrolysis step (Table 4) were treated in this same fashion. Lactose standards were analyzed along with fermentation broth samples to minimize the effect of storage time on the activity of lactase and glucostat.

Table 4. Volumes, reagents and the steps used in enzymatic hydrolysis of lactose[a]

Reagents and Instructions	Sample	Sample blank	Standard	Standard blank
To labeled test tubes, add:				
phosphate buffer	0.2 ml	0.2 ml	0.2 ml	0.2 ml
lactase activator	0.1	0.1	0.1	0.1
distilled water	0.1	0.1	--	--
dilution salts[b]	--	--	0.1	0.1
lactase	0.1	--	0.1	--
Place in 37 C bath, add:				
sample[c]	0.8	0.8	--	--
lactose standard	--	--	0.8	0.8
Mix by hand by vortexing				
Time 29 min., 55 sec., then add:				
perchloric acid	0.3	0.3	0.3	0.3
lactase	--	0.1	--	0.1
Mix by hand vortexing and Store in ice bath				

[a]The final volume of the lactose hydrolysis solution is 1.6 ml.

[b]Dilution salts are diluted 1 to 1, 1 to 3, 1 to 10 or 0.7 to 25 (v/v), to simulate assaying for lactose in media which is diluted by the same respective factors.

[c]Appropriately prepared fermentation broth is diluted so that the lactose concentration in the sample is less than 1.5 g/l.

Table 5. The formulations of the reagents used in the enzymatic hydrolysis of lactose

Component solution	Formulation
Phosphate buffer[a]	0.530 M Na_2HPO_4
	0.171 M KH_2PO_4
Dilution salts[b,c]	30.6 g/l yeast extract[d]
	20.0 g/l KH_2PO_4
	8.0 g/l $MgSO_4 \cdot 7H_2O$
	24.0 g/l KHphthalate[e]
Lactase activator	12.7 g/l yeast extract[d]
	8.33 g/l KH_2PO_4
	8.33 g/l $MgSO_4 \cdot 7H_2O$
Lactase[f]	16 unit/ml lactase in 50% glycerol
Perchloric acid[a]	3.5% perchloric acid

[a]Sigma Chemical Co., 1982.

[b]pH adjusted to pH 5.5 with 50% NaOH.

[c]One milliliter of dilution salts contains the same mass of each of the major constituents contained in 8 ml of media, excluding lactose and antifoam.

[d]Difco Laboratories, Detroit, MI.

[e]Potassium hydrogen phthalate, acidometric standard, Fisher Scientific Co., Pittsburgh, PA.

[f]This activity-concentration gives approximately 1 unit/ml of lactose in the lactose-hydrolysis solution, as recommended by Kurz and Wallenfels (1974).

The concentration of lactose in the fermentation broth, L (g/l), was calculated as

$$L = (DF)(A_{450,S} - A_{450,SB}) \frac{\text{conc. of lactose std.}}{(A_{450,L} - A_{450,LB})} \qquad (9)$$

where DF is the dilution factor used in preparing the fermentation broth for the assay, $A_{450,S}$ is the absorbance at 450 nm for the sample, $A_{450,SB}$ is the absorbance of the sample blank, $A_{450,L}$ is the absorbance of the lactose standard, and $A_{450,LB}$ is the absorbance of the lactose-standard blank.

Lipid content

The analysis for lipid content is a modification of the alcoholic-KOH extraction method of Moon et al. (1978). The maximum ratio of cells to alcoholic KOH was 250 mg cell dry weight to 10 ml 12% alcoholic KOH. The reaction mixture was held at 2-5 C overnight and then heated to 70 C for about 4 hr. The fatty acid potassium salts were extracted by vortex-mixing of the digested cells with 3 to 5 ml of distilled water. This extraction was repeated until foaming was not observed upon further mixing of the digested cells and water. The water extracts were combined and acidified with 12 N HCl to a pH less than one, and then extracted with ca. 10 ml distilled hexane three times. The hexane extracts were filtered through a Whatman #40 filter paper presoaked with hexane. After each filtration, the filter paper was washed with ca. 2 ml of hexane. The combined hexane extracts were again filtered in this same fashion and collected into

tared 50-ml beakers. The hexane in the beakers was evaporated at 50 to 60 C, heated with a rheostat-controlled hot plate, under a light stream of nitrogen 0.5 hr beyond the apparent removal of hexane. The beakers were covered with aluminum foil during this time to prevent the inclusion of dust into the sample. After the hexane was evaporated, the beakers were weighed until constant weights were obtained. Between weighings, the beakers were returned to the hot plate set at 35 to 45 C.

The concentration of the lipid in the fermentation broth was calculated as the difference between the final weight and the tare weight of the beaker, divided by the volume of the fermentation broth from which the cells were obtained for this analysis.

Cell and extracellular nitrogen

Nitrogen was determined based on a Kjeldahl procedure for the analysis of nitrogen in beer (A.O.A.C., 1980). The sample size was varied from 5 to 40 ml of fermentation broth; preferentially 20 ml were used. Digestion was initiated with 3 ml of conc. H_2SO_4 and 5 gm of catalyst. This resulted in the removal of water as indicated by the formation of a black sludge-like foam. The remaining 21 ml of conc. H_2SO_4 were then added. The digestion was continued 0.5 hr beyond clearing. The Kjeldahl flasks containing the digested samples were corked and stored at room temperature.

Distillation was carried out in a modified distillation unit. A rubber stopper which sealed the Kjeldahl flask to the condensing

column was modified by inserting a small glass tube through it. A drying tube attached to the glass tubing by means of Tygon tubing aided in adding based directly to the contents of the Kjeldahl flask while the flask was connected to the condensing column. After the addition of base was complete, the Tygon tubing could be clamped shut. This modification was implemented to eliminate the loss of ammonia nitrogen during the addition of liquid base.

Sixty milliliters of 50% NaOH were added drop by drop with the flask set in the adjacent porcelain base. The Tygon tubing was clamped shut after all but a small portion of the base was added. The flask was gently, then more vigorously swirled. The flame under the flask was lit and kept as low as practical such that 90 to 100 ml of distillate were collected in 1 to 2 hr. The distillate was collected in a flask containing an accurately measured volume of 0.025 N HCl of around 40 ml. The unreacted acid was back titrated with 0.025 N NaOH using 0.5% N NaOH with 0.5% alcoholic methyl red as the indicator. The normalities of the acid and base solutions were determined according to the procedure of Ayres (1968).

The concentration of nitrogen in the sample, N (g/l), was determined as

$$N = \frac{\text{ml HCl} - (\text{ml NaOH})\ (A/B)}{\text{ml sample}} \quad \frac{\text{N HCl}}{1} \quad \frac{\text{mol N}}{\text{mol HCl}} \quad \frac{14\ \text{g}}{\text{mol N}} \qquad (10)$$

where ml HCl is the volume of acid measured into the receiving flask, ml NaOH is the volume of base required to neutralize the unreacted

acid, A/B is the acid to base normality ratio, N HCl is the normality of the acid, and mol N is moles of nitrogen which has a molecular weight of 14 g/mol.

Numerical analysis

The batch fermentation model was a set of ordinary, first order, simultaneous differential equations. This set of equations was integrated numerically with a set of parameter estimates using the I.M.S.L. subroutine DGEAR (I.M.S.L., 1982). The continuous fermentation kinetic model was however simply an algebraic set of equations obtained from a mass-balance of the fermenter.

The parameter estimates providing the best fit by either model of their respective fermentation data were determined using a simplex-pattern search procedure (Carpenter and Sweeney, 1965; Fan et al., 1969). The function which the search procedure minimized was the sum of the normalized residual sum of squares between the model predictions and the observed concentrations of the fermentation broth constituents: extracellular nitrogen, cellular nitrogen, lactose, lipid, and nonlipid biomass. The residual sum of squares obtained from fitting the concentrations of each constituent was normalized by dividing each residual sum of squares by the respective average standard deviation of the largest measured concentrations of the respective constituent.

RESULTS AND DISCUSSION

Development of Assays

Lactose assay

Hettinga et al. (1970) developed an assay for lactose in which lactose was first hydrolyzed by a combination of heat and acid. The glucose released by this treatment was assayed enzymatically using glucostat (Worthington Biochemical Corp., Freehold, NJ). Their lactose assay was used by Moon et al. (1978) to follow the disappearance of lactose in batch fermentations of C. curvata D and R. But because acid and heat can also hydrolyze glucose-containing carbohydrates other than lactose, the method of Hettinga et al. (1970) can not correctly determine the lactose concentration if other glucose-containing carbohydrates are also present in the sample of cell-free broth being analyzed. This type of interference could have occurred in samples analyzed by Moon et al. (1978), since these authors reported that these yeast strains produced a soluble, extracellular, nondialyzeable slime during the first 20-30 hr of the fermentations. Therefore, enzymatic hydrolysis of lactose seemed to be a more accurate method to measure the concentration of lactose in the fermentation broth of C. curvata D.

Enzymatic hydrolysis of lactose was done initially according to the procedure outlined in the technical bulletin accompanying the lactose ordered from Sigma Chemical Company (Sigma Chemical Co., 1983). In evaluating the accuracy of the assay, the concentration

of lactose was known in both the diluted fermentation broth and the lactose standard solutions. Examination of these results indicated that lactose from the standard solutions was hydrolyzed to a lesser extent than was lactose assayed from the diluted fermentation broth.

These results indicated that it was necessary to evaluate the effect of the three major components of the broth, $MgSO_4 \cdot 7H_2O$, KH_2PO_4 and yeast extract (Difco Laboratories, Detroit, MI), for their possible combined effect on the activity of lactase during the hydrolysis of lactose. Therefore, the concentration of these components were varied in the lactose hydrolysis solution; however the weight to weight ratio of these three components were kept the same as that in the original medium. Because the weight to weight ratio was kept constant, the effect of these three components on the activity of lactase was simply expressed in Figure 4 in terms of the concentrations of $MgSO_4 \cdot 7H_2O$ in the solution.

Above concentrations of ca. 0.2, 0.5, and 0.76 mg/ml of $MgSO_4 \cdot 7H_2O$, KH_2PO_4, and yeast extract, respectively, the activity of lactase increased slightly (Figure 4). This may have resulted from the effect on the activity of lactase from a decrease in the buffered pH of the hydrolysis solution. The high concentrations of yeast extract and KH_2PO_4 relative to the molarity of the buffer could have resulted in the decrease in the buffered pH.

But the observed increase in lactase activity up to concentrations of ca. 0.2, 0.5, and 0.76 mg/ml of $MgSO_4 \cdot 7H_2O$, KH_2PO_4, and

Figure 4. Extent of hydrolysis, as determined by absorbance at 450 nm, of lactose standards by lactase as affected by various concentrations of $MgSO_4 \cdot 7H_2O$:KH_2PO_4: yeast extract in a fixed ratio of 1:2.5:3.8 (w/w), respectively. Lactose standards of 0.59 g/l (▽) and 0.50 g/l (△); $(NH_4)_2SO_4$ substituted for Yeast Extract and lactose standard at 0.50 g/l (□). Concentrations based on final reaction volume of lactose-hydrolysis solution

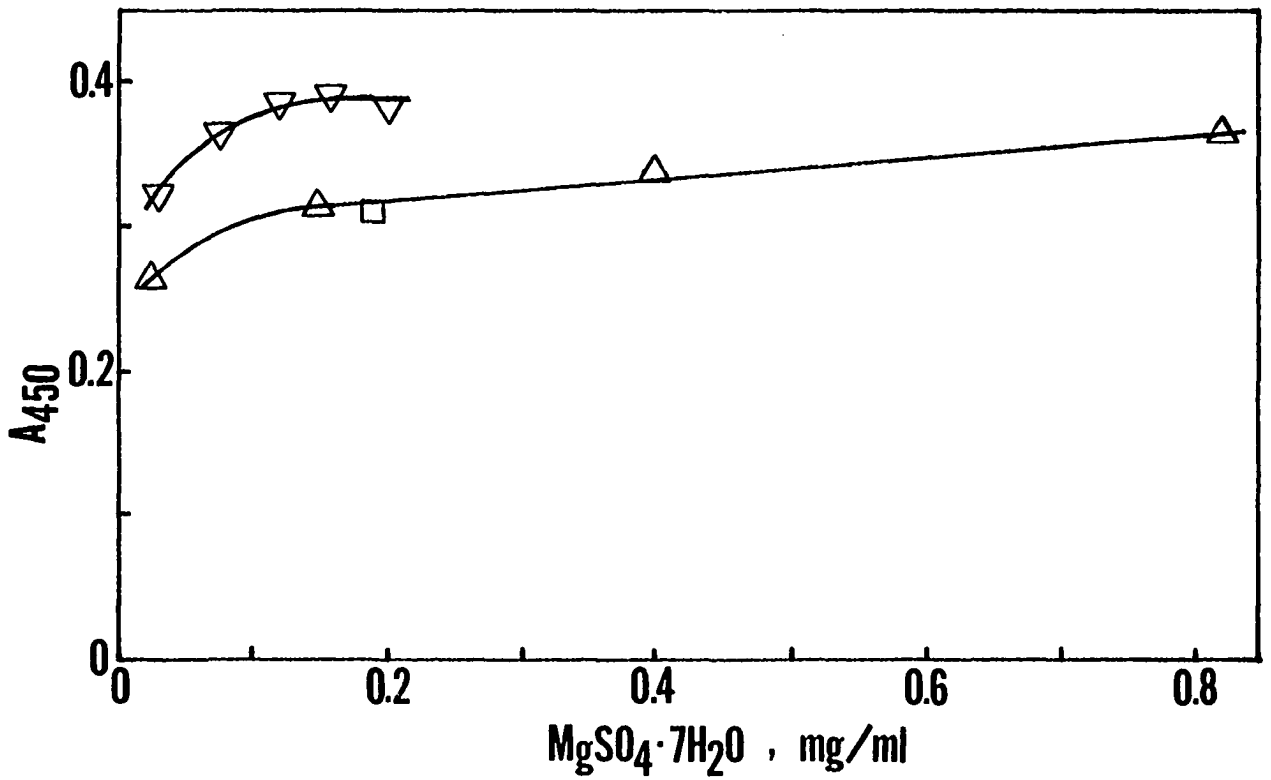
0.4
0.2
0
A_{450}
0
0.2
0.4
0.6
0.8
$MgSO_4 \cdot 7H_2O$, mg/ml

yeast extract, respectively, can be more reasonably attributed to activation of the lactase by one or more of the three added components (Figure 4). Yeast extract and $(NH_4)_2SO_4$ were found to be interchangeable, indicating yeast extract was not responsible for activating lactase (Figure 4). Potassium ion (K^+) has been reported to activate lactase obtained from Saccharomyces lactis (Sprössler and Plainer, 1983). But the buffer used in this assay contains a considerable amount of K^+. This suggests that magnesium ion might be the potential activator of the lactase used in this study. The lactase activator was not however identified.

From the results observed in Figure 4, $MgSO_4 \cdot 7H_2O$, KH_2PO_4, and yeast extract were incorporated into the lactose-hydrolysis solution at the final-volume concentrations of 0.21, 0.52, and 0.79 mg/ml, respectively. These concentrations were chosen in order to eliminate the lactase-activating effect of the ions. High concentrations of these three components in the hydrolysis solution were observed however to increase to some extent the activity of lactase (Figure 4). To overcome this, lactose standard curves were run simulating the diluting of media 1 to 1, 1 to 3, 1 to 10, and 0.7 to 25 (v/v). These dilution simulations were accomplished as described in the Materials and Methods, by adding appropriate amounts of the major constituents of the media, excluding lactose and antifoam, to the hydrolysis solution. The effect of the four dilution simulations are observed from the extent of the hydrolysis of four

concentrations of the lactose standard (Figure 5). As anticipated from Figure 4, dilution simulations of 1 to 1 and 1 to 3 (v/v) slightly increased the activity of lactase. This is evidenced in Figure 5 from the slightly steeper slopes of the plot of absorbance vs. lactose concentration. But dilution simulations of 1 to 10 and 0.7 to 25 (v/v) were not observed to have any difference in their effect on the activity of lactase. Figure 6 compares the results from Figure 4 and 5. From this comparison it was concluded that the inclusion of dilution salts in the lactose-hydrolysis solution when assaying the lactose standard was only necessary for dilution simulations of 1 to 1 and 1 to 3 (v/v).

Corrections for the volume changes in the batch 1 fermentation

Because the air used in aerating the batch 1 fermentation was not humidified prior to being dispersed into the broth and because the run was conducted in January, the incoming air was estimated to have a relative humidity of 20% at 20 C. And because of the dispersion and breakup of the air bubbles in the fermentation broth, the air exiting the fermenter was estimated to be at 30 C with a relative humidity close to 100%. From this analysis, it was evident that the contents of the fermenter were being concentrated by the removal of water by evaporation.

Combined with the volumetric air flow rate, the amount of water removed by the aeration of the culture could be estimated. During the first 25 hr of the fermentation, ca. 510 ml of 1% silicone

Figure 5. Standard curves for the lactose assay as affected by simulating the dilution of fermentation broth. Dilutions of 1 to 1 (▽), 1 to 3 (△), 1 to 10 (○) and 0.7 to 25 (□). Concentrations based on final reaction volume of lactose-hydrolysis solution

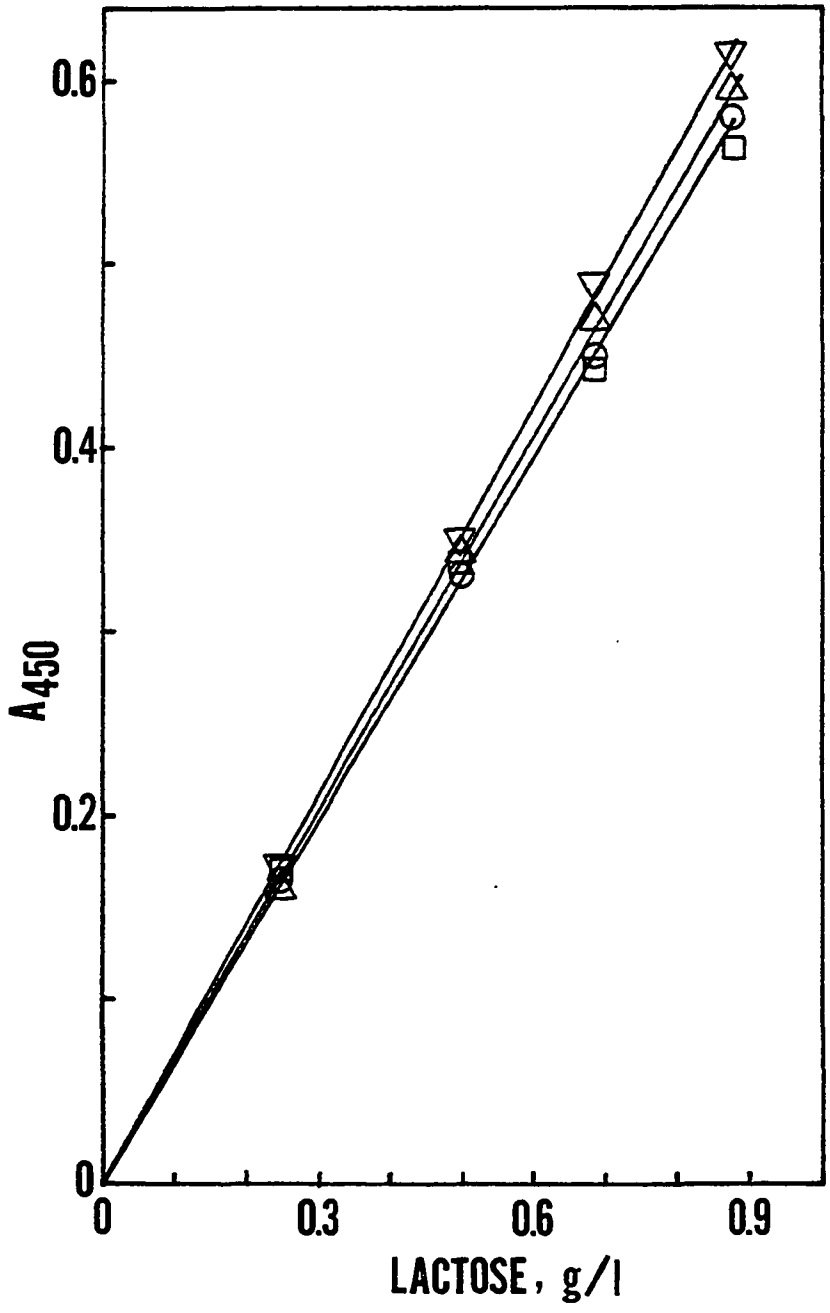
0.6
0.4
0.2
0
A450
0
0.3
0.6
0.9
LACTOSE, g/l

Figure 6. Comparison of the effect of the dilution simulations with the effect of varying $MgSO_4 \cdot 7H_2O$:KH_2PO_4:Yeast Extract (1:2.5:3.8, w/w) on the hydrolysis by lactase of standard lactose at 0.5 g/l. Results from Figure 4 (△), and Figure 5 (○)

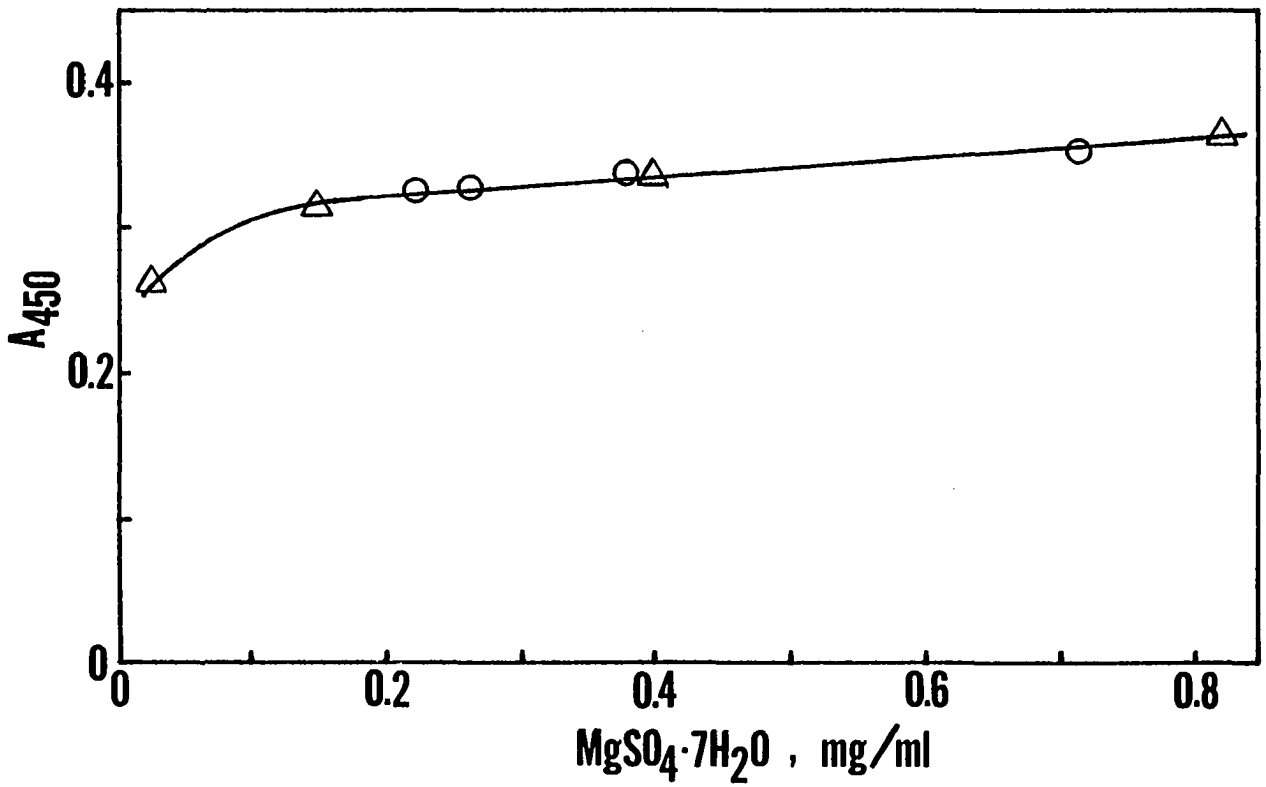
0.4
0.2
0
A_{450}
0
0.2
0.4
0.6
0.8
$MgSO_4 \cdot 7H_2O$, mg/ml

antifoam were added to the broth. Combining these two factors, the change in the volume of the broth could be estimated between samlings of ca. 100 ml of the broth. The volume-concentration correction factor was calculated as the ratio of the estimated volume of the broth just after sampling to the estimated volume just before the next sampling. The cumulative volume-concentration correction factor at a particular sampling time was the product of all previous volume-concentration factors up to that time of sampling (Figure 7). It can be observed in Figure 7 that for the first 30 hr the volume of water evaporated roughly balanced the volume of antifoam added. After the first 30 hr, the evaporation of water is observed to concentrate the contents of the broth by as much as 12% by the end of the fermentation.

Correction of the nonfilterable dry weight concentrations

For the batch 2 fermentation, two shake flasks were prepared identically and simultaneously. The first was used to inoculate the fermenter and the second was analyzed for microscopic cell count, nonfilterable dry weight, lipid, and cellular and extracellular nitrogen. The results from the analysis of the second flask are summarized in Table 6 under F0. Two flasks were used because the entire volume of broth in one of the flasks was used to inoculate the fermenter.

Five minutes after inoculation, the fermentation broth was sampled. The results of this analysis are summarized in Table 6 under

Figure 7. The cumulative volume concentration factor resulting from addition of antifoam and evaporation of water from the fermentation broth of batch 1 fermentation

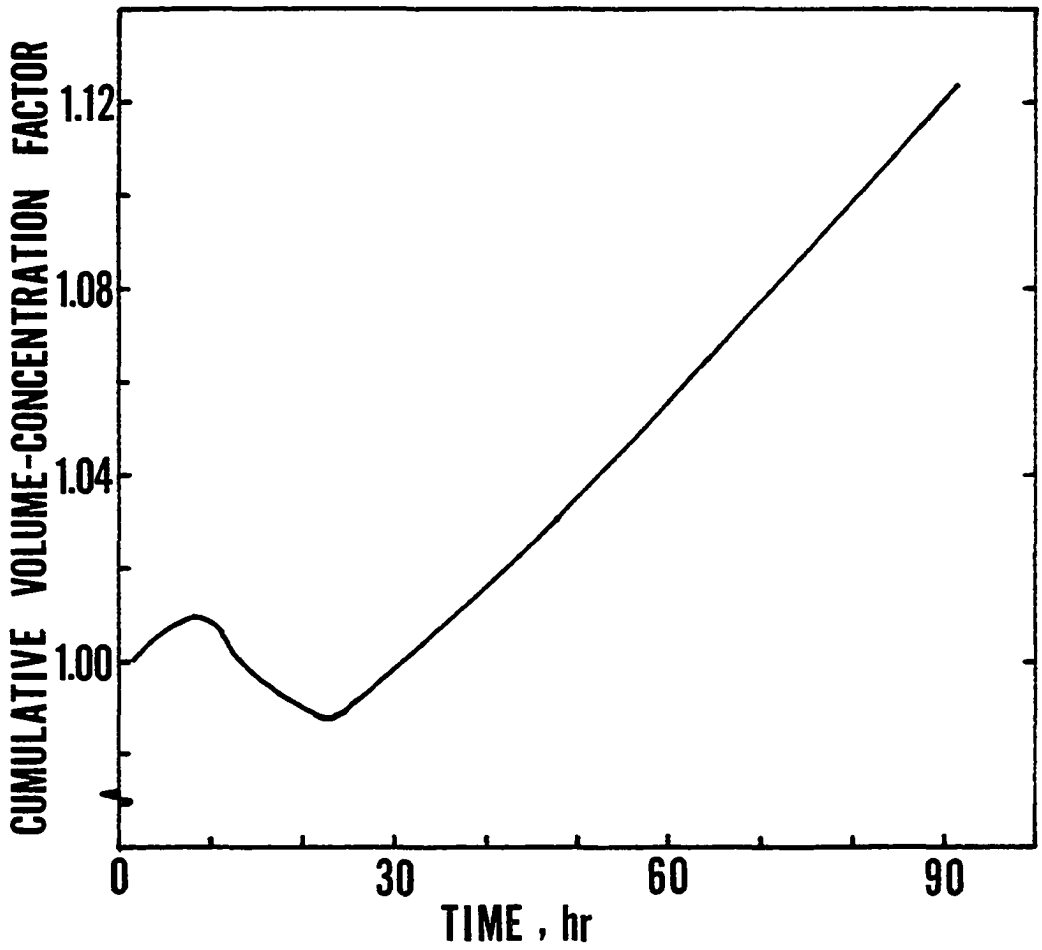
CUMULATIVE VOLUME-CONCENTRATION FACTOR
1.12
1.08
1.04
1.00
0
30
60
90
TIME , hr

Table 6. The comparison of the observed fermenter biomass concentrations 5 minutes after inoculation (F1), with the estimated concentration ($\hat{F1}$), based on the inoculum concentration (F0) and using the dilution factor of 20 ml of inoculum into 5700 ml of fermentation broth.

Assay	F0	$\hat{F1}$	F1
Microscopic cell count	4.0×10^8/ml	1.4×10^6/ml	1.4×10^6/ml
Nonfilterable dry weight	4.43 g/l	0.0155g/l	0.16 g/l
Cellular nitrogen	0.277	9.7×10^{-4}	--
Extracellular nitrogen	0.151	--	0.398
Lipid	0.30	1.1×10^{-3}	--

F1. It was assumed that the two shake flasks contained identical concentrations of cellular and extracellular constituents and that these concentrations did not change appreciably in the first 5 min in the fermenter after inoculation. Based on these assumptions, the concentrations in the fermenter were estimated from the concentrations of the shake flask using the volumes of the inoculum and the fermentation broth (20 ml and 5700 ml, respectively). These estimated concentrations are shown in Table 6 under $\hat{F1}$.

Examination of Table 6 indicates that the estimated and measured microscopic cell count are in agreement. But the estimated and measured nonfilterable dry weight concentrations differ by a factor of ca. 10. This indicated that at least initially the nonfilterable dry weight concentration in the fermentation broth did not correctly indicate the biomass concentration. Therefore it seemed reasonable that nonfilterable noncell solids in the broth were interfering in the determination of the biomass concentrations using nonfilterable dry weight analysis. These nonfilterable noncell solids may have been soluble or suspended solids originating from the media. Based on Table 6, the concentration of the nonfilterable noncell solids was estimated to be 2.8 mg in 20 ml of fermentation broth. The corrected and uncorrected nonfilterable dry weight concentrations are compared for the first 20 hr in Figure 8. Only the nonfilterable dry weight concentrations from the first 10 hr were significantly affected.

Figure 8. Comparison of the nonfilterable dry weight concentrations uncorrected and corrected for the nonfilterable noncell solids in the fermentation broth. Uncorrected (△) and corrected (○) nonfilterable dry weight concentrations

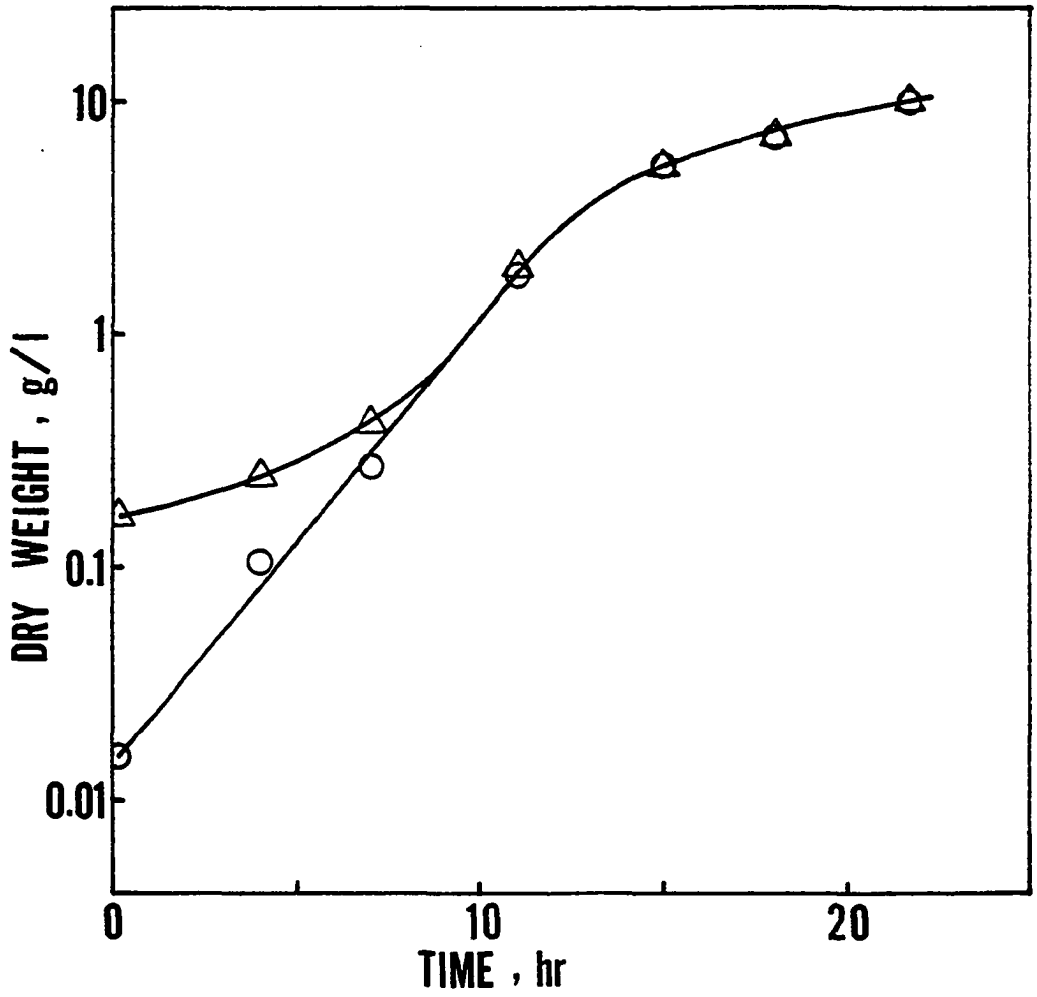
10
1
0.1
0.01
DRY WEIGHT , g/l
0
10
20
TIME , hr

The same procedure was used in inoculating the batch 1 fermentation. The initial microscopic cell counts were observed to be roughly the same for both fermentations (1.3×10^6/ml and 1.6×10^6/ml for batch 1 and batch 2 fermentations, respectively). Because of these points, it was felt that the time-traces for the nonfilterable dry weight concentrations would also be reasonably similar between the two fermentations. Based on this, the concentration of the nonfilterable noncell solids in the batch 1 fermentation broth could be estimated as 1.8 mg in 20 ml of broth, similar to that estimated for batch 2. The time-traces of the corrected nonfilterable dry weight concentrations for both fermentations are compared in Figure 9 and observed to be in good agreement. The corrected nonfilterable dry weight concentrations were considered to correctly indicate the total biomass concentrations in the fermentation broth.

Examination of C. curvata D in Batch and Continuous Fermentations

In order to develop a substantive kinetic model of growth and lipid accumulation for C. curvata D, it was necessary to examine in some detail batch fermentations of this yeast. Additional information on the kinetics was sought by analyzing the effect of dilution rate on the growth and lipid accumulation of this yeast in single-stage continuous fermentations. Because the overall kinetics of the yeast would be the same regardless of the fermentation system, and batch and continuous fermentations each provided a different

Figure 9. The nonfilterable dry weight concentrations corrected for the nonfilterable noncell solids in the fermentation broth as obtained for the two batch fermentations. Corrected nonfilterable dry weight concentrations from batch 1 (△) and batch 2 (○) fermentations

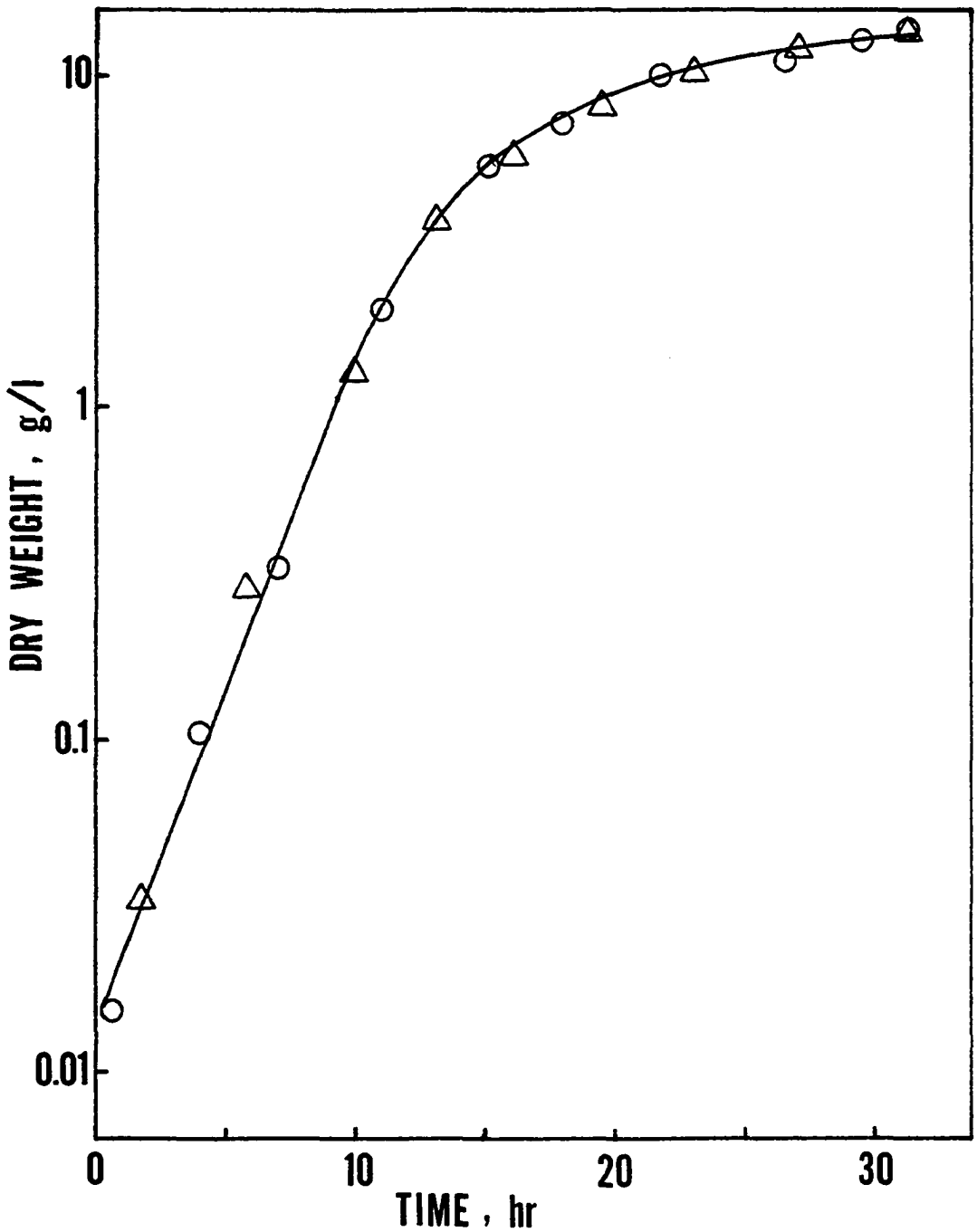
10
1
0.1
0.01
DRY WEIGHT, g/l
0
10
20
30
TIME, hr

perspective of these same kinetics, the kinetics of this yeast would be elucidated more effectively by analyzing both fermentation systems.

Batch fermentations

Two batch fermentations, batch 1 and batch 2, were conducted in which the concentrations of the major constituents of the yeast biomass and the media were monitored frequently for over 90 hr. For batch 1, pH and the concentrations of lactose (L), extracellular nitrogen (N), total biomass, and lipid (X_f) were monitored starting just after the inoculation of the fermenter (Figure 10). In order to better understand the growth of the yeast, the concentration of nonlipid biomass (X_s) was recorded in Figure 10 rather than the concentration of total biomass. The concentration of nonlipid biomass is the difference between the concentrations of total biomass and lipid.

General trends can be observed in batch 1 for growth and lipid accumulation of this yeast. In the first 13 hr, most of the cellular uptake of nitrogen occurred. Although X_s is observed to increase during this period, changes in X_f and L are not however readily evident. The pH is observed to go through a peak, evidently corresponding to the cellular absorption of nitrogen.

From 13 to 25 hr, most of the accumulation of nonlipid biomass was completed. Significant cellular uptake of lactose also occurred. Accumulation of lipid was more evident during this

Figure 10. Changes in the concentrations of the major components of the fermentation broth and biomass for batch 1 fermentation. pH(●); concentrations of lactose, L(○), extracellular nitrogen, N(□), nonlipid biomass, X_s(△), and lipid, X_f(▽)

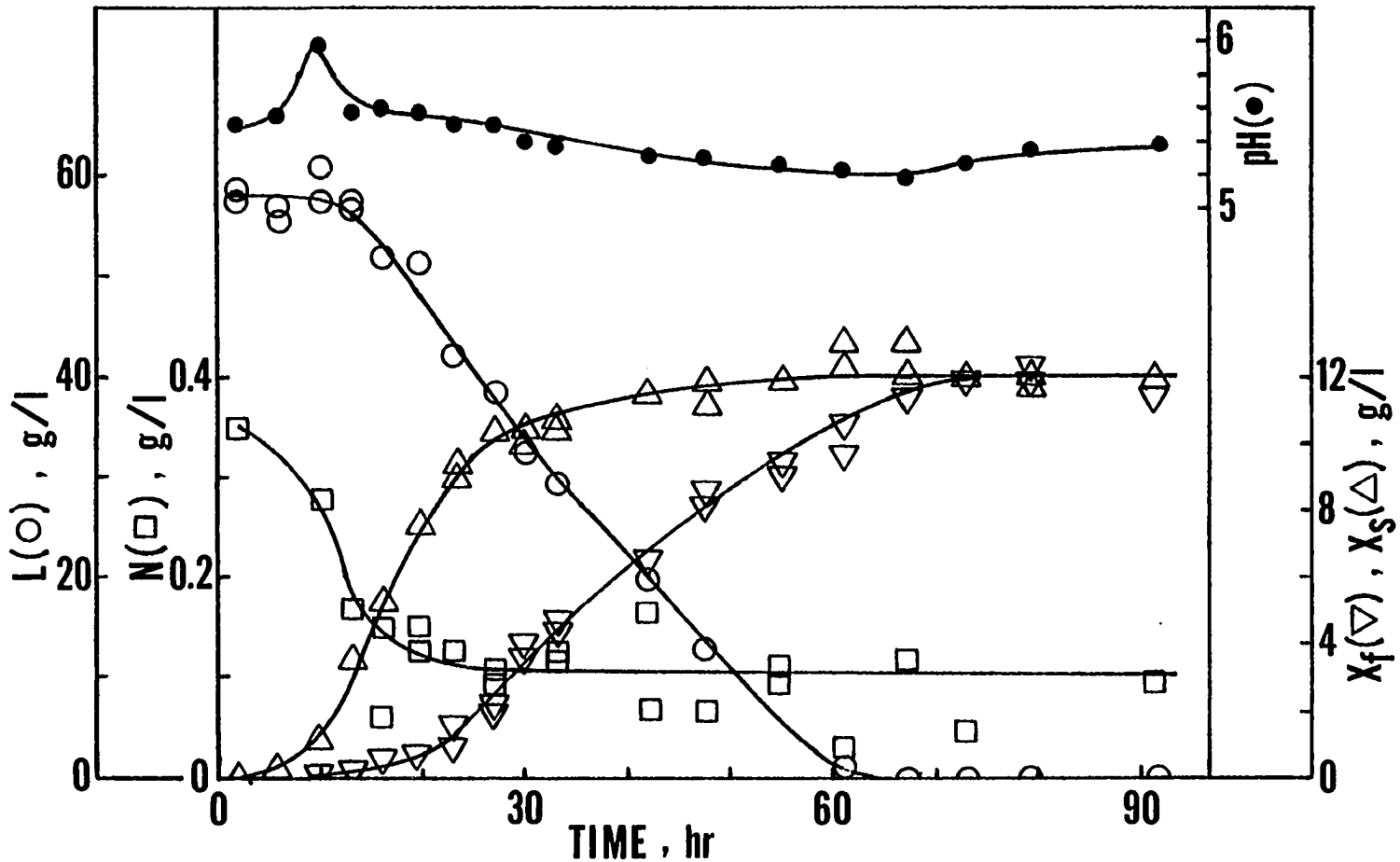
L(○) , g/l
N(□) , g/l
pH(●)
Xf(▽) , Xs(△) , g/l
TIME , hr
0
20
40
60
0
0.2
0.4
5
6
0
4
8
12
0
30
60
90

period. Additional cellular uptake of nitrogen seemed to occur. However the pH was fairly constant.

From 25 to 65 hr, most of the lipid accumulated. Lactose was exhausted by the end of this period, evidently terminating lipid accumulation. Some increase in X_s occurred during this period, but no additional cellular uptake of nitrogen seemed to occur. The decrease in pH seems to correspond to the increase in X_f. But after 65 hr, only pH is observed to change increasing to some extent.

These same trends for pH, L, N, X_s and X_f are also observed for batch 2 fermentation (Figure 11). Although the data for N differ in absolute concentration between the two fermentations, the change in concentrations from the beginning to the end of each fermentation is reasonably similar for the two fermentations.

In comparing the two fermentations, the ratio of X_f to X_s (X_f/X_s) suggests that accumulation of lipid in batch 1 lagged by ca. 3 hr behind that in batch 2 (Figure 12). At the end of the fermentations, X_f/X_s for batch 2 seems slightly greater than that for batch 1. This can be attributed to the combination of the slightly greater final concentrations of nonlipid biomass observed in batch 1 and the similar final concentrations of lipid for both fermentations. Considering the overall patterns of the two fermentations, these two batch fermentations can be considered reasonably similar.

Figure 11. Changes in the concentrations of the major components of the fermentation broth and biomass for batch 2 fermentation. pH(●); concentrations of lactose, L(○), extracellular nitrogen, N(□), nonlipid biomass, X_s(△), and lipid, X_f(▽)

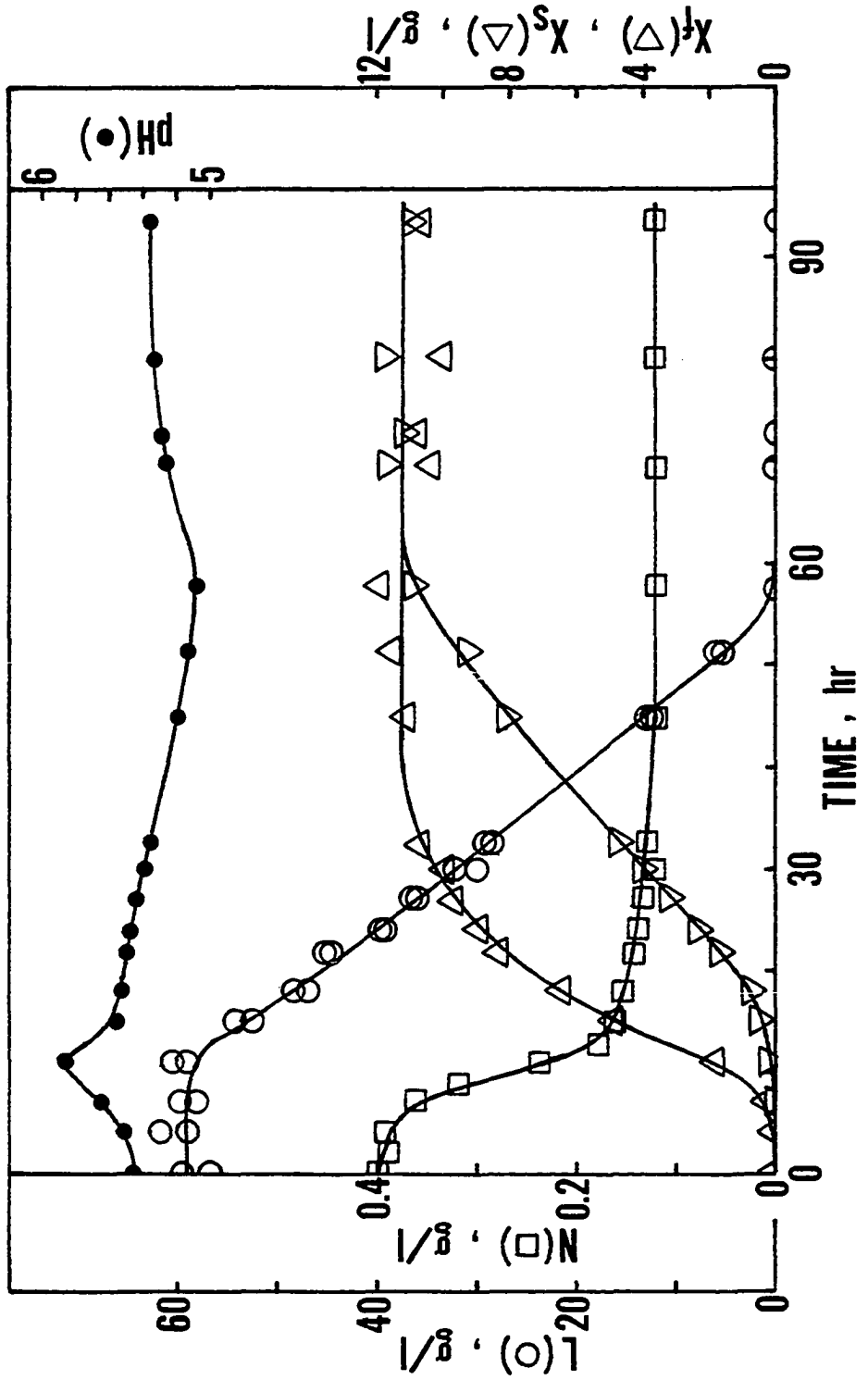
pH(●)
L(○), gg/l
N(□), gg/l
Xf(▽), Xs(△), gg/l
TIME, hr

Figure 12. Changes in biomass concentrations during the batch fermentations. Batch 1 (hollow symbols) and batch 2 (solid symbols) fermentations; concentrations of nonlipid biomass, X_s(□, ■); microscopic cell count, MCC(△, ▲); viable cell count, VCC(○); ratio of lipid to nonlipid biomass, X_f/X_s(▽, ▼)

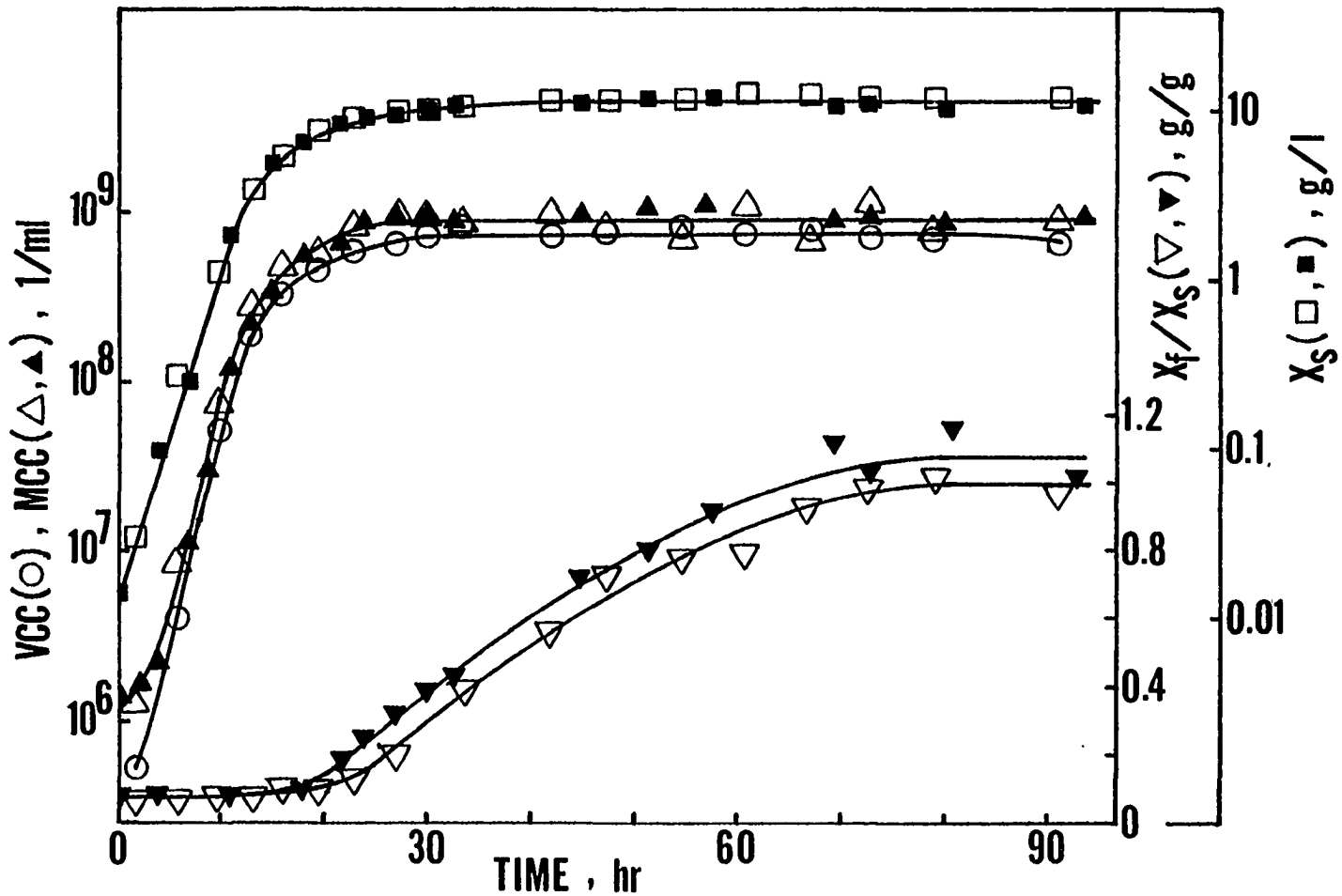
VCC(○), MCC(△,▲), 1/ml
10^9
10^8
10^7
10^6
0
30
60
90
TIME , hr
χ_f/χ_x
1.2
0.8
0.4
0
χ_s/χ_x(▲,△), g/g
χ_s(□,■), g/l
10
1
0.1
0.01

In batch 2, the concentration of cellular nitrogen (N_x) was also monitored (Figure 13). Lundin (1950) first showed that the percentage of nonlipid biomass as nitrogen in an oleaginous yeast correlated with the respiration rate of the nonlipid biomass. He considered that this correlation resulted because most of the cellular nitrogen was biologically active as cellular enzymes. Although nucleic acids contribute a portion of the cellular nitrogen, most of the cellular nitrogen in yeast seems to be contributed by protein (Almazan et al., 1981). Based on the concept that cellular nitrogen concentration was proportional to the cellular enzyme concentration, the specific rates of uptake or accumulation could be expressed with respect to N_x. These specific rates of change of a particular constituent at a particular time were calculated by dividing the slope of a line tangent to the plot of the concentration of that constituent vs. time, by the concentration of cellular nitrogen at that particular time. The specific rates were estimated from the data of the batch 2 fermentation because N_x was only monitored in that batch fermentation. But since the two batch fermentations are reasonably similar, the observed trends can be interpreted as applying in general to batch fermentations of this yeast under the conditions of this study.

In both batch fermentations, the major increases in N_x, X_s, and X_f seemed to be somewhat sequential. This has also been observed to occur in batch fermentations of other oleaginous yeast

Figure 13. Transfer of nitrogen from the fermentation broth to the biomass during batch 2 fermentation. Concentrations of total nitrogen, N_x + N(○), extracellular nitrogen, N(□), and cellular nitrogen, N_x(△)

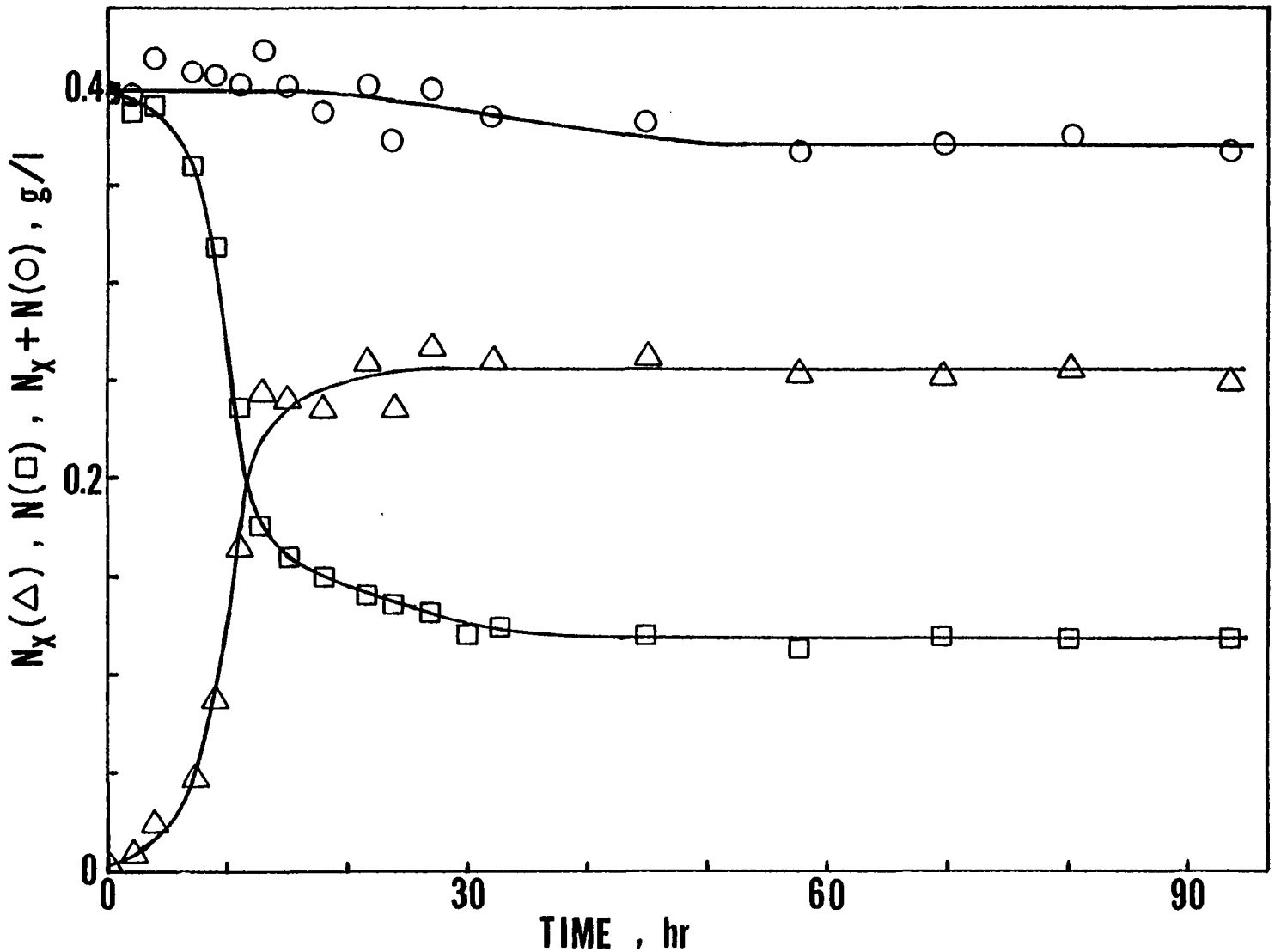
0.4
0.2
0
0
30
60
90
TIME , hr
$N_X(\triangle)$, $N(\square)$, $N_X+N(\bigcirc)$, g/l

(Enebo et al., 1946; Kessel, 1968; Yamauchi et al., 1983).

But other studies indicated that not all oleaginous yeast in a batch fermentation behaved as observed here. In several cases, the major increases in X_s and N_x seemed concurrent rather than sequential (Misra et al., 1984; Yoon et al., 1982). In these fermentations, the period of the increase in X_s and N_x preceded and overlapped to some extent the period of the increase in X_f. In another case, it was observed that the major increases in N_x, X_s, and X_f were largely concurrent as indicated by the relatively constant lipid content in the biomass (50-70%) throughout the fermentation (Pedersen, 1961). The concurrence of the major increases of N_x, X_s, and X_f evidently resulted because of that yeast's very slow maximum growth rate (Ratledge, 1978).

With this backdrop of diversity in the general trends of oleaginous yeasts in a batch fermentation, the batch fermentations of this study will be further evaluated.

Cellular and extracellular nitrogen Most of the utilizable extracellular nitrogen was taken up by the cell in the first 13 hr. A semilog plot of N_x and the difference between the total nitrogen concentration (N_o) and N suggests that uptake of nitrogen was rapid initially with N_x increasing from 2-11 hr at an exponential rate of ca. 0.32 1/hr (Figure 14). The rapid uptake of nitrogen observed for this yeast may contribute to this yeast's ability to out-compete other microorganisms in a mixed-culture, nitrogen-

Figure 14. Changes in biomass concentrations during the growth phase of batch 2 fermentation. Concentrations of nonlipid biomass, X_s(□), and cellular nitrogen, N_x(△); the difference between the initial total nitrogen and the extracellular nitrogen concentrations, N_o - N(○); microscopic cell counts, MCC(▽)

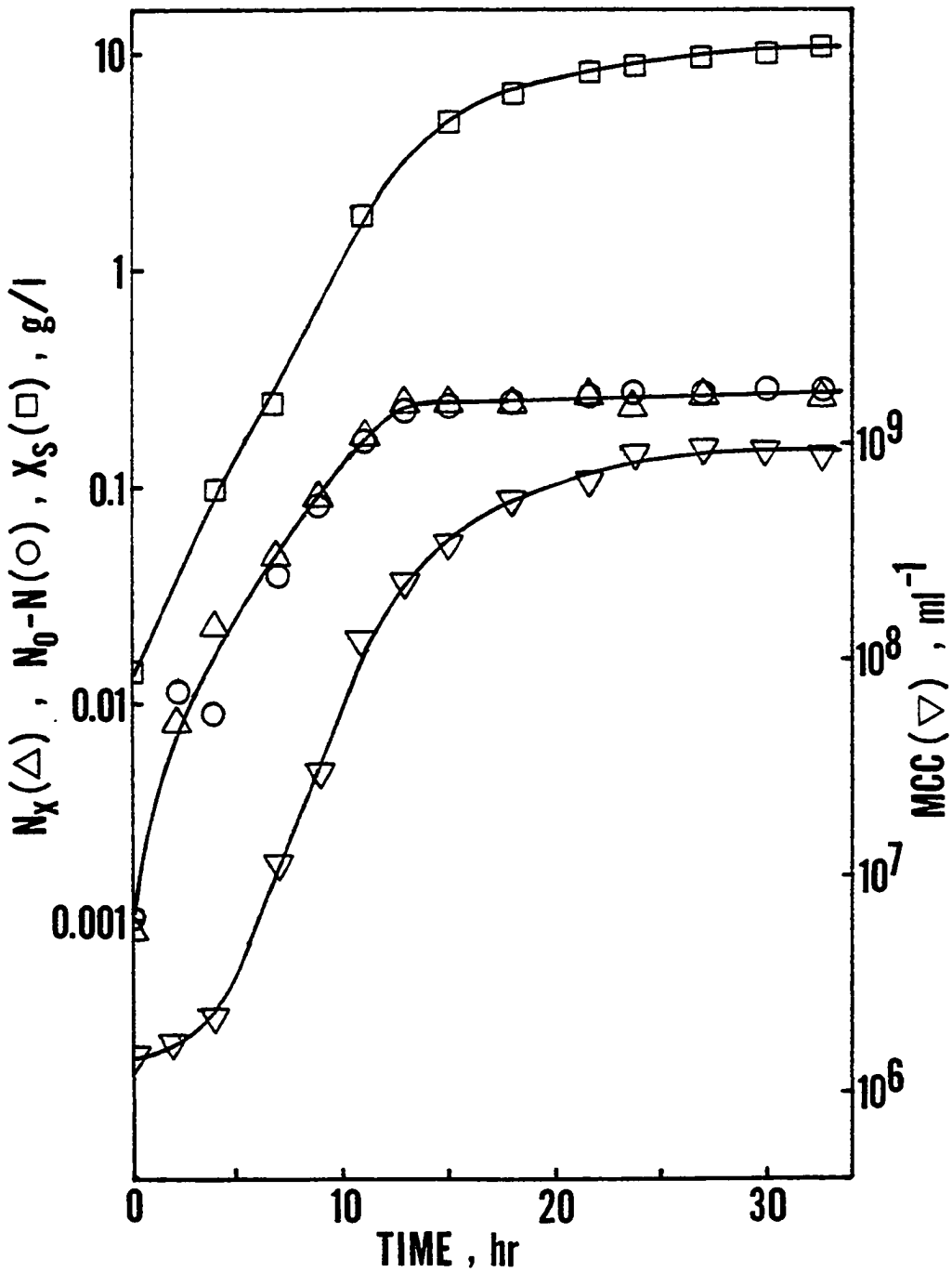
10
1
0.1
0.01
0.001
$N_X(\triangle)$, N_0-N(○) , $X_S(\square)$, g/l
10^9
10^8
10^7
10^6
MCC (▽) , ml^{-1}
0
10
20
30
TIME , hr

limited batch fermentation (Hammond et al., 1981).

The ratio of the change in X_s to the change in N_x ($\Delta X_s/\Delta N_x$) suggests that for the first 7 hr, uptake of nutrients was primarily that of nitrogenous compounds such as amino acids. This is based on observing $\Delta X_s/\Delta N_x$ to be ca. 5.4 for the first 7 hr; this value is similar to 5.9 which is estimated to be the mass ratio of protein to nitrogen for yeast protein (Moon et al., 1978; Zabriskie et al., 1980). The effect of the uptake of predominantly nitrogenous compounds is evident in the approach of the ratio of X_s to N_x (X_s/N_x) to ca. 6 in the first 7 hr (Figure 15).

Assuming a mass to nitrogen ratio of 5.4 for nitrogenous compounds, the percentage of nitrogenous compounds in the nonlipid biomass can be estimated to range from 50 to 90% during the first 11 hr of a batch fermentation. In comparison, when R. glutinis has been cultivated for protein, ca. 62% of the nonlipid biomass was estimated as protein (N $\times$ 6.25) (Lundin, 1950). At the end of the batch fermentation of this study, ca. 13% of the nonlipid biomass can be estimated to be nitrogenous compounds based on observing ca. 42 for X_s/N_x (Figure 15). This final value of 13% is similar to the estimated protein (N $\times$ 6.25) content of the nonlipid biomass for other oleaginous yeast at the end of batch fermentation (Table 7). Thus, the percentage of nonlipid biomass of C. curvata D estimated as nitrogenous compound is observed to change dramatically over the course of a batch fermentation.

Figure 15. Changes in cell composition during batch 2 fermentation. Ratio of nonlipid biomass to microscopic cell count, X_s/MCC(○); ratio of nonlipid biomass to cellular nitrogen, X_s/N_x(□); ratio of lipid to nonlipid biomass, X_f/X_s(△)

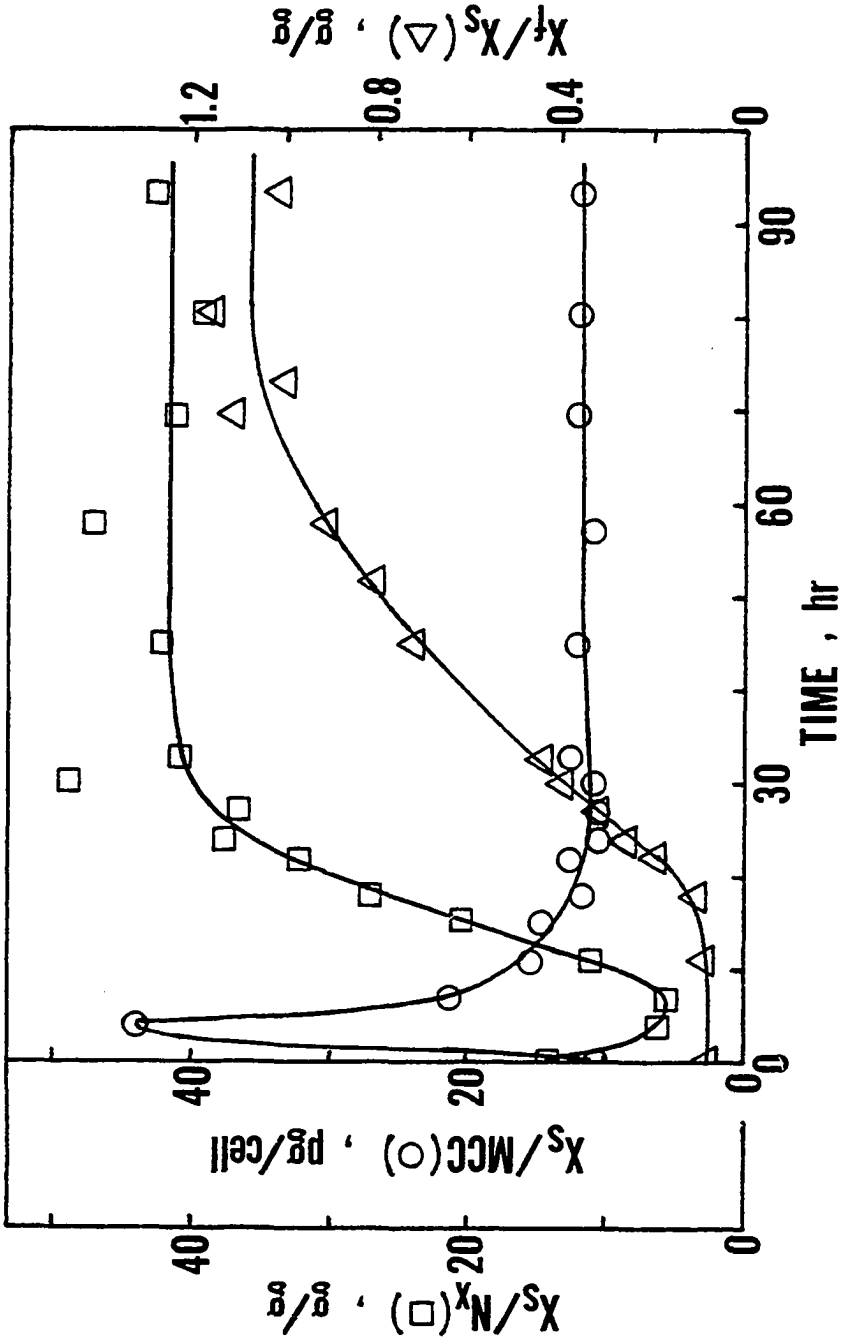
X_f/X_S (△) , g/g
1.2
0.8
0.4
0
90
60
30
TIME , hr
0
X_S/MCC(○) , pg/cell
40
20
0
X_S/N_X(□) , g/g
40
20
0

Table 7. Values reported at the end of batch fermentations of oleaginous yeast of the ratio of cell protein[a] to nonlipid biomass (X_p/X_s) and the ratio lipid to nonlipid biomass (X_f/X_s)

Species	X_p/X_s	X_f/X_s	Reference
Candida curvata D	0.22	1.3	Moon et al., 1978
Candida curvata R	0.18	1.0	Moon et al., 1978
Cryptococcus terricolus	0.10	2.0	Pedersen, 1961
Hansenula ciferri	0.13	0.25	Hopton and Woodbine, 1960
Hansenula saturnus	0.12	0.33	Hopton and Woodbine, 1960
Lipomyces starkeyi	0.23	0.58	Roy et al., 1978
Rhodotorula glutinis	0.31	0.67	Allen et al., 1964
	0.30	1.5	Enebo et al., 1946
	0.25	0.58	Hopton and Woodbine, 1960
	0.26	1.0	Lundin, 1950
	0.27	1.1	Yoon et al., 1982
Trichosporon cutaneum 24	0.19	0.25	Moon et al., 1978
Trichosporon cutaneum 40	0.25	0.82	Moon et al., 1978

[a]Protein = N × 6.25.

During the period of rapid cellular uptake of nitrogen (the first ca. 11 hr of batch fermentation), the pH of the buffered fermentation broth was observed to increase (Figures 10 and 11). Utilizing the mass balance on the buffer and the Henderson-Hesselbach equation, the molarity of a protonated form of the buffer, [acid], can be estimated at various pHs as follows

$$[\text{acid}] = [\text{buffer}]\ 10^{pK - pH}/(1 + 10^{pK - pH}) \qquad (11)$$

where [buffer] is the molarity of the buffer, and pK is the pH at which equimolar concentrations of the protonated and corresponding unprotonated form of the buffer exist. The molarity of the buffer was estimated to be 15 mM and the pK for the combination of mono- and dibasic o-phthalate was given as 5.51 (Weast, 1974). Using the change in pH from 5.5 to a peak of 5.9, a decrease of 3.6 mM of monobasic o-phthalate could be calculated. This coresponded to a decrease of ca. 0.16 g/l of extracellular nitrogen or ca. 8.4 mM of amino acids. This assumes that the uptake of nitrogen represented the uptake of amino acids of an amino acid profile similar to that of yeast extract as reported by Zabriskie et al. (1980). The coincidence of the pH rise with the rapid uptake of nitrogen may reflect the uptake of a basic amino acid such as glutamine, which composes 15% (mole/mole) of yeast extract amino acids (Zabriskie et al., 1980).

The exponential increase in N_x ended after 11 hr (Figure 14). The initial decrease in the specific rate of cellular nitrogen

accumulation after this period seems to be approximately linearly related to a decrease in N (Figure 16). But at specific rates less than 0.04 1/hr, the decrease in specific rates does not seem to be linearly related to the decrease in N. The overall nonlinear relationship between the decreasing specific rates of cellular nitrogen accumulation and the utilizable extracellular nitrogen concentration may result from the heterogeneity of the nitrogenous compounds in yeast extract.

A decrease is noted in the total nitrogen concentration (N_x + N) after 20 hr of fermentation (Figure 13). This seems to result because not all of the extracellular nitrogen removed from the broth is recovered from the cells. Such a result may however be an artifact of the Kjeldahl nitrogen procedure resulting from the cellular conversion of primary amines to other nitrogenous compounds less readily reduced during the digestion step (Ayres, 1968). This is supported by observing that after ca. 40 hr, both X_s and N_x + N remained constant (Figures 11 and 13).

As evident in these batch fermentations, not all of the nitrogen was assimilated. An estimated 70% of the nitrogen was utilized however. This compares favorably with an estimated 80% of the nitrogen in yeast extract which can be attributed to amino acids (Zabriskie et al., 1980). The remaining unutilized nitrogen may have been contributed by amino acid peptides or nucleic acid. Peptides may not be available to this yeast because of a lack of

Figure 16. Relationship between the specific rate of cellular nitrogen accumulation and the concentration of extracellular nitrogen during batch 2 fermentation. Specific rates of extracellular nitrogen uptake, $\frac{-1}{N_x}\frac{dN}{dt}$ (○); and of cellular nitrogen accumulation, $\frac{1}{N_x}\frac{dN_x}{dt}$ (●)

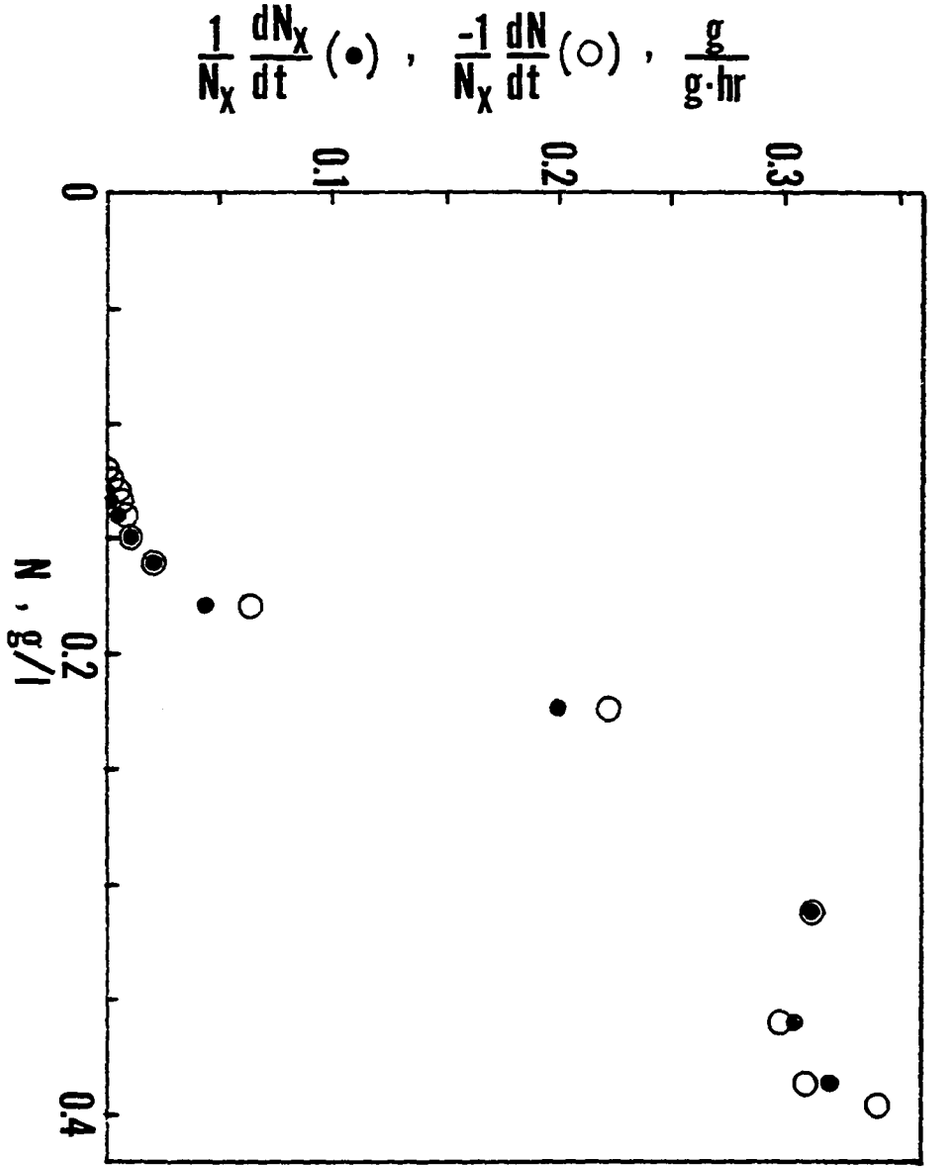
$\frac{1}{N_X}\frac{dN_X}{dt}$ (•) , $\frac{-1}{N_X}\frac{dN}{dt}$ (○) , $\frac{g}{g \cdot hr}$
0
0.1
0.2
0.3
0.2
0.4
N , g/l

proteolytic ability (Moon et al., 1978). Nucleic acids are evident in yeast extract because the ratio of the absorbance of a solution of yeast extract at 260 nm to that at 280 nm is greater than such a ratio for a solution of casamino acids (Difco Laboratories, Detroit, MI). For yeast extract the ratio was 2.8, and for casamino acids the ratio was 1.0. Nucleic acids provided by yeast extract may have been available in excess or were not readily metabolizable by this yeast.

Nonlipid biomass and cells Figure 12 suggests that accumulation of X_s in the batch fermentation entered an exponential phase without an evident lag. But the ratio of the change in X_s to the change in N_x observed for the first 7 hr suggested that the change in X_s for this period could be attributed essentially to the uptake of nitrogenous compounds. The nonnitrogenous nonlipid biomass concentration could be estimated as the difference between X_s and N_x times 5.4. The factor 5.4 was used because during the first 7 hr of the fermentation the ratio of the change in X_s to the change in N_x was observed to be ca. 5.4. Thus, the increase in X_c would not be evident until after ca. 7 hr into the batch fermentation. In agreement with this, the specific rate of nonnitrogenous nonlipid biomass accumulation was estimated to be close to zero for the first 7 hr, increasing significantly thereafter (Figure 17).

An apparent lag of ca. 10 hr was observed for lactose uptake in the batch fermentation (Figure 11). But during this period,

Figure 17. Changes in specific rates of biomass accumulation during batch 2 fermentation. Specific rates of accumulation of nonlipid biomass, $\frac{1}{N_x}\frac{dX_s}{dt}$ (○); of nonnitrogenous nonlipid biomass, $\frac{1}{N_x}\frac{dX_c}{dt}$ (●); and of cellular nitrogen, $\frac{1}{N_x}\frac{dN_x}{dt}$ (□)

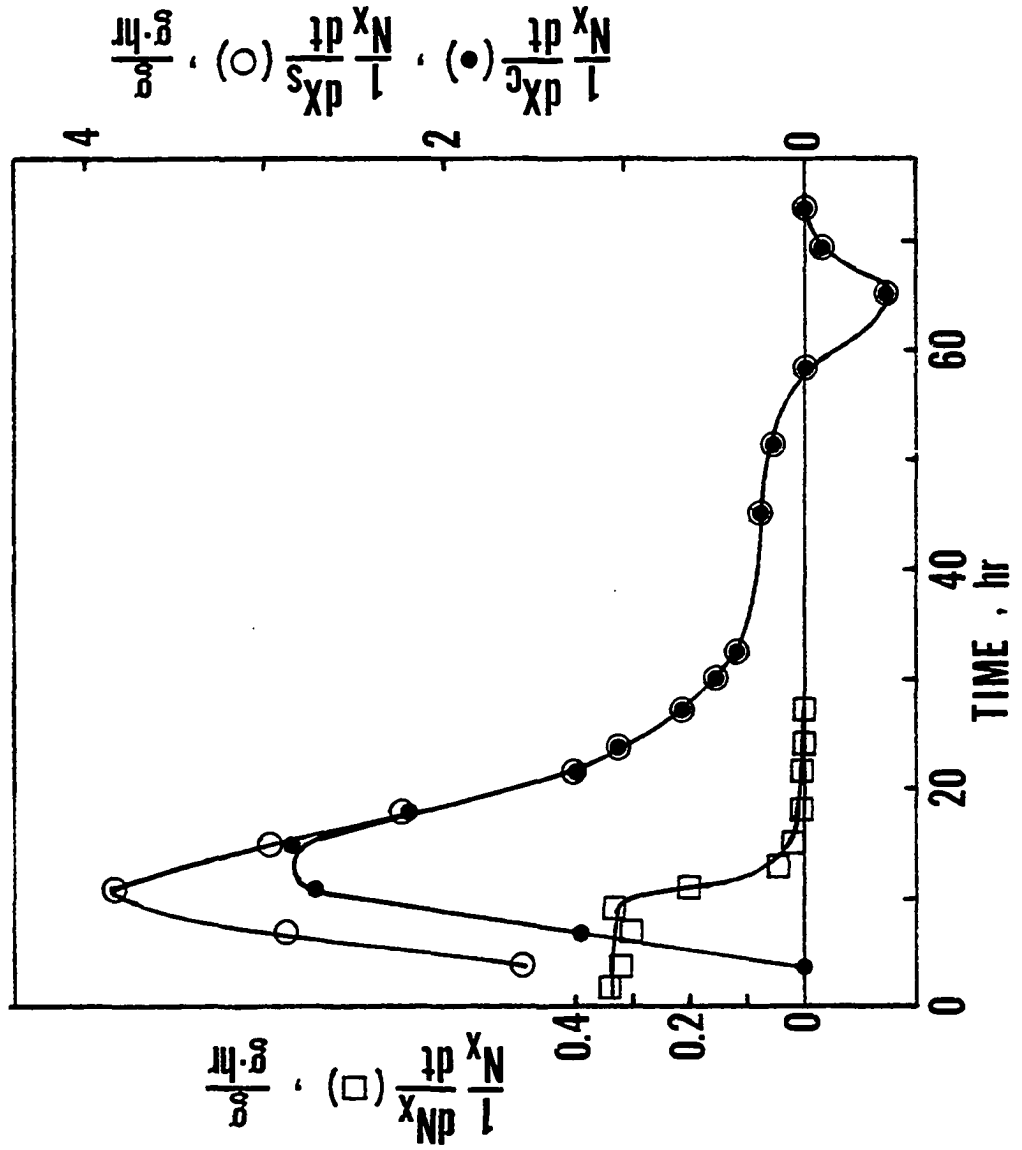
$\frac{1}{N_X}\frac{dX_C}{dt}$ (●), $\frac{1}{N_X}\frac{dX_S}{dt}$ (○), $\frac{eq}{eq\cdot hr}$
$\frac{1}{N_X}\frac{dN_X}{dt}$ (□), $\frac{eq}{eq\cdot hr}$
TIME, hr
0
20
40
60
0
0.2
0.4
0
2
4

ca. 0.9 g/l of nonnitrogenous nonlipid biomass and ca. 0.2 g/l of lipid accumulated. This discrepancy could be caused by the large standard deviation of 1.3 g/l for the measurement of lactose at 60 g/l, which would make the change in the lactose concentration not noticeable during this period.

Glucose was also present initially in the fermentation broth at 0.09 g/l. It was almost completely utilized after 7 hr. Glucose originated in part from yeast extract which contained ca. 1.3% glucose (w/w). It is not likely that the presence of such a small concentration of glucose inhibited lactose uptake. These concentrations of glucose are much smaller than that which has been reported to be inhibitory to the uptake of other sugars, eg. galactose, fructose, or sucrose (Hong et al., 1983; Imanaka et al., 1972).

Both the concentrations of cellular nitrogen and cells, as determined by microscopic cell count, increased exponentially in the first 11 hr (Figure 14). The exponential rates were estimated at 0.32 1/hr and 0.54 1/hr for the concentrations of cellular nitrogen and cells, respectively. The changing ratio of X_s to the concentration of cells (X_s/MCC) and X_s/N_x (Figure 15) substantiate that growth was not balanced during this period.

The proportionality between X_s and the concentration of cells was evident after 20 hr in the fairly constant value of X_s/MCC (Figure 15). The overall pattern of X_s/MCC is actually quite similar to that for nonoleaginous microorganisms.

From ca. 7 to ca. 40 hr, the increase in X_c was evident from the increase in X_s/N_x (Figure 15). The specific rate of nonnitrogenous nonlipid biomass accumulation was estimated to peak at ca. 13 hr and decrease to around zero after ca. 40 hr (Figure 17). After ca. 40 hr, a maximum and essentially constant X_s/N_x is observed (Figure 15). Because X_s and cell concentration were proportional and X_s essentially stopped increasing before lactose was exhausted from the fermentation broth (Figure 11), it seems reasonable that X_s stopped increasing because a minimum amount of cellular nitrogen was required per cell for the essential cellular metabolic processes.

After ca. 30 hr, the cell concentration was essentially constant (Figure 12). In addition, the concentration of viable cells was also essentially constant. The viable cell count was not observed to decrease immediately after the exhaustion of lactose at ca. 60 hr (Figure 10), as it was observed to occur after the exhaustion of glucose in a carbon-limited fermentation of a niacin-producing yeast (Tseng and Phillips, 1982). Thus in a nitrogen-limited fermentation, C. curvata D is suggested to be hardier than this nonoleaginous niacin-producing yeast in a carbon-limited fermentation.

Microscopic examination of the yeast cells during the stationary phase for X_s and the concentration of cells observed in Figure 12 suggested that budding and separation activity had essentially ceased. The duration of this stationary phase was at least 40 hr. Tsuchiya et al. (1980) also observed a stationary phase for

the biomass concentration of an adenine-requiring strain of Bacillus subtilis prior to the exhaustion of glucose. Adenine in their study was present at a fairly constant concentration in the fermentation broth during this period. They concluded that this stationary phase observed for 4 hr resulted because of the balance between cell death and lysis and cell division. Since cell death and lysis was not evident for C. curvata D over a 40 hr interval, it suggested that cells of C. curvata D have a much longer average lifespan under nitrogen-limited conditions than those cells of B. subtilis under adenine-limited conditions.

Lipid For the first 15 hr of the batch fermentations, X_f/X_s is observed to be essentially constant (Figure 12). This has also been observed with other oleaginous yeasts in which the constant X_f/X_s ranged from 10-40% (Enebo et al., 1946; Fahmy et al., 1962; Yamauchi et al., 1983; Yoon et al., 1982). In contrast, when R. glutinis, an oleaginous yeast, was cultivated instead for protein, Lundin (1950) observed X_f/X_s to be 3%. Thus, during the initial period of nonlipid biomass accumulation in a lipid-accumulating fermentation, the lipid which is synthesized is probably in excess of that required for maintenance of cell membranes in the oleaginous yeast.

Figure 18 shows the relationship between X_f and L during the batch fermentations. Both the linearity of the curve below 40 g/l of lactose and the coincidence of the termination of lipid

Figure 18. The relationship between the concentrations of lipid, X_f, and lactose, L, observed during batch fermentation. Batch 1 (○) and batch 2 (□) fermentations.

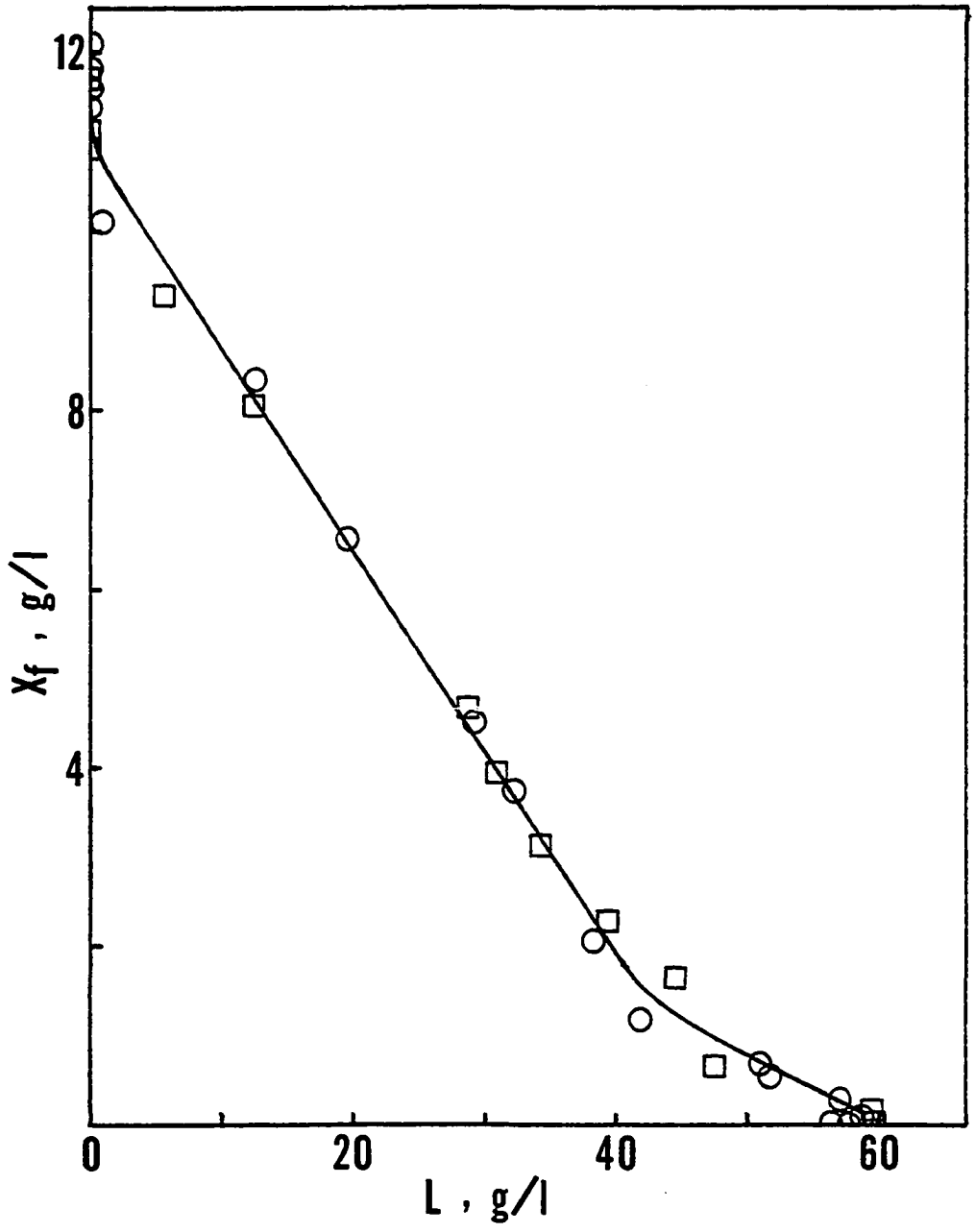
12
8
4
0
20
40
60
X_f , g/l
L , g/l

accumulation with lactose exhaustion suggest that lactose was converted to lipid without the additional accumulation of metabolites such as citrate, ethanol or acetic acid. Some additional lipid is observed to have accumulated after the exhaustion of lactose (Figure 18). This coincides with a negative specific rate of non-nitrogenous nonlipid biomass accumulation (Figure 17), thus suggesting that a time-lag exists between the uptake of lactose and the formation of lipid.

Some studies of oleaginous yeast in batch fermentations have also indicated that during significant lipid accumulation the concentrations of lipid and glucose were linearly related (Kessel, 1968; Misra et al., 1984; Yoon et al., 1982). Other oleaginous yeast may behave differently. For instance, Hansenula sp. seems to accumulate ethanol, ethyl acetate, and acetic acid along with lipid (Davies et al., 1951; Fahmy et al., 1962). These metabolites are evidently converted in part to lipid after the exhaustion of glucose.

The dramatic increase in X_f/X_s observed after 15 hr in Figure 12 is observed to coincide with the dramatic increase in the specific rate of lipid accumulation (Figure 19). The dramatic increase in X_f/X_s for this yeast in batch fermentation has also been observed to coincide with the increase in the specific activity of enzymes required for fatty acid synthesis (Evans and Ratledge, 1983b). Thus, this increase in the specific rate of lipid

Figure 19. Changes in specific rates of substrate absorption and biomass accumulation during batch 2 fermentation. Specific rates of lactose uptake, $\frac{-1}{N_x}\frac{dL}{dt}$ ($\triangle$); and the accumulation of nonlipid biomass, $\frac{1}{N_x}\frac{dX_s}{dt}$ ($\bigcirc$); of nonnitrogenous nonlipid biomass, $\frac{1}{N_x}\frac{dX_c}{dt}$ ($\bullet$); and of lipid, $\frac{1}{N_x}\frac{dX_f}{dt}$ ($\bigtriangledown$)

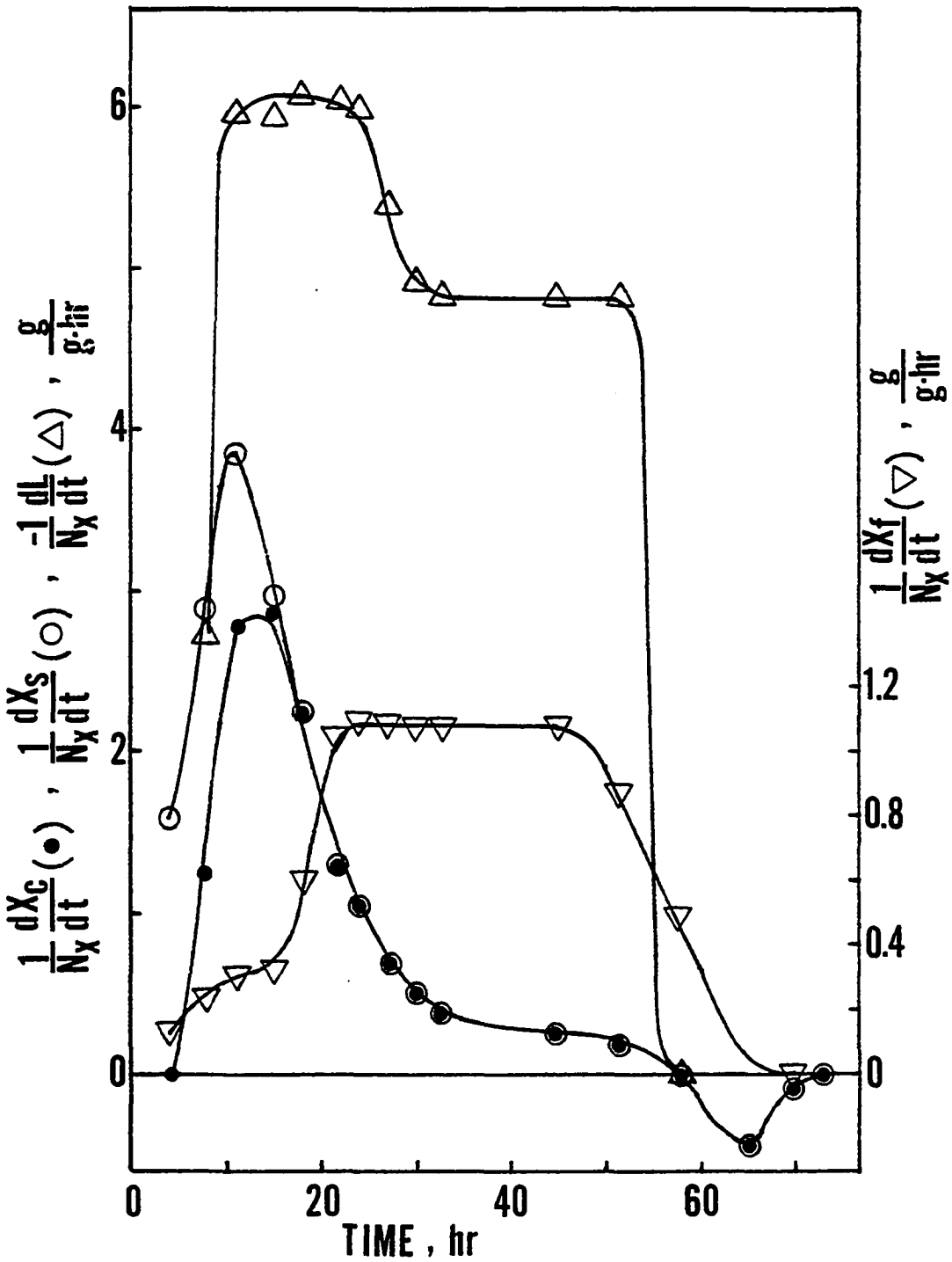
6
4
2
0
0
20
40
60
TIME , hr
1.2
0.8
0.4
0
$\frac{1}{N_X}\frac{dX_c}{dt}(\bullet)$, $\frac{1}{N_X}\frac{dX_s}{dt}(\circ)$, $\frac{-1}{N_X}\frac{dL}{dt}(\triangle)$, $\frac{g}{g\cdot hr}$
$\frac{1}{N_X}\frac{dX_f}{dt}(\triangledown)$, $\frac{g}{g\cdot hr}$

accumulation corresponds to the reported increase in the specific activity of these enzymes and can be considered to represent an increase in the flux of metabolites through the fatty acid synthesis pathway. That a maximum and constant specific rate of lipid accumulation is observed from 24 to 45 hr in Figure 19 supports the proposal that the rate of fatty acid synthesis is limited by the specific activity of ATP:citrate lyase (Boulton and Ratledge, 1981).

But what causes the increase in the specific rate of lipid accumulation? Increased lactose uptake can be ruled out since during the dramatic increase in the specific rate of lipid accumulation the specific rate of lactose uptake was constant (Figure 19). The beginning of this increase in the specific rate of lipid accumulation is however observed to coincide with the beginning of the decrease in the specific rate of nonnitrogenous nonlipid biomass accumulation (Figure 19). In addition, the specific rate of lactose uptake is observed to decrease after the constant and maximum specific rate of lipid accumulation was attained. These observations suggest that the initial decrease in the specific rate of demand for lactose for nonnitrogenous nonlipid biomass accumulation is balanced by the increase in the specific rate of demand for lactose for lipid accumulation. The continued decrease in the specific rate of demand for lactose for nonnitrogenous nonlipid biomass accumulation after the attainment of the maximum and constant specific rate of lipid accumulation would

result in a decrease in the specific rate of lactose uptake in order to prevent the accumulation of metabolites. The presently accepted biochemical mechanism of lipid accumulation attributes the increase in the flux of metabolites through the fatty acid synthesis pathway to a decreased demand for energy produced by the Krebs cycle. Decreased demand for energy produced by the Krebs cycle would reasonably result from the decrease in the specific rate of nonnitrogenous nonlipid biomass accumulation. Thus, the dramatic increase in the specific rate of lipid accumulation observed from 15 to 24 hr in Figure 18 might result from the combination of a constant specific rate of lactose uptake and a decrease in the specific rate of demand for lactose for nonnitrogenous nonlipid biomass accumulation.

Continuous fermentations

The first in a series of steady state continuous fermentations was initiated from a batch fermentation. Subsequent steady states in that series were a result of changes in the dilution rates. A new dilution rate was imposed on the system after the previous continuous fermentation had reached a steady state and samples of fermentation broth had been removed. A steady state at each dilution rate was verified by observing the absorbance of the effluent, an example of which is shown in Figure 20. After removing samples of fermentation broth and prior to imposing a new dilution rate on the system, batch growth conditions prevailed for several hours.

Figure 20. Transient responses of biomass concentration following a change from batch operation to that of continuous operation at a dilution rate of 0.102 1/hr. Absorbance at 540 nm of the effluent fermentation broth, A_{540}(●)

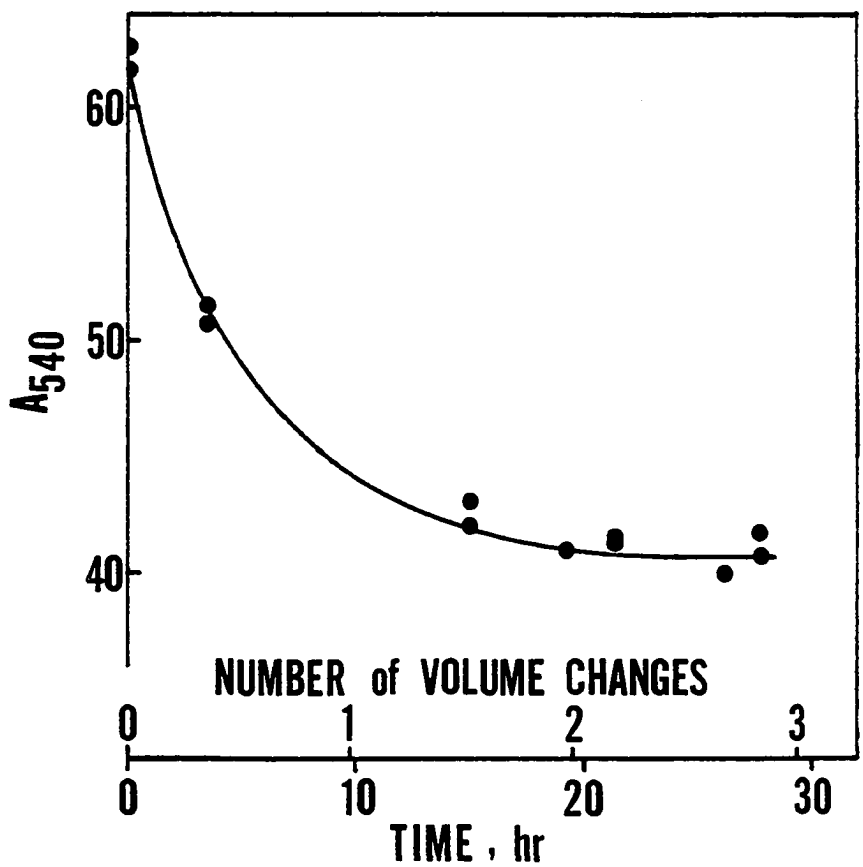
60
50
40
A_{540}
NUMBER of VOLUME CHANGES
0
1
2
3
0
10
20
30
TIME , hr

As a result, the absorbance of the effluent was always greater at the time a new dilution rate was first imposed on the system.

Figure 21 shows the transient responses of the different cell fractions resulting from imposing at 0 hr a step change in the dilution rate, from 0.05 1/hr to 0.14 1/hr. Steady state concentrations of each cell fraction were attained at differing rates, with X_f requiring the longest period (ca. 3 volume changes).

Figure 22 summarizes the effect of dilution rate on the steady state pH, L, N, X_s and X_f. The culture was observed to be washed out at a dilution rate of ca. 0.305 1/hr. This is similar to the wash-out dilution rate of 0.30 1/hr reported for this yeast by Evans and Ratledge (1983a). The bulk of the extracellular nitrogen was utilized at dilution rates near the wash-out dilution rate. An additional small decrease in N is also observed at dilution rates less than 0.295 1/hr. In previous reports of this type, N has not been explicitly reported; but the relationships between dilution rate and steady state X_s, X_f, and L are similar to those reported for other continuous fermentations of oleaginous yeast (Choi et al., 1982; Evans and Ratledge, 1983a; Gill et al., 1977; Ratledge and Hall, 1979; Yoon and Rhee, 1983).

Microscopic cell counts have not always been reported for continuous fermentations of oleaginous yeast. In Figure 23, X_s/MCC is observed to be relatively constant over the range of dilution rates evaluated, indicating again the proportionality between X_s

Figure 21. Transient behavior of a single-stage continuous culture following a change from a dilution rate of 0.05 1/hr to 0.14 1/hr. Absorbance at 540 nm of the effluent fermentation broth, A_{540}(●); concentrations of nonlipid biomass, X_s(○), cellular nitrogen, N_x(□), and lipid, X_f(△)

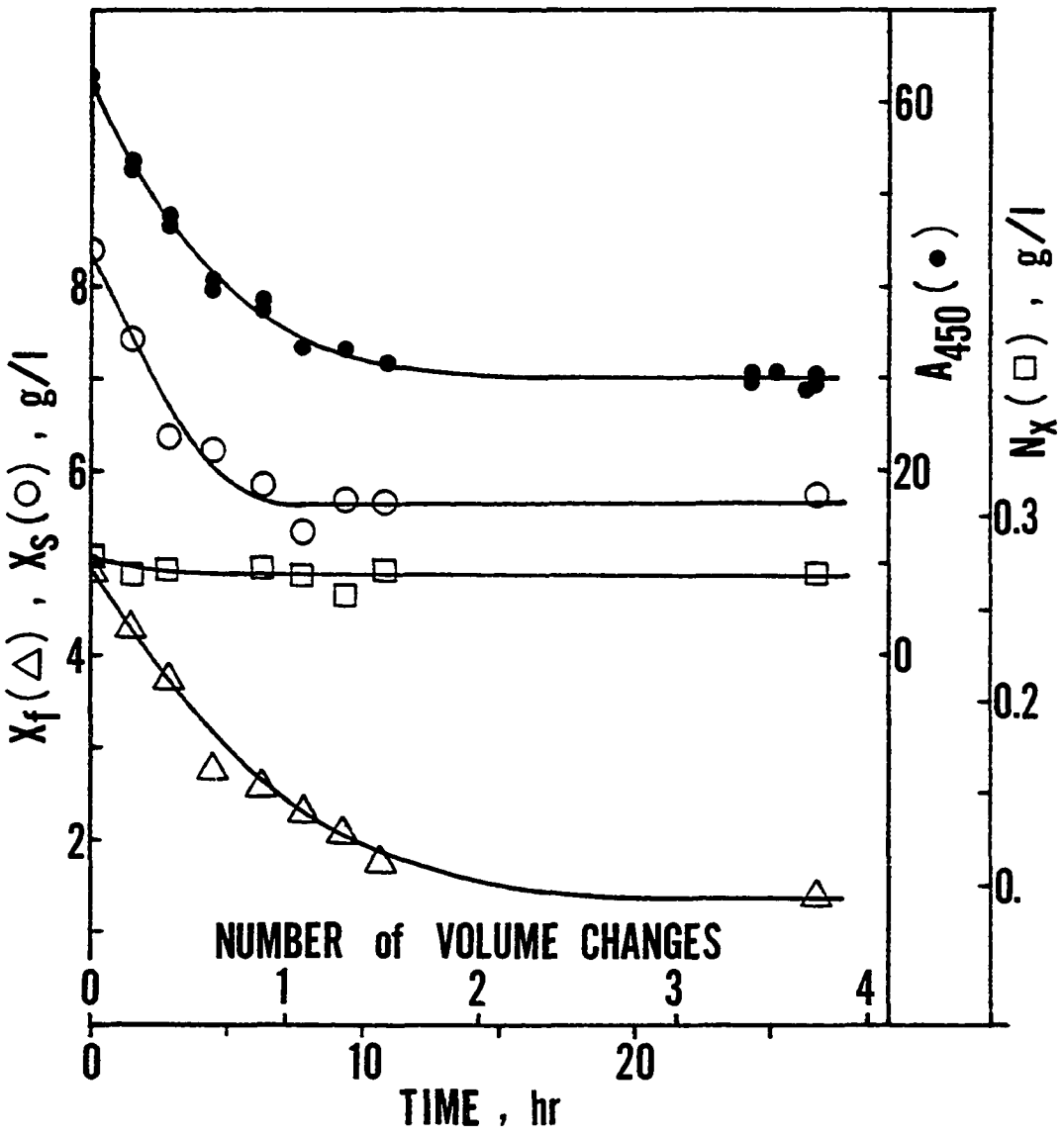
X_f (△) , X_S (○) , g/l
A_{450} (●)
N_X (□) , g/l
NUMBER of VOLUME CHANGES
TIME , hr
0
2
4
6
8
20
60
0.
0.2
0.3
1
2
3
10

Figure 22. Steady-state concentrations of the major substrates and components of the biomass at various dilution rates. Fermentation broth pH(●); concentrations of nonlipid biomass, X_s(○), lipid, X_f(□), lactose, L(▽), extracellular nitrogen, N(△)

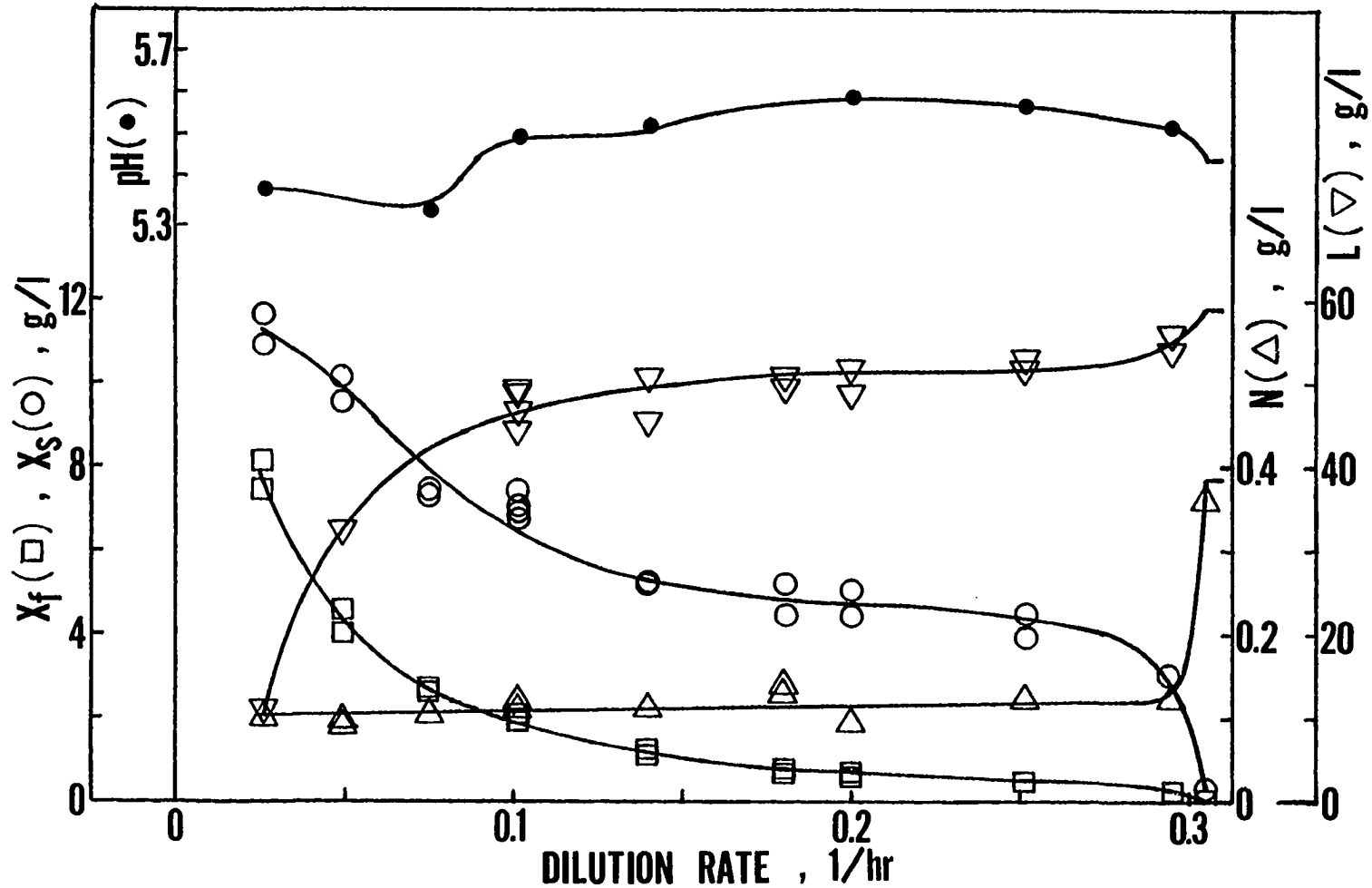
5.7
5.3
pH(●)
12
8
4
0
X_f(□) , X_s(○) , g/l
0.4
0.2
0
N(△) , g/l
60
40
20
0
L(△) , g/l
0
0.1
0.2
0.3
DILUTION RATE , 1/hr

Figure 23. Steady-state cell compositions at various dilution rates. Ratio of nonlipid biomass to cellular nitrogen, X_s/N_x(△); ratio of lipid to nonlipid biomass, X_f/X_s(□); ratio of nonlipid biomass to the microscopic cell count, X_s/MCC(○)

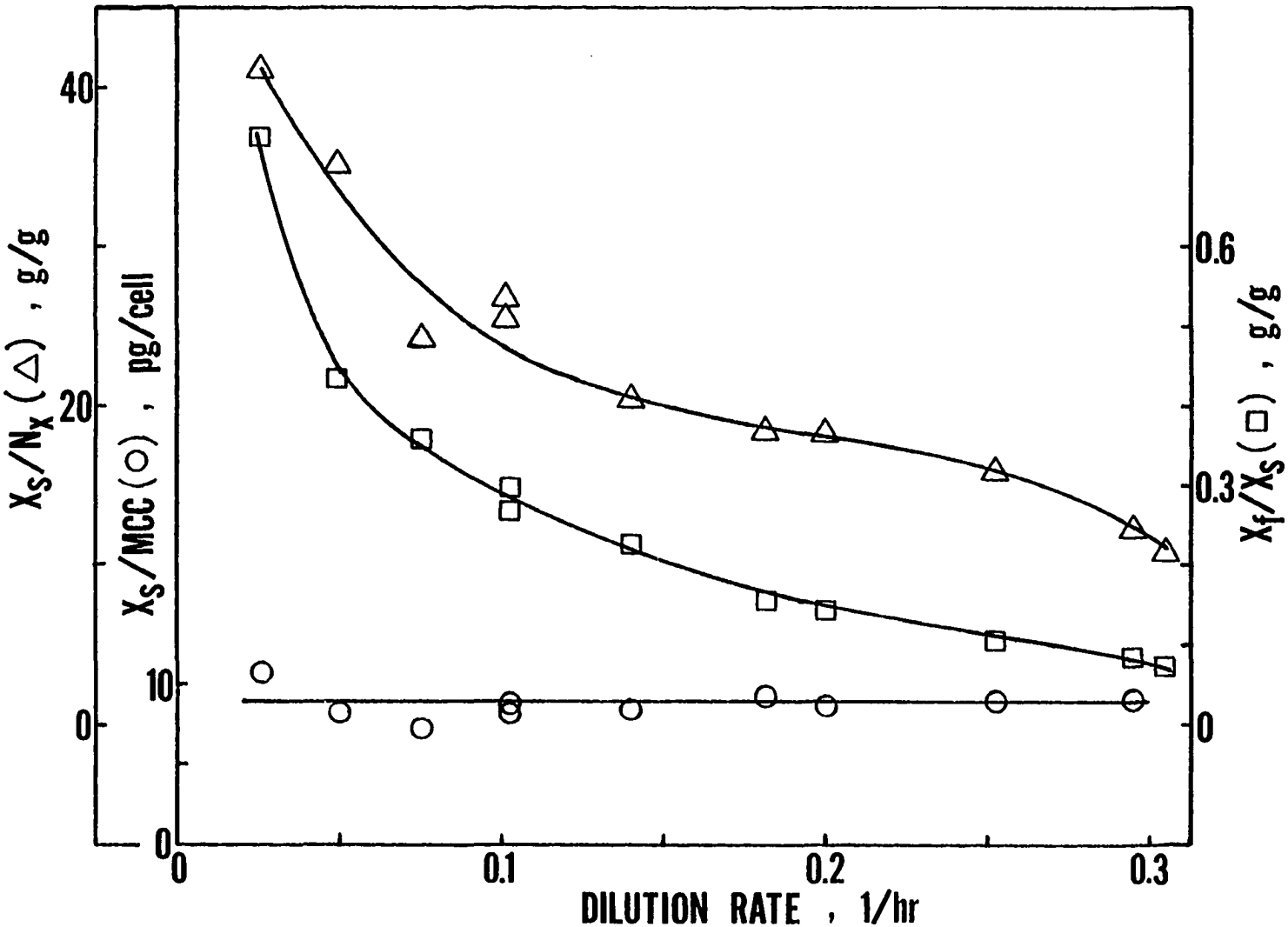
40
20
0
10
0
0
0.1
0.2
0.3
0.6
0.3
0
X_S/N_X (△) , g/g
X_S/MCC (○) , pg/cell
X_f/X_S (□) , g/g
DILUTION RATE , 1/hr

and the concentration of cells. At the slowest dilution rate, 0.026 1/hr, a value of 41 for X_s/N_x is observed (Figure 23). This value is similar to the maximum X_s/N_x observed in batch fermentation (Figure 15). This suggests that X_s at 0.026 1/hr is near its maximum concentration, which appears roughly double that observed at 0.20 1/hr.

The steady state X_f/X_s is observed to be greater at slower dilution rates over the range of dilution rates evaluated (Figure 23). This trend has also been observed in other single-stage continuous fermentations of oleaginous yeast (Choi et al., 1982; Evans and Ratledge, 1983a; Gill et al., 1977; Ratledge and Hall, 1979; Yoon and Rhee, 1983).

Figure 24 depicts the effect of the dilution rate on the specific rates of lactose utilization and lipid, nonlipid biomass, and nonnitrogenous nonlipid biomass production. The concentration of cellular nitrogenous compounds was again estimated as 5.4 times N_x, as was estimated in the analysis of the batch fermentation. The specific rates obtained from continuous fermentation data were expressed with respect to N_x unless otherwise stated. They were calculated as the difference between the concentrations of a constituent in the fermenter and that in the influent stream times dilution rate and divided by N_x.

Three ranges of dilution rates can be defined in Figure 24 based on the trends in the specific rates of lipid and nonnitrogenous

Figure 24. Steady-state specific rates of substrate utilization and biomass production at various dilution rates. Specific rates of lactose uptake, $D(L_o - L)/N_x$ (□); and the accumulation of nonlipid biomass, $D \cdot X_s/N_x$ (○); of nonnitrogenous nonlipid biomass, $D \cdot X_c/N_x$ (●); and of lipid, $D \cdot X_f/N_x$ (△)

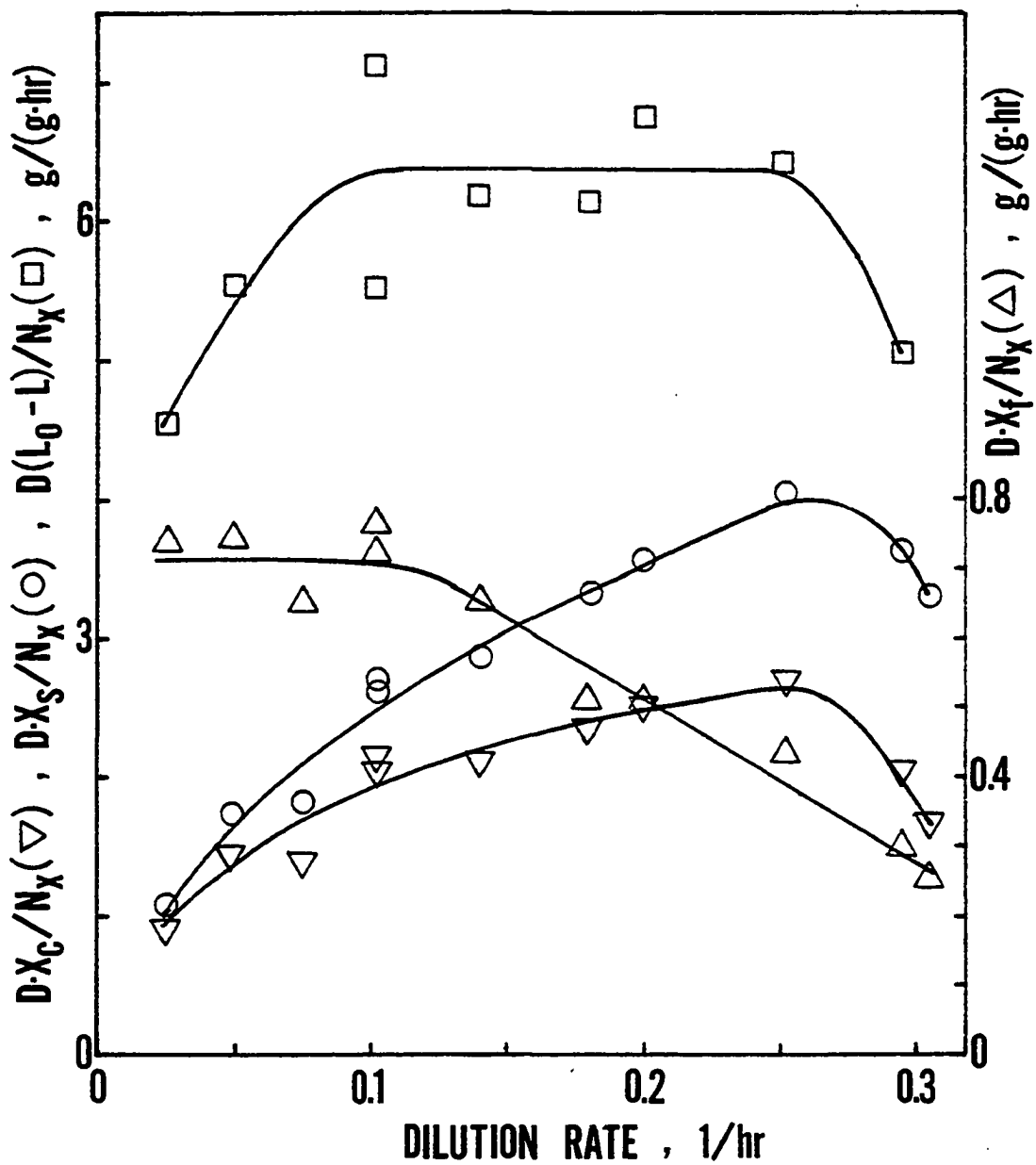
D·Xc/Nx(▽) , D·Xs/Nx(○) , D(Lo-L)/Nx(□) , g/(g·hr)
D·Xf/Nx(△) , g/(g·hr)
0
3
6
0.4
0.8
0
0.1
0.2
0.3
DILUTION RATE , 1/hr

nonlipid biomass production and lactose utilization. At dilution rates greater than 0.25 1/hr, the specific rate of lactose utilization was slower, corresponding to slower specific rates of lipid and nonnitrogenous nonlipid biomass production. For this dilution rate range, X_f/X_s was roughly 0.1 or slightly smaller (Figure 23).

In the middle range of dilution rates from 0.1 to 0.25 1/hr, the specific rate of lactose utilization is observed to be roughly constant. But at the slower dilution rates in this range, the specific rate of nonnitrogenous nonlipid biomass production was slower while the specific rate of lipid production was faster.

For those dilution rates from 0.026 to 0.1 1/hr, the specific rate of lipid production is observed to be roughly constant. But at slower dilution rates in this range, the specific rate of lactose utilization was slower corresponding with slower specific rates of nonnitrogenous nonlipid biomass production.

From the observed relationships of the specific rates of lipid and nonnitrogenous nonlipid biomass production and lactose utilization, it seems that lactose is utilized only as required for the production of lipid and nonnitrogenous nonlipid biomass. Based on this concept, the roughly constant specific rates of lactose utilization observed between dilution rates of 0.1 and 0.25 1/hr can be interpreted as resulting because the decreased demand for lactose for nonnitrogenous nonlipid biomass production is balanced by the increase in the demand for lactose for lipid production.

Specific rates were also estimated with respect to X_s. The effect of dilution rate on these specific rates is observed in Figure 25. These specific rates can also be considered to be proportional to the rates of production or utilization per cell because of the relatively constant X_s/MCC over the range of dilution rates evaluated (Figure 23).

The rate of production of lipid per cell was, therefore, slightly slower at 0.026 1/hr than it was at 0.295 1/hr. But the rate of utilization of lactose per cell was dramatically slower at 0.026 1/hr than it was at 0.295 1/hr. That X_f/X_s was greater at the slower dilution rates (Figure 23) suggests that a greater percentage of the lactose utilized by the cell at the slower dilution rates was utilized for lipid production.

The rate of lactose utilization per cell is observed in general to be slower at the slower dilution rates (Figure 25). This corresponds to larger X_s/N_x at slower dilution rates (Figure 23). Thus, the decrease in the rate of lactose utilization per cell can be seen to correlate additionally with the decreased nitrogen content per cell. This additional correlation seems reasonable since the nitrogen content per cell is proportional to the concentration of enzymes in a cell. Therefore the decreased nitrogen content per cell would suggest a decreased metabolic activity per cell. Thus in describing the metabolic rates, the concentration of cellular nitrogen would be important rather than the concentration of cells.

Figure 25. Steady-state specific rates of substrate utilization and biomass production at various dilution rates. Specific rates (relative to the nonlipid biomass concentration, X_s) of lipid accumulation, $D \cdot X_f/X_s$ ($\triangle$); and uptake of lactose, $D(L_o - L)/X_s$ ($\square$); and of extracellular nitrogen, $D(N_o - N)/X_s$ ($\bigcirc$). The specific rate (relative to the total biomass concentration, X) of extracellular nitrogen uptake, $D(N_o - N)/X$ ($\bullet$)

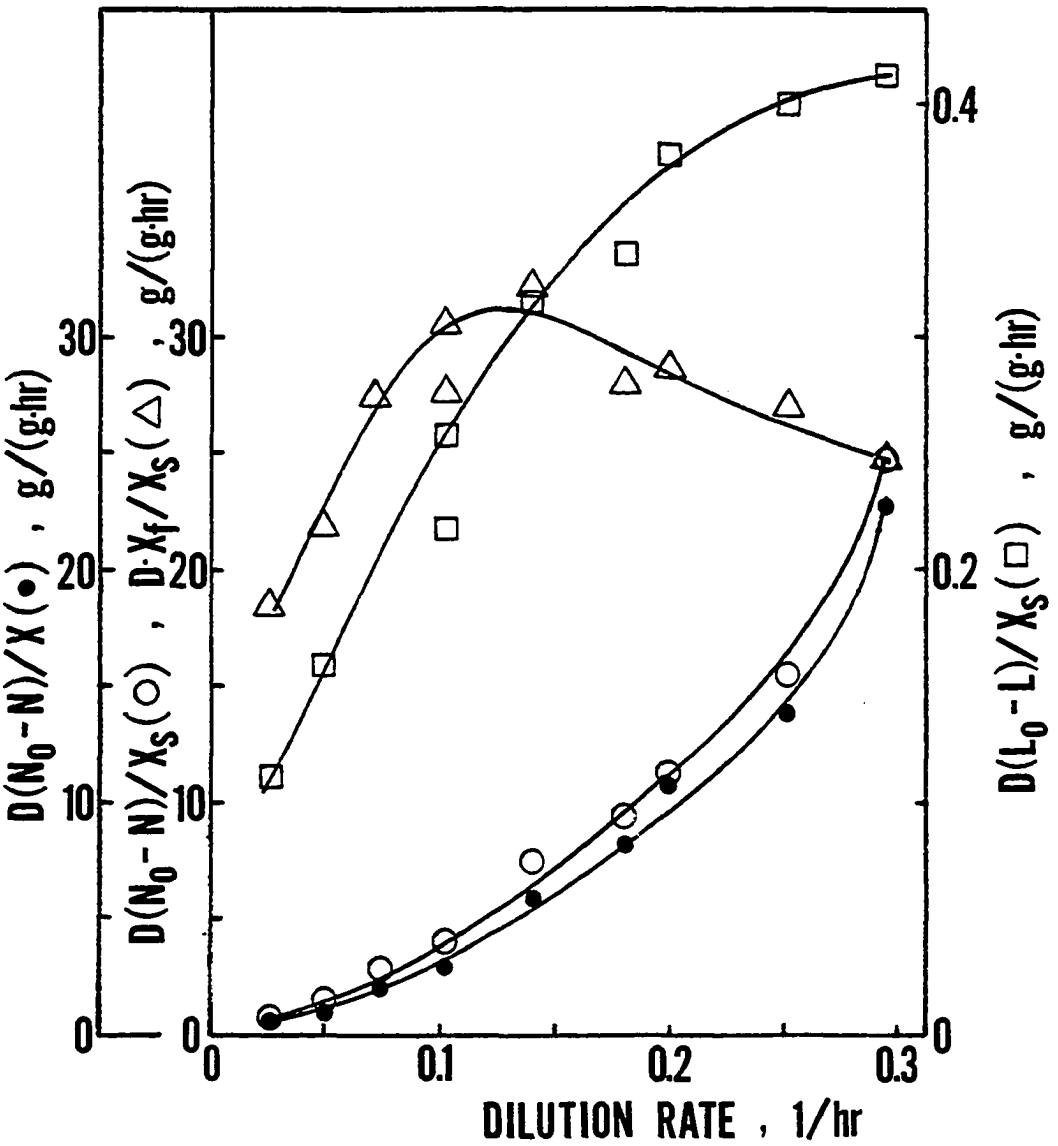
D(N0-N)/X(●) , g/(g·hr)
D(N0-N)/Xs(○) , D·Xf/Xs(△) , g/(g·hr)
D(L0-L)/Xs(□) , g/(g·hr)
0
10
20
30
0.1
0.2
0.3
0.4
DILUTION RATE , 1/hr

This observed relationship between the rate of lactose utilization per cell and X_s/N_x suggests caution should be exercised in drawing correlations between specific rates relative to X_s and specific rates relative to N_x. These correlations may not be valid if X_s/N_x changes significantly over the different conditions to which the correlation is applied. Such a correlation has however been drawn by Boulton and Ratledge (1981) and Evans and Ratledge (1983b) when comparing the specific rates (relative to X_s) of lipid synthesis to the specific activities (relative to extracted cell protein) of enzymes such as ATP:citrate lyase. And because the study of Evans and Ratledge (1983b) was also conducted on C. curvata D, it is quite likely that the ratio of nonlipid biomass to cellular nitrogen in their study changed with the dilution rate as observed in this study (Figure 23).

The specific rates of nitrogen utilization expressed with respect to X_s or expressed with respect to the concentration of total biomass (X) are observed in Figure 25 to be similar: both specific rates decreased nonlinearly with a decrease in dilution rate. The nonlinear relationship between the specific rate expressed with respect to X_s and dilution rate resulted because X_s/N_x was greater at slower dilution rates (Figure 23). This same effect of dilution rate on X_s/N_x has been observed by other investigators (Almazan et al., 1981; Choi et al., 1982). In contrast, Yoon and Rhee (1983) observed that in their study of an oleaginous yeast the specific

rate of nitrogen utilization expressed with respect to X decreased linearly with a decrease in dilution rate. Thus, it can be inferred that the relationship observed in this study between dilution rate and the specific rates of nitrogen utilization (relative to X_s or relative to X) does not hold for all oleaginous yeast.

Characteristics of growth and lipid accumulation of C. curvata D

Several characteristics of growth and lipid accumulation of C. curvata D were evident from the evaluation of the batch and continuous fermentations. The nonlipid biomass concentration was observed to be proportional to the concentration of cells (Figures 15 and 23). The percentage of the nonlipid biomass estimated as nitrogenous compounds changed dramatically during the course of the batch fermentation (Figure 15) and was affected dramatically by the dilution rate in the continuous fermentations (Figure 23). The nonlipid biomass seemed to be limited by the concentration of cellular nitrogen (Figure 15).

Cellular nitrogen seemed to represent the catalytic element in the nonlipid biomass. The dramatic increase in the specific rate of lipid accumulation in the batch fermentation corresponded with the increase in the specific activity of enzymes required for fatty acid synthesis as reported by Evans and Ratledge (1983b). Thus, the increase in the specific rate of lipid accumulation seemed to indicate an increased flux of metabolites through the fatty acid synthesis pathway. The increase in this specific rate seemed to be caused by

a combination of the decrease in the specific rate of demand for lactose for nonnitrogenous nonlipid biomass accumulation and a constant specific rate of lactose uptake. This suggested causal relationship was consistent with the presently accepted biochemical mechanism of fatty acid synthesis. After the attainment of a maximum and constant specific rate of lipid accumulation, further decreases in the specific rate of nonnitrogenous nonlipid biomass accumulation corresponded with the decrease in the specific rate of lactose uptake. The combined decreases in these specific rates also indicated that metabolites were not accumulated by this yeast.

Similar relationships were observed for the continuous fermentations between the specific rates (relative to N_x) of lactose utilization and nonnitrogenous nonlipid biomass and lipid production. Faster specific rates of lipid production corresponded with slower specific rates of nonnitrogenous nonlipid biomass production at slower dilution rates in the range of 0.1 to 0.25 1/hr (Figure 24). The specific rate of lactose utilization was observed to be constant over this range of dilution rates. A maximum and constant specific rate of lipid production was observed from 0.026 to 0.1 1/hr. Both specific rates of nonnitrogenous nonlipid biomass production and lactose utilization were slower at the slower dilution rates of this range.

This yeast seemed to display two characteristics which were similar to other oleaginous yeast. First, during the initial accumulation of nonlipid biomass in the batch fermentation, the ratio of lipid to

nonlipid biomass was essentially constant (Figure 12). Second, at the end of the batch fermentation, the fraction of nonlipid biomass estimated as nitrogenous compounds ($N_x \times 5.4$), was similar to the reported estimated protein ($N \times 6.25$) content of the nonlipid biomass for other oleaginous yeast (Table 7).

This yeast seemed to also display two characteristics which not all oleaginous yeasts seemed to display. First, the major increases as observed in the batch fermentation for the concentration of cellular nitrogen, nonlipid biomass, and lipid seemed somewhat sequential rather than concurrent (Figures 10 and 11). Second, lactose seemed to be converted to lipid during lipid accumulation without the additional accumulation of metabolites (Figure 18).

These characteristics of C. curvata D obtained from batch and continuous fermentations seemed to shed additional light on the presently accepted biochemical mechanism for lipid accumulation. The biochemical mechanism has been summarized in the Literature Review. In this mechanism, two primary points of control of lipid accumulation are evident and both are controlled by the energy state of the cell. One of these control points is at NAD^+:isocitrate dehydrogenase (ICDH). Located in the mitochondria, this enzyme controls the flux through the Krebs cycle of carbon compounds originating from citrate. Therefore, this enzyme can be thought to be controlling the rate of energy production by the Krebs cycle. This enzyme has been shown to be inhibited by a high energy state of adenosine

phosphates which evidently occurs in the oleaginous yeast cell during lipid accumulation (Botham and Ratledge, 1979). The other major control point is considered to be at the L-malate/citrate translocase (MCT). Located in the mitochondrial membrane, this translocase has been shown to be activated by a high energy state of adenosine phosphates (Evans et al., 1983b).

The specific rate of nonnitrogenous nonlipid biomass accumulation can therefore be shown to be inversely controlling the specific rate of lipid accumulation by assuming that energy derived from the Krebs cycle is used predominantly for the accumulation of nonnitrogenous nonlipid biomass. Figure 26 summarizes this concept in which nonnitrogenous nonlipid biomass accumulation is represented by carbohydrate synthesis. In essence, the specific rate of carbohydrate synthesis can be assumed to influence the specific rate of lipid synthesis through its demand on energy produced by the mitochondria. Therefore, a decrease in the specific rate of carbohydrate synthesis would result in an increase in the energy state of the cell, inhibiting ICDH and activating MCT. And by increasing the flux of citrate into the cytosol, the specific rate of lipid synthesis would increase. This assumes that the specific activities of the enzymes of fatty acid synthesis are sufficient to handle the increase in the flux of citrate into the cytosol.

The maximum specific rate of lipid synthesis would result when the increasing flux of carbon substrate reached the maximum capacity

Figure 26. Overall biochemical pathways of lactose utilization for carbohydrate and lipid synthesis. Energy produced in the mitochondria is considered to be utilized for carbohydrate synthesis. Cell membrane (1); mitochondrial cell membrane (2); NAD^+:isocitrate dehydrogenase (3); L-malate/citrate translocase (4); membrane translocases (⫲→); enzyme activation (⊕→); enzyme inhibition (⊖→)

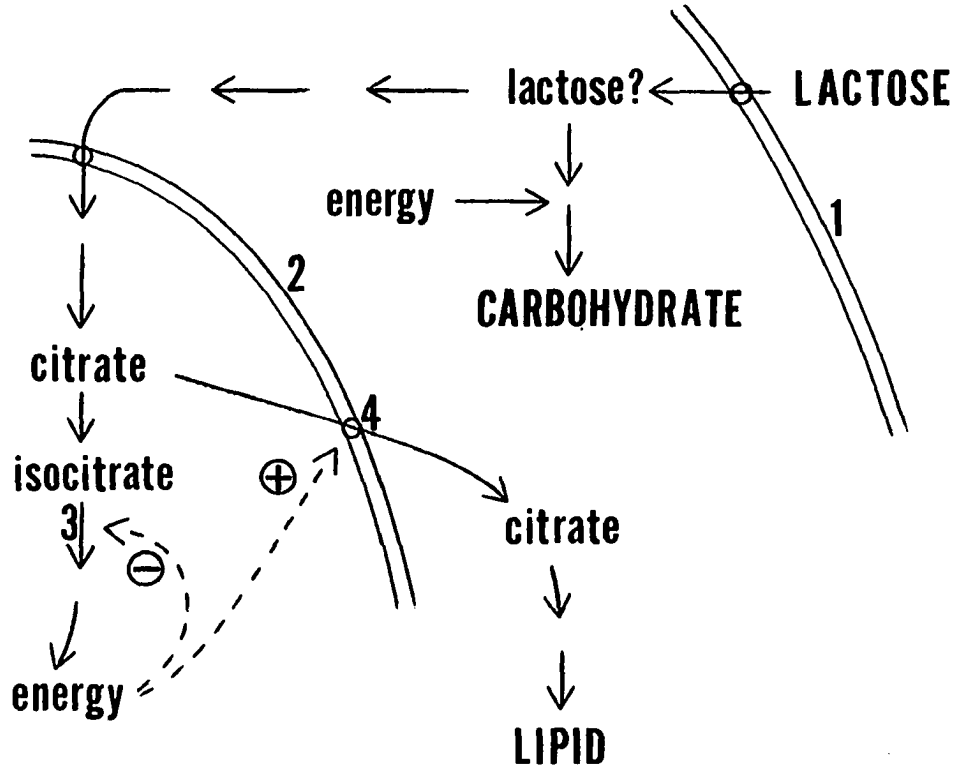
lactose?
LACTOSE
energy
1
2
CARBOHYDRATE
citrate
4
isocitrate
3
citrate
energy
LIPID

of the metabolic pathways leading to fatty acid synthesis. In particular, ATP:citrate lyase has been suggested as the rate-limiting enzyme for fatty acid synthesis in oleaginous yeast (Boulton and Ratledge, 1981). After a maximum specific rate of lipid synthesis is attained, further reductions in the specific rate of carbohydrate synthesis would effect, via feedback inhibition, a proportional decrease in the specific rate of lactose uptake (Smith et al., 1983). This feedback inhibition mechanism would prevent the excessive accumulation of intracellular metabolites.

Synthesis of enzymes essential to fatty acid synthesis has been suggested by Evans and Ratledge (1983b) to occur during the transition to lipid accumulation in batch fermentations. Intracellular citrate was not observed to accumulate excessively during this transitional period (Evans and Ratledge, 1983b). It therefore seems reasonable to consider that the increase in the specific activity of these enzymes kept pace with the increase in the flux of metabolites into the pathway for fatty acid synthesis. Therefore, it is more likely that the increase of the specific rate of lipid accumulation observed during the batch fermentation is the result of a constant specific rate of lactose uptake occurring in conjunction with a decreasing specific rate of demand for lactose for nonnitrogenous nonlipid biomass accumulation.

Model Development

Nitrogen

In the batch fermentation, nitrogen uptake was observed immediately after the inoculation of the fermenter (Figure 11). In the first 11 hr, the cellular nitrogen concentration increased exponentially (Figure 14). After 11 hr, the specific rate of this cellular nitrogen accumulation decreased dramtically. Overall, the decrease in the specific rate did not seem to be linearly related to the decrease in the utilizable, extracellular nitrogen concentration.

Accumulation of cellular nitrogen primarily resulted from the uptake of amino acids in the fermentation broth. Since the uptake of amino acids has been shown to occur by active transport, the dependence of the rate of amino acid uptake on the concentration of amino acids in the fermentation broth can be described by Michaelis-Menten kinetics (Schultz et al., 1974). The rate of amino acid uptake is also dependent on the rate the absorbed amino acids are being utilized internally by the cell (Smith et al., 1983). This multiple control of the rate of amino acid uptake is similar to the multiple control of substrate utilization as described by Dabes et al. (1973). The concepts of their model are summarized in the Literature Review. Therefore, the 3-parameter model as proposed by them was used to describe the specific rate of cellular nitrogen accumulation as a function of the utilizable extracellular nitrogen

concentration, N_u. It follows that

$$N_u = N - N_b = \mu_1(A + B/(\mu_{m1} - \mu_1)) \tag{12}$$

or

$$\mu_1 = \frac{-1}{2}\left(\mu_{m1} + \frac{N_u + B}{A} + \left(\left(\mu_{m1} + \frac{N_u + B}{A}\right)^2 - \frac{4\mu_{m1} \cdot N_u}{A}\right)^{\frac{1}{2}}\right) \tag{13}$$

where N is the extracellular nitrogen concentration, g/l; N_b is the concentration of nonutilizable extracellular nitrogen, g/l; μ_1 is the specific rate of cellular nitrogen accumulation, 1/hr; μ_{m1} is the maximum specific rate of cellular nitrogen accumulation, 1/hr; A is the inverse of the first order rate dependence on N_u of μ_1, g·hr/l; and B is a saturation parameter, g/l.

Specific rates were expressed with respect to N_x, because N_x was considered to represent the enzyme or rate-determining portion of the cell. It follows that

$$\mu_1 = \frac{1}{N_x}\frac{dN_x}{dt} = \frac{1}{N_x}\frac{d(N_{uo} - N_u)}{dt} = \frac{-1}{N_x}\frac{dN_u}{dt} \tag{14}$$

where N_{uo} is the total concentration of utilizable nitrogen in the medium, g/l; and N_x is the cellular nitrogen concentration, g/l. Although the nitrogen from yeast extract represented a mixture of nitrogenous compounds, the utilizable extracellular nitrogen was treated as one entity.

Nonlipid biomass

In the batch fermentations, cellular nitrogen accumulation largely preceded nonlipid biomass accumulation (Figures 10 and 11).

Thus, the accumulation of nonlipid biomass could be considered to result from two sequential but somewhat overlapping events: first, the absorption of nitrogenous compounds, and second, the accumulation of nonnitrogenous nonlipid biomass. The total nonlipid biomass in the batch fermentations seemed to be limited also by the cellular nitrogen concentration (Figure 15).

From these observations, the equation describing the specific rate of nonlipid biomass accumulation can be constructed as

$$\frac{1}{N_x}\frac{dX_s}{dt} = \alpha \cdot \mu_1 + \frac{\mu_{m2}(1 - \mu_1/\mu_{m1})^n}{\left(1 + \frac{k_i}{\left(1 - \frac{X_s}{K \cdot N_x}\right)}\right)\left(1 + \frac{K_L}{L}\right)} \qquad (15)$$

where X_s is the nonlipid biomass concentration, g/l; α is the contribution to the nonlipid biomass resulting from the accumulation cellular nitrogen; μ_{m2} is the maximum specific rate of nonnitrogenous nonlipid biomass accumulation, proportional to N_x, 1/hr; n is an exponential factor; k_i is a saturation parameter determining the asymptotic approach of X_s/N_x to its maximum value, K; K_L is the saturation parameter for active transport of lactose into the cell, g/l; and L is the lactose concentration in the fermentation broth, g/l.

To reflect that the major increase in X_s followed the increase in N_x, the function $(1-\mu_1/\mu_{m1})^n$ was introduced. The function stated that as μ_1 decreased and deviated from μ_{m1}, the specific rate

of nonnitrogenous nonlipid biomass accumulation would be increased. The inclusion of the function $(1 + K_L/L)^{-1}$ in Equation (15) indicated that the uptake of lactose was by active transport and was required for nonnitrogenous nonlipid biomass accumulation.

Lactose

Lactose was required only for the accumulation of nonnitrogenous nonlipid biomass and lipid. The specific rate of lactose consumption could be considered to occur in three phases. The first phase is characterized by the lactose consumption in the first 13 hr of the batch fermentation during which the specific rate of nonnitrogenous nonlipid biomass accumulation was estimated as initially zero and then increasing (Figure 18), and the ratio of lipid to nonlipid biomass was roughly constant (Figure 12). Lactose during this period could be considered to be consumed at a rate proportional to the rates of accumulation of both nonnitrogenous nonlipid biomass and lipid (Figure 18).

In the second phase, the specific rate of lactose uptake was suggested to be maintained at a constant specific rate because a decrease in the demand for lactose for nonnitrogenous nonlipid biomass accumulation was compensated by an increase in the demand for lactose for lipid accumulation. This relationship between these specific rates is evident in the batch fermentations from 15 to 24 hr (Figure 18) and in the continuous fermentations between the dilution rates of 0.10 and 0.25 1/hr (Figure 24).

In the third phase, lipid accumulation was occurring at a maximum and constant specific rate, while the specific rate of nonnitrogenous nonlipid biomass accumulation continued to decrease (Figure 18). The lactose consumption rate during this phase was again proportional to the rates of accumulation of both nonnitrogenous nonlipid biomass and lipid.

The first phase of lactose consumption, $\left(\frac{-1}{N_x}\frac{dL}{dt}\right)_1$, can be described as

$$\left(\frac{-1}{N_x}\frac{dL}{dt}\right)_1 = \frac{1}{Y_1(1 + K_L/L)}\left((\alpha - \beta)\mu_1 + \frac{\mu_{m2}(1 - \mu_1/\mu_{m1})^n}{1 + k_i/(1 - \alpha/K)}\right)$$

$$+ \frac{\gamma}{Y_2(1 + K_L/L)}\left(\alpha\cdot\mu + \frac{\mu_{m2}(1 - \mu_1/\mu_{m1})^n}{1 + k_i/(1 - \alpha/K)}\right) \qquad (16)$$

where β represents the mass to nitrogen ratio of the nitrogenous compounds absorbed by the cell, γ represents the mass ratio of lipid to nonlipid biomass which was observed to be constant during this phase of lactose consumption, $1/Y_1$ is the grams of lactose required per gram of nonnitrogenous nonlipid biomass accumulated, and $1/Y_2$ is the grams of lactose required per gram of lipid accumulated.

The first term of Equation (16) describes the demand for lactose for the accumulation of nonnitrogenous nonlipid biomass. The second term of Equation (16) describes the demand for lactose for lipid accumulation during the first phase of lactose consumption when X_f/X_s was observed to be constant. In Equation (16), X_s/N_x was approximated by α in the function describing the asymptotic

approach of X_s/N_x to K. This was considered to introduce, at most, a 10% error into Equation (16) because of the type of function into which α was substituted and because X_s/N_x remained considerably removed from its final value of K during the first phase of lactose consumption (Figure 15). This substitution simplified the description of the second phase of lactose absorption.

The peaking in the specific rate of nonnitrogenous nonlipid biomass accumulation can be considered to initiate the transition from the first to the second phase of lactose consumption. The resulting maximum for Equation (16) would describe the second phase of lactose consumption. Estimating this maximum was further simplified because, at the transition from the first to the second phase of lactose consumption, the lactose concentration would be so much greater than K_L that the function $(1 + K_L/L)^{-1}$ would approximate unity. By setting the first derivative with respect to μ_1/μ_{m1} of Equation (16) equal to zero and solving for μ_1/μ_{m1}, the value of μ_1/μ_{m1} at which Equation (16) has a maximum can be determined as follows

$$\left(\frac{\mu_1}{\mu_{m1}}\right)_{max} = 1 - \left(\frac{\mu_{m1} \left(\frac{\alpha - \beta}{Y_1} + \frac{\alpha \cdot \gamma}{Y_2}\right)\left(1 + \frac{k_i}{1 - \alpha/K}\right)}{n \cdot \mu_{m2} \quad (1/Y_1 + \gamma/Y_2)} \right)^{\frac{1}{n-1}} \qquad (17)$$

where $(\mu_1/\mu_{m1})_{max}$ is the value of μ_1/μ_{m1} at which Equation (16) has a maximum. Equation (17) indicates $(\mu_1/\mu_{m1})_{max}$ would be less than one

and could be negative, since the parameters can only be positive. If $(\mu_1/\mu_{m1})_{max}$ is calculated to be negative, Equation (16) is maximum at a value of zero for μ_1/μ_{m1}, since μ_1/μ_{m1} cannot be negative.

The second derivative of Equation (16) with respect to μ_1/μ_{m1} indicates the conditions under which $(\mu_1/\mu_{m1})_{max}$ determines a maximum for Equation (16). Again $(1 + K_L/L)^{-1}$ was approximated as one.

$$\frac{d^2\left(\frac{1}{N_x}\frac{dL}{dt}\right)_1}{d(\mu_1/\mu_{m1})^2} = \frac{(1/Y_1 + \gamma/Y_2)\mu_{m2}\cdot n(n-1)(1-(\mu_1/\mu_{m1})_{max})^{n-2}}{1 + k_{i2}/(1-\alpha/K)} \quad (18)$$

A negative value for Equation (18) is required for Equation (16) to have a maximum. Equation (18) is only negative when n is between 0 and 1.

Thus, the specific rate of lactose consumption during the second phase, $\left(\frac{-1}{N_x}\frac{dL}{dt}\right)_2$, can be described as follows when $(\mu_1/\mu_{m1})_{max}$ is calculated as positive.

$$\left(\frac{1}{N_x}\frac{dL}{dt}\right)_2 = \frac{1}{1 + K_L/L}\left(\left(\frac{\alpha-\beta}{Y_1} + \frac{\alpha\cdot\gamma}{Y_2}\right)\mu_1 + \left(\frac{1}{Y_1} + \frac{\gamma}{Y_2}\right)\frac{\mu_{m2}(1-(\mu_1/\mu_{m1})_{max})^n}{1 + k_i/(1-\alpha/K)}\right) \quad (19)$$

where $(\mu_1/\mu_{m1})_{max}$ is between 0 and 1.

The specific rate of lactose consumption during the third phase $\left(\frac{-1}{N_x}\frac{dL}{dt}\right)_3$, can be described as

$$\left(\frac{-1}{N_x}\frac{dL}{dt}\right)_3 = \frac{1}{Y_1}\left(\frac{1}{N_x}\frac{dX_s}{dt} - \beta\cdot\mu_1\right) + \frac{\mu_{m3}}{Y_2(1 + K_L/L)} \quad (20)$$

where μ_{m3} is the maximum specific rate of lipid accumulation, 1/hr.

The first term in Equation (20) describes the demand for lactose for nonnitrogenous nonlipid biomass accumulation and the second term describes the demand for lactose for lipid accumulation.

Equations (16) to (20) were combined as follows to describe the specific rate of lactose uptake.

$$\frac{-1}{N_x}\frac{dL}{dt} = \begin{cases} \left(\frac{-1}{N_x}\frac{dL}{dt}\right)_1 ; & \text{or} \begin{cases} \frac{\mu_1}{\mu_{m1}} \geqslant \left(\frac{\mu_1}{\mu_{m1}}\right)_{max} > 0 \\ \text{and} \begin{cases} \left(\frac{\mu_1}{\mu_{m1}}\right)_{max} \leqslant 0 \\ \left(\frac{-1}{N_x}\frac{dL}{dt}\right)_3 > \left(\frac{-1}{N_x}\frac{dL}{dt}\right)_1 \end{cases} \end{cases} & (21a) \\ \left(\frac{-1}{N_x}\frac{dL}{dt}\right)_2 ; & \text{and} \begin{cases} \left(\frac{\mu_1}{\mu_{m1}}\right)_{max} > \frac{\mu_1}{\mu_{m1}} \geqslant 0 \\ \left(\frac{-1}{N_x}\frac{dL}{dt}\right)_3 > \left(\frac{-1}{N_x}\frac{dL}{dt}\right)_2 \end{cases} & (21b) \\ \left(\frac{-1}{N_x}\frac{dL}{dt}\right)_3 ; & \text{or} \begin{cases} \text{and} \begin{cases} \left(\frac{\mu_1}{\mu_{m1}}\right)_{max} > \frac{\mu_1}{\mu_{m1}} \geqslant 0 \\ \left(\frac{-1}{N_x}\frac{dL}{dt}\right)_3 \leqslant \left(\frac{-1}{N_x}\frac{dL}{dt}\right)_2 \end{cases} \\ \text{and} \begin{cases} \left(\frac{\mu_1}{\mu_{m1}}\right)_{max} \leqslant 0 \\ \left(\frac{-1}{N_x}\frac{dL}{dt}\right)_3 \leqslant \left(\frac{-1}{N_x}\frac{dL}{dt}\right)_1 \end{cases} \end{cases} & (21c) \end{cases}$$

In principle, the specific rate of lactose consumption is

determined by the slowest of the specific rates as calculated by Equations (21a) to (21c). This is to reflect the fact that lactose is consumed by the cell only to meet the demand for the accumulation of lipid and nonnitrogenous nonlipid biomass.

Lipid

Based on the previous developments, the specific rate of lipid accumulation can be described as

$$\frac{1}{N_x}\frac{dX_f}{dt} = Y_2\left(\frac{-1}{N_x}\frac{dL}{dt} - \frac{1}{Y_1}\left(\frac{1}{N_x}\frac{dX_s}{dt} - \beta\cdot\mu_1\right)\right) \qquad (22)$$

where X_f is the lipid concentration, g/l. The specific rate of lipid accumulation is proportional to the difference between the specific rates of lactose consumption and the demand for lactose for nonnitrogenous nonlipid biomass accumulation.

Evaluation of Model

The proposed model consisted of a set of ordinary first-order differential equations containing 15 parameters. The model can be verified by comparing the predicted N, L, X_s, X_f and N_x with the experimental data.

For the batch fermentations, this required numerical integration of the set of differential equations and some estimates of the parameters. Estimates of the 15 parameters were obtained by using a simplex-pattern search which minimized the sum of squares of the differences between the predicted and experimental values. This is

described in the Materials and Methods. The estimates of the parameters determined by this procedure are presented in Table 8. The predicted and observed X_s, X_f, and L for batch 1 and 2 are compared in Figures 27 and 28, respectively. The period of transition from growth to lipid accumulation which occurred around 20 hr was well-described by the model. The specific rates of lipid, nonlipid biomass, and nonnitrogenous nonlipid biomass accumulation and lactose uptake predicted by the model are compared in Figure 29 with those calculated from the experimental data. The trends observed for these specific rates are reasonably represented by the model.

The kinetic model was constructed based on the hypothesis that during the transition from growth to lipid accumulation, the specific rate of lipid accumulation increased because of both the decreasing specific rate of demand for lactose for nonnitrogenous nonlipid biomass accumulation and the constant specific rate of lactose uptake. This hypothesis is supported by the good agreement between the model predictions and the observed X_s, X_f, and L during this transitional period at around 20 hr (Figures 27 and 28).

Evans and Ratledge (1983b) measured the specific activity of ATP:citrate lyase at various times during the course of a batch fermentation of C. curvata D. They considered this enzyme to be the rate-controlling enzyme of fatty acid synthesis. The activity of the enzyme was determined in cell-free extracts and dialyzed cell-free extracts. They concluded that a 3-fold increase in the

Table 8. Identified parameters for batch fermentations

Parameter	Units	Estimates	
		Batch 1	Batch 2
μ_{m1}	1/hr	0.59	0.56
A	g•hr/l	0.43	0.55
B	g/l	1.3×10^{-5}	1.3×10^{-5}
N_{uo}	g/l	0.24	0.26
β	g/g	5.7	5.6
α	g/g	5.8	5.7
μ_{m2}	g/(g•hr)	4.4	5.3
n		0.65	0.71
k_i		0.49	0.52
K	g/g	49	42
$1/Y_1$	g/g	1.5	1.4
$1/Y_2$	g/g	3.8	4.1
K_L	g/l	1.9	1.4
γ	g/g	0.076	0.099
μ_{m3}	g/(g•hr)	1.3	1.2

Figure 27. The substrate and biomass concentrations predicted by the model and compared with those observed in batch 1 fermentation. Concentrations of lactose, L(△), extracellular nitrogen, N(▽), nonlipid biomass, X_s(○), and lipid, X_f(□). Model predictions (——)

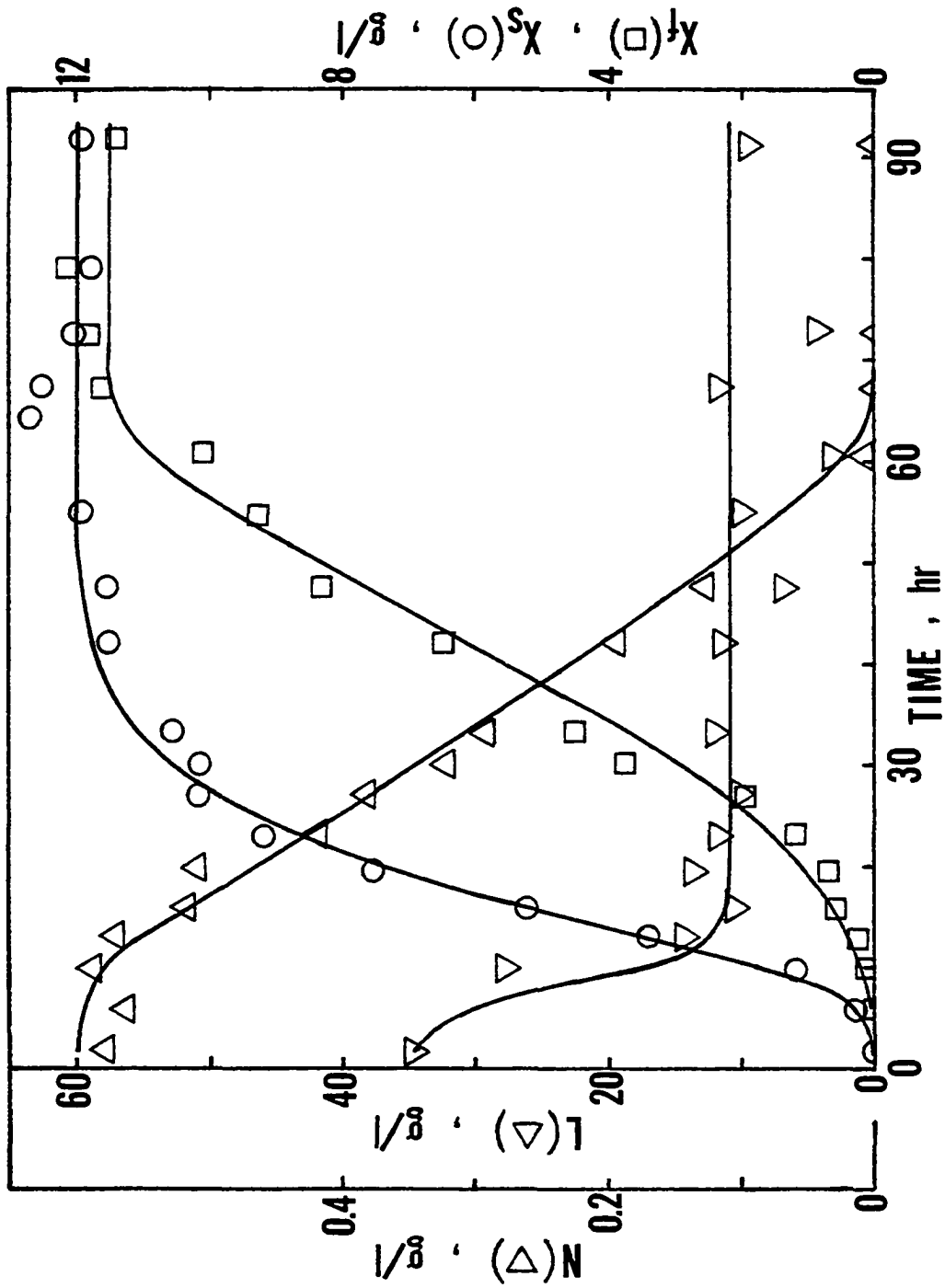
$X_f(\square)$, $X_s(\circ)$, g/l
12
8
4
0
90
60
30
TIME , hr
0
60
40
20
0
$L(\triangle)$, g/l
0.4
0.2
0
$N(\triangle)$, g/l

Figure 28. The substrate and biomass concentrations predicted by the model and compared with those observed in batch 2 fermentation. Concentrations of lactose, L(△), extracellular nitrogen, N(▽), nonlipid biomass, X_s(○), and lipid, X_f(□), and cellular nitrogen, N_x(●). Model predictions (——)

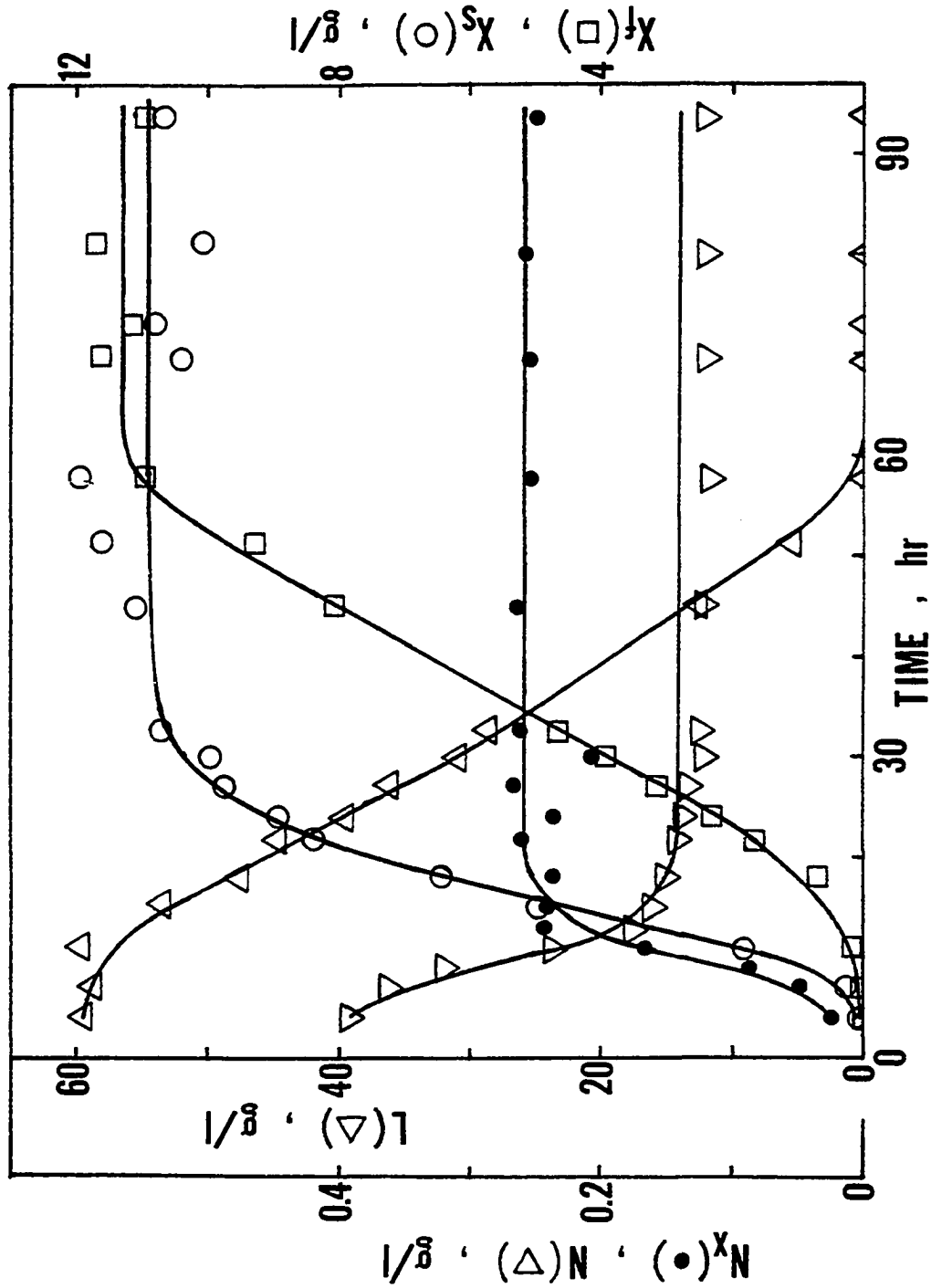
$X_f(\square)$, $X_s(\circ)$, g/l
12
8
4
0
90
60
30
TIME , hr
0
20
40
60
L(△) , g/l
0
0.2
0.4
$N_x(\bullet)$, N(△) , g/l

Figure 29. The specific rates of substrate absorption and biomass accumulation predicted by the model and compared with those calculated from the batch 2 fermentation data. Specific rates of the uptake of lactose, $\frac{-1}{N_x}\frac{dL}{dt}$ ($\triangle$); the accumulation of nonlipid biomass, $\frac{1}{N_x}\frac{dX_s}{dt}$ ($\bigcirc$); nonnitrogenous nonlipid biomass, $\frac{1}{N_x}\frac{dX_c}{dt}$ ($\bullet$); and lipid, $\frac{1}{N_x}\frac{dX_f}{dt}$ ($\bigtriangledown$). Model predictions (——)

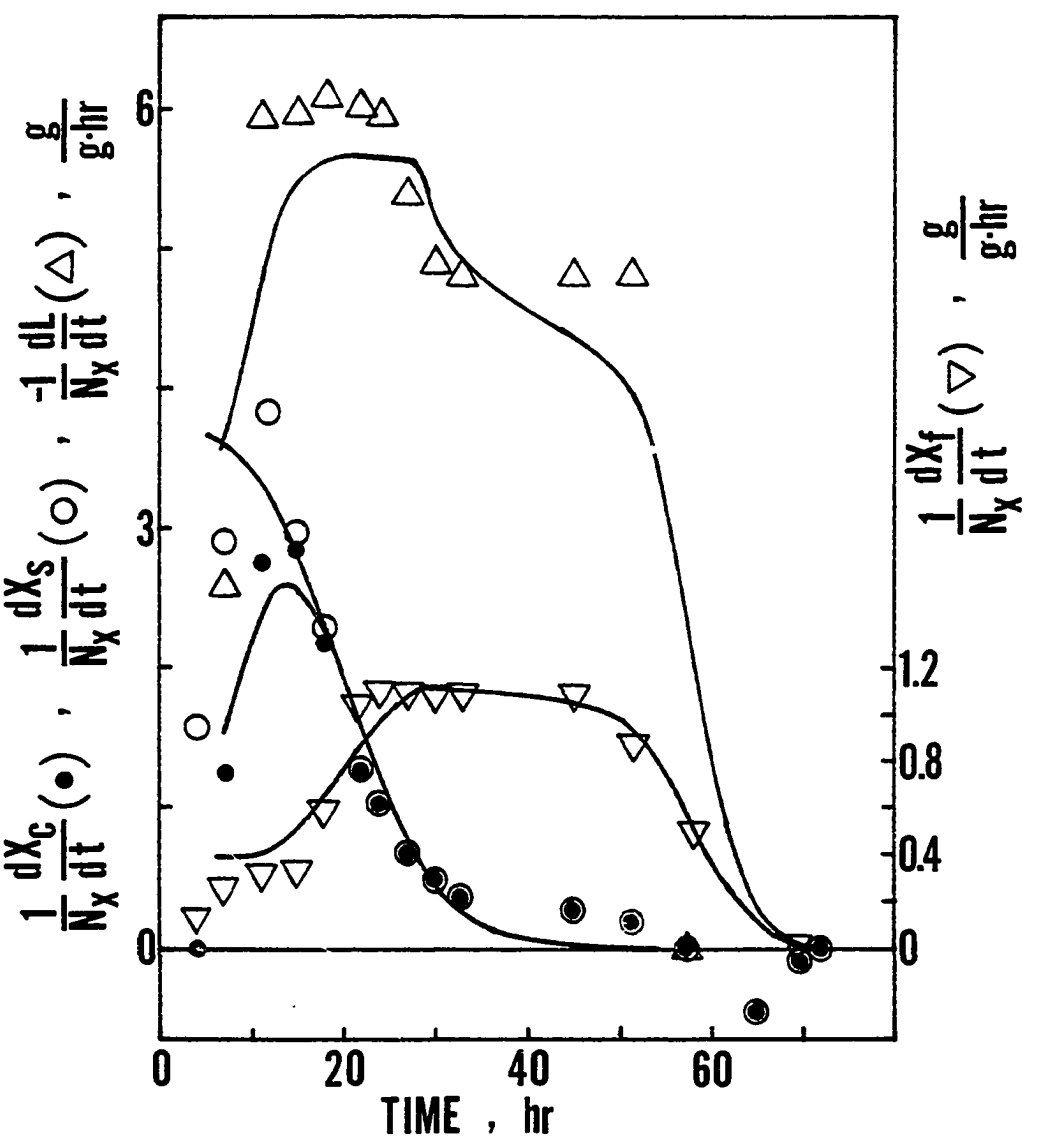
$\frac{1}{N_X}\frac{dX_c}{dt}(\bullet)$, $\frac{1}{N_X}\frac{dX_s}{dt}(\circ)$, $\frac{-1}{N_X}\frac{dL}{dt}(\triangle)$, $\frac{g}{g\cdot hr}$
$\frac{1}{N_X}\frac{dX_f}{dt}(\triangledown)$, $\frac{g}{g\cdot hr}$
6
3
0
1.2
0.8
0.4
0
0
20
40
60
TIME , hr

specific activity of ATP:citrate lyase during the transition from growth to lipid accumulation was "not due to the presence of low molecular weight effectors in the extract and thus was more likely to be due to increased synthesis of the active enzyme." Therefore, it seems reasonable to assume that if synthesis of enzymes such as ATP:citrate lyase is indeed required for the increase in the specific rate of lipid accumulation, the synthesis of these enzymes must be rapid enough so as not to delay the increase in the specific rate of lipid accumulation.

The predicted and observed N for batch 1, and N and N_x for batch 2 are compared in Figures 27 and 28, respectively. The model satisfactorily described changes in these concentrations, although N from batch 2 was slightly overestimated beyond 20 hr.

The specific rates of cellular nitrogen accumulation predicted by the model are compared with those estimated from the data in Figure 30. The model predicted a simple first-order dependence of the specific rate of cellular nitrogen accumulation on the utilizable extracellular nitrogen concentration. This can be seen to be a reasonable approximation of the specific rates estimated from the experimental data.

The parameters obtained from fitting batch 1 and batch 2 are quite similar (Table 8). In general, the estimates for each parameter differ by less than 10%. Such good agreement between the parameter estimates was expected because the two fermentations were considered to be similar.

Figure 30. The relationship between the specific rates of cellular nitrogen accumulation and the extracellular nitrogen concentration, N, predicted by the model and compared with that calculated from batch 2 fermentation data. Specific rates of extracellular nitrogen uptake, $\frac{-1}{N_x}\frac{dN}{dt}$ (O); and cellular nitrogen accumulation, $\frac{1}{N_x}\frac{dN_x}{dt}$ (●). Model predictions (——)

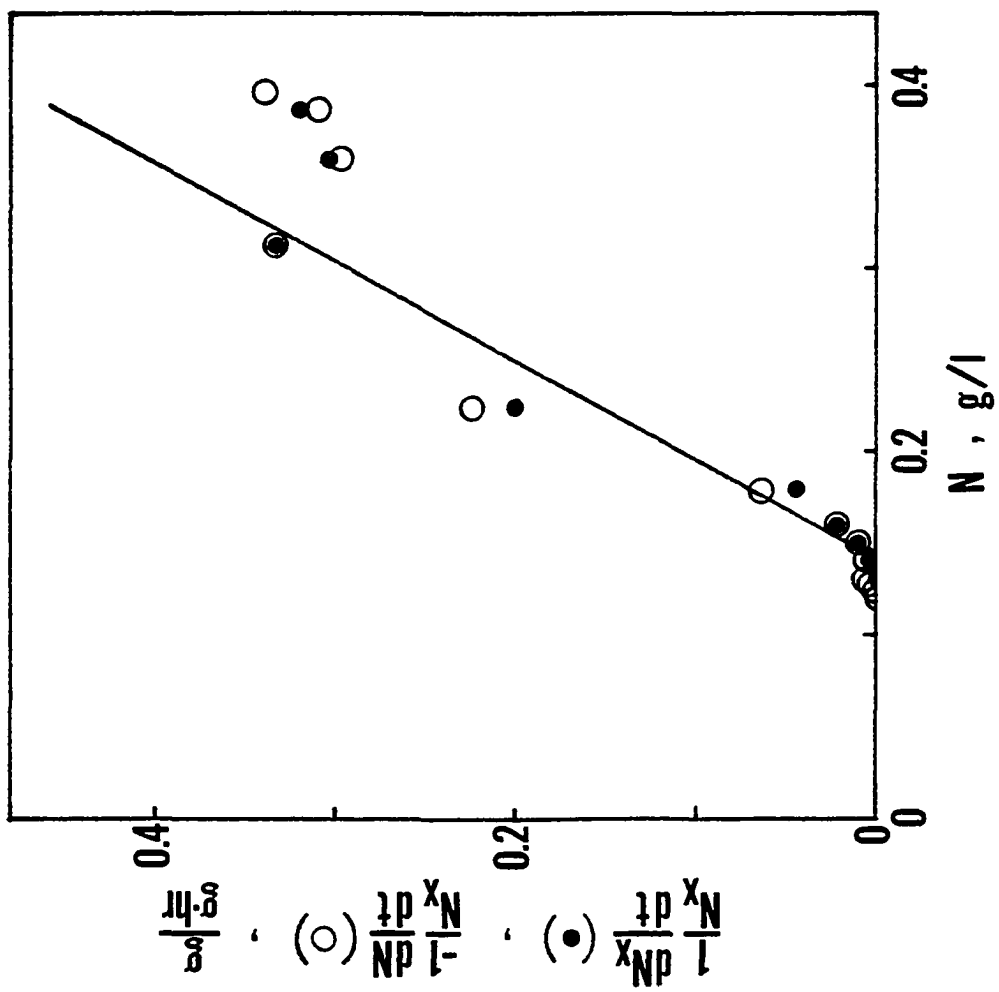
0
0.2
0.4
N , g/l
0
0.2
0.4
$\frac{1}{N_X}\frac{dN_X}{dt}$ (●) , $\frac{-1}{N_X}\frac{dN}{dt}$ (○) , $\frac{g}{g\cdot hr}$

The continuous fermentation data was described with the model developed in the previous section by making a steady-state macroscopic mass balance over the fermenter. The continuous fermentation data was hence described by a set of nonlinear algebraic equations. These were solved for the steady-state concentrations of extracellular nitrogen, cellular nitrogen, nonlipid biomass, lactose, and lipid, and resulted in the following equations:

$$\mu_1 = D \tag{23}$$

$$N = N_b + N_u = N_b + D(A + B/(\mu_{m1} - D)) \tag{24}$$

$$N_x = N_{uo} - N_u \tag{25}$$

$$\begin{aligned} X_s = {} & \frac{N_x}{2}\left(\alpha + K(1 + k_i) + \frac{\mu_{m2}}{D}(1 - D/\mu_{m1})^n\right) \\ & - \frac{N_x}{2}\left(\left(\alpha + K(1 + k_i) + \frac{\mu_{m2}}{D}(1 - D/\mu_{m1})^n\right)^2\right. \\ & \left. - 4K\left(\alpha(1 + k_i) + \frac{\mu_{m2}}{D}(1 - D/\mu_{m1})^n\right)\right)^{1/2} \end{aligned} \tag{26}$$

$$\begin{aligned} L_1 = {} & L_o - N_x\left(\left(\frac{\alpha - \beta}{Y_1} + \frac{\gamma \cdot \alpha}{Y_2}\right)\right. \\ & \left. + \frac{\mu_{m2}(1 - D/\mu_{m1})^n(1/Y_1 + \gamma/Y_2)}{D(1 + k_i/(1 - \alpha/K}\right) \end{aligned} \tag{27}$$

$$\begin{aligned} L_2 = {} & L_o - N_x\left(\left(\left(\frac{\alpha - \beta}{Y_1} + \frac{\gamma \cdot \alpha}{Y_2}\right)\frac{\mu_{m1} \cdot (\mu_1/\mu_{m1})_{max}}{D}\right.\right. \\ & \left.\left. + \frac{\mu_{m2}(1 - (\mu_1/\mu_{m1})_{max})^n(1/Y_1 + \gamma/Y_2)}{D(1 + k_i/(1 - \alpha/K))}\right)\right) \end{aligned} \tag{28}$$

$$L_3 = L_o - \frac{1}{Y_1}(X_s - \beta \cdot N_x) - \frac{N_x \cdot \mu_{m3}}{Y_2 \cdot D} \tag{29}$$

$$L = \begin{cases} L_1 \; ; \; \begin{cases} D/\mu_{m1} \geqslant (\mu_1/\mu_{m1})_{max} > 0 \\ \text{or} \\ (\mu_1/\mu_{m1})_{max} \leqslant 0 \text{ and } L_3 < L_1 \end{cases} & \text{(30a)} \\ L_2 \; ; \; (\mu_1/\mu_{m1})_{max} > D/\mu_{m1} \geqslant 0 \text{ and } L_3 < L_2 & \text{(30b)} \\ L_3 \; ; \; \begin{cases} (\mu_1/\mu_{m1})_{max} > D/\mu_{m1} \geqslant 0 \text{ and } L_3 \geqslant L_2 \\ \text{or} \\ (\mu_1/\mu_{m1})_{max} \leqslant 0 \text{ and } L_3 \geqslant L_1 \end{cases} & \text{(30c)} \end{cases}$$

$$X_f = Y_2(L_o - L - \frac{1}{Y_1}(X_s - \beta \cdot N_x)) \tag{31}$$

where D is the dilution rate, 1/hr; and L_1, L_2, and L_3 estimate the lactose concentration under the specified conditions, g/l.

The parameter K_L was not included in these equations because the lactose concentration was never observed to be less than 10 g/l in the continuous fermentations. The value of $(\mu_1/\mu_{m1})_{max}$ was determined by Equation (17). The dilution rate equaled μ_1 as a result of designating N_x as the basic catalytic element in the development of the model.

Modeling continuous fermentations by making a macroscopic mass balance over the fermenter has been used successfully in describing microbial growth in continuous fermentations resulting from the sequential utilization of two carbon-substrates (Barford and Hall, 1981; Bellgardt et al., 1982; Imanaka et al., 1972; Pamment et al., 1978). Thus, it seems reasonable to use this approach in modeling

the continuous fermentations of this study.

The parameter estimates which provided the best description of the continuous fermentations were determined by using the simplex-pattern search procedure as described in the Materials and Methods. These estimates are presented in Table 9. The model predicts the observed N_x, X_s, X_f, N, and L reasonably well (Figure 31). The specific rates of lactose utilization, and nonlipid biomass and lipid production predicted by the model also exhibit the same trends as those calculated from the data (Figure 32).

The kinetic model has been shown to describe both batch and continuous fermentations. This suggests that the kinetic model satisfactorily represents the kinetics of cellular growth and lipid accumulation for this yeast under the conditions examined for batch and continuous fermentations.

The parameter estimates giving the best description of the continuous fermentations were compared using the t-test with those giving the best description of the batch fermentations (Table 10). The use of the t-test assumed that the estimates were normally distributed about the true value of the parameter. For four of the parameters, the estimates obtained by fitting the continuous fermentations were significantly different from the estimates obtained by fitting the batch fermentations (Table 10). This indicates that a different set of parameter estimates is required to describe the batch fermentations than is required to describe the

Table 9. Identified parameters for continuous fermentations

Parameter[a]	Estimate
μ_{m1}	0.31
A	0.11
B	1.5×10^{-5}
N_{uo}	0.29
β	5.4
α	8.5
μ_{m2}	4.1
n	0.13
k_i	0.66
K	48
$1/Y_1$	1.9
$1/Y_2$	3.8
γ	0.10
μ_{m3}	0.73

[a]The units of the parameters are given in Table 8.

Figure 31. The steady-state substrate and biomass concentrations predicted by the model and compared with those observed in the continuous fermentations. Steady-state concentrations of lactose, L(△); cellular nitrogen, N_x(●); nonlipid biomass, X_s(○); extracellular nitrogen, N(▽); and lipid, X_f(□). Model predictions (——)

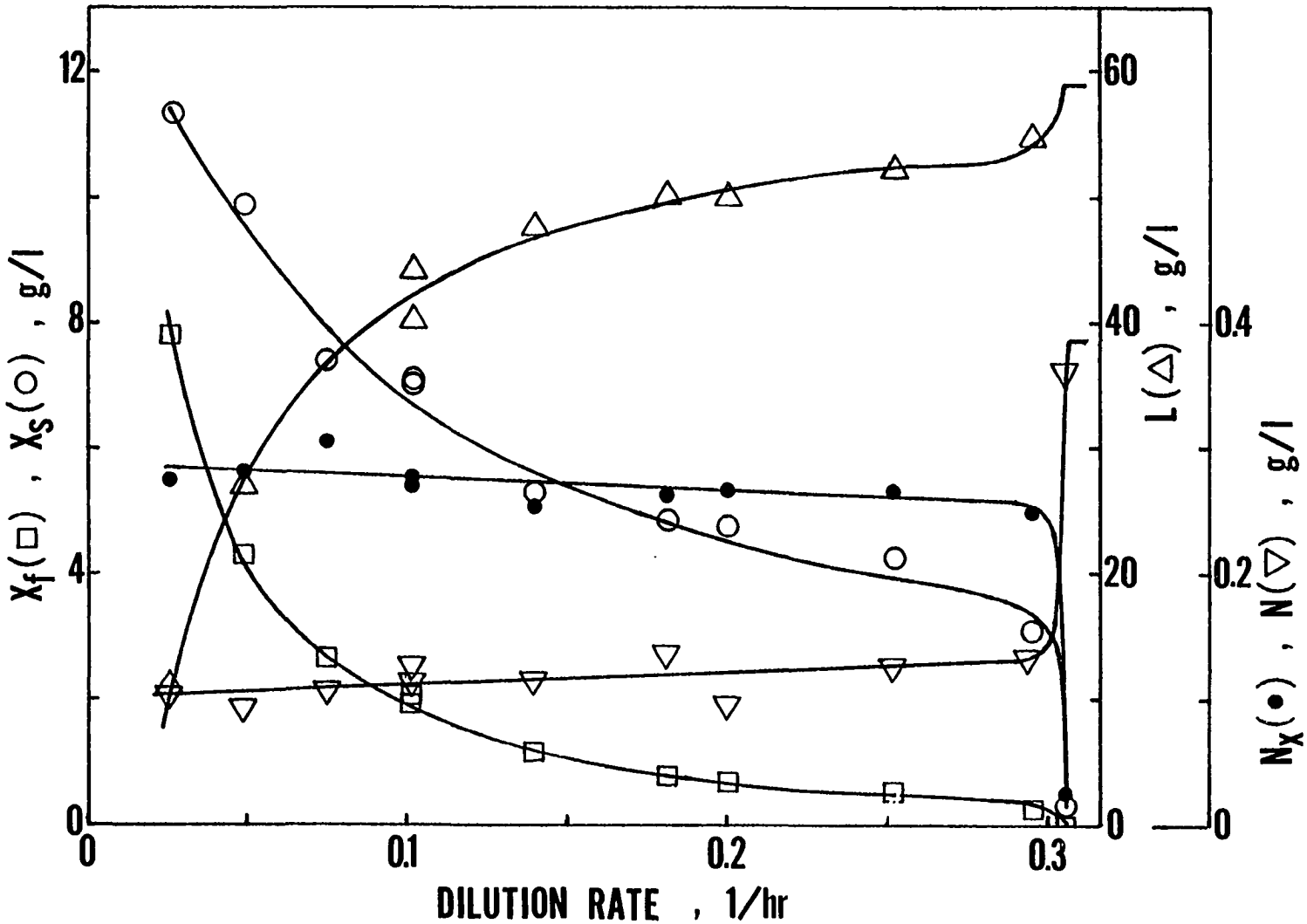
12
8
4
0
0
0.1
0.2
0.3
60
40
20
0
0.4
0.2
0
$X_f(\square)$, $X_S(\bigcirc)$, g/l
L(△) , g/l
$N_X(\bullet)$, N(▽) , g/l
DILUTION RATE , 1/hr

Figure 32. Steady-state specific rates of substrate utilization and biomass production predicted by the model and compared with those calculated from the continuous fermentation data. Specific rates of lactose uptake, $D(L_o - L)/N_x$ ($\triangle$); and the accumulation of nonlipid biomass, $D \cdot X_s/N_x$ (O); and lipid, $D \cdot X_f/N_x$ ($\square$). Model predictions (——)

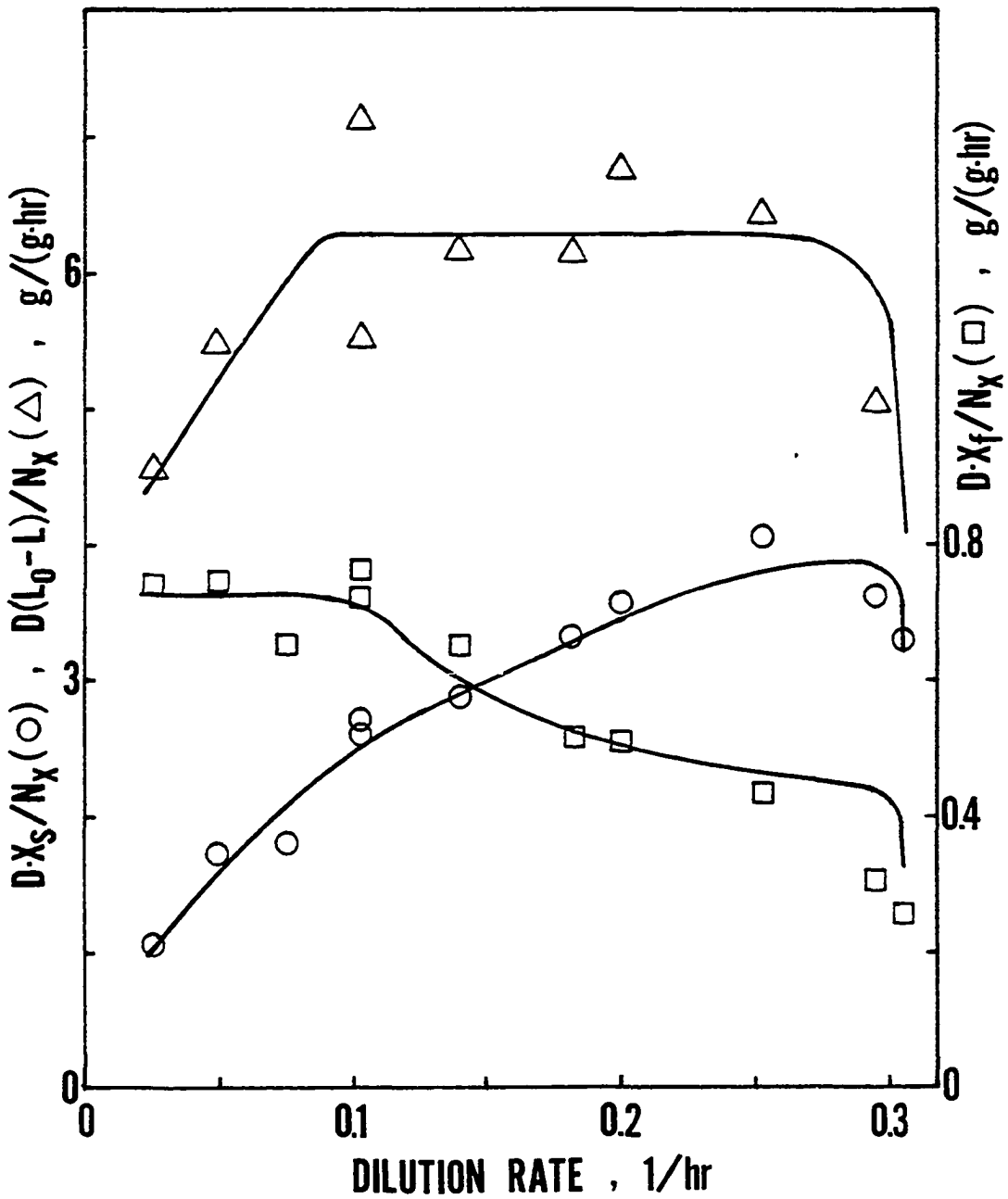
D·Xs/Nx(○) , D(L0-L)/Nx(△) , g/(g·hr)
D·Xf/Nx(□) , g/(g·hr)
6
3
0
0.8
0.4
0
0
0.1
0.2
0.3
DILUTION RATE , 1/hr

Table 10. Comparison of the identified parameters for continuous fermentations with the identified parameters for batch fermentations

Parameter[a]	Estimate		
	Batch		Continuous
	Average	(SD[b])	
μ_{m1}	0.58	(0.018)	0.31*
A	0.49	(0.085)	0.10
B	1.3×10^{-5}	(2.1×10^{-7})	1.5×10^{-5}
N_{uo}	0.25	(0.010)	0.29
β	5.6	(0.068)	5.4
α	5.7	(0.079)	8.5*
μ_{m2}	4.9	(0.64)	4.1
n	0.68	(0.042)	0.13*
k_i	0.51	(0.022)	0.66*
K	46	(4.8)	48
$1/Y_1$	1.4	(0.13)	1.9
$1/Y_2$	4.0	(0.24)	3.8
K_L	1.6	(0.37)	--[c]
γ	0.088	(0.017)	0.10
μ_{m3}	1.2	(0.088)	0.73

[a] The units of the parameters are given in Table 8.

[b] Standard deviation of estimates.

[c] Parameter was not estimated from continuous fermentation data.

* $p < 0.10$.

continuous fermentations. Other investigators have also observed this when using one kinetic model to describe microbial growth resulting from the sequential utilization of glucose and ethanol in either batch or continuous fermentations (Barford and Hall, 1981; Pamment et al., 1978).

The significant differences between certain parameter estimates in Table 10 probably reflects that cellular nitrogen, nonnitrogenous nonlipid biomass, and lipid accumulation were somewhat sequential in the batch fermentations but more concurrent in the continuous fermentations. This is consistent with the generally accepted concept that cells are acting more homogenously in the continuous fermentations than they are in the batch fermentations.

In Table 10, similar estimates were obtained for those parameters reflecting critical biomass ratios, K and γ, reflecting the use of yeast extract as the nitrogen source, N_{uo} and β, and reflecting the conversion efficiency of lactose to nonnitrogenous nonlipid biomass and lipid, $1/Y_1$ and $1/Y_2$, respectively. Since these parameters would be independent of the fermentation system, the similarity of the estimates for these parameters is further evidence of the validity of the kinetic model in its description of growth and lipid accumulation.

On the average, 3.9 g of lactose is required by this yeast in order to accumulate 1.0 g of lipid. The efficiency with which this yeast produces lipid from lactose is estimated to be ca. 77% as

efficient as that estimated based on the biochemical pathways and energy requirements of the process (Smith et al., 1983). Some of the monosaccharides from lactose may also be incorporated into the carbohydrate-lipid compounds that were observed to be present in the polar lipid of this yeast (Hammond et al., 1981). But these compounds evidently represented only a small portion of the polar and neutral lipid, inasmuch as the fatty acids were reported to compose ca. 90% (w/w) of the polar and neutral lipid. Thus, this yeast can be concluded to utilize lactose efficiently for lipid accumulation.

On extrapolating the continuous fermentation model using the parameter estimates in Table 9, the model predicts that lactose would be completely utilized at a steady state dilution rate of ca. 0.020 1/hr. The average residence time for the continuous fermentation is then estimated to be 50 hr for the complete utilization of lactose. This is 10-15 hr shorter than that required for the batch fermentations (Figures 27 and 28). Thus, the single-stage continuous fermentation seems to be more efficient than the batch fermentation in terms of the average residence time required for complete lactose removal. This conclusion is similar to that drawn by Gill et al. (1977).

The shorter residence time required in the continuous fermentation for the complete utilization of lactose may be best improved by decreasing the time required for lipid accumulation, since this is the slowest rate of the oleaginous fermentation. This may be

accomplished by modifying the fermentation broth. For instance, an optimum pH has been reported for this yeast for lipid accumulation (Moon et al., 1978). Yeast strains may also be isolated which accumulate lipid at a faster rate. Alternatively, it may be preferred for economic reasons to cultivate the oleaginous yeast with a lower percentage of the biomass as lipid as suggested by Almazan et al. (1981). This would also shorten the time required for lipid accumulation.

Compared to a single-stage continuous fermentation, a two-stage continuous fermentation may offer only a marginal decrease in the overall average residence time for the complete utilization of lactose. A two-stage system may be desirable if the optimal conditions for the accumulation of nonlipid biomass and lipid are sufficiently different. This may not occur since the optimum pHs for the accumulation of nonlipid biomass and lipid are fairly similar for this yeast (Moon et al., 1978). Therefore, a two-stage system may not offer any significant advantage over a single-stage system. This conclusion is similar to that drawn by Hall and Ratledge (1977).

CONCLUSION

Candida curvata D was grown in batch and continuous fermentations. In the batch fermentations, the concentrations of cellular nitrogen, nonlipid biomass, and lipid increased more or less sequentially. The concentration of nonlipid biomass was proportional to the concentration of cells, and both concentrations seemed limited by the available nitrogen. A constant ratio of lipid to nonlipid biomass was observed in the batch fermentations during the initial period when most of the accumulation of nonlipid biomass occurred. Nitrogenous compounds (predominantly amino acids) contributed significantly to this initial accumulation of nonlipid biomass, but the percentage of cellular nitrogen in the nonlipid biomass changed dramatically over the course of the batch fermentation and was greatly affected by the dilution rate in the continuous fermentations. Lactose was used both for the accumulation of nonnitrogenous nonlipid biomass and lipid. Unlike some species of oleaginous yeast, metabolites did not seem to accumulate during or after the transition to the period in which lipid accumulation predominated.

Expressing specific rates with respect to cellular nitrogen concentration seemed to be a logical approach, since the concentration of cellular nitrogen best represented the concentration of cellular enzymes. The trends in specific rates relative to

cellular nitrogen indicated a transitional phase from growth to lipid accumulation. The increase in the specific rate of lipid accumulation during batch fermentations was paralleled by a decrease in the specific rate of demand for lactose to produce nonnitrogenous nonlipid biomass. The specific rate of lactose consumption was constant during the transition from growth to predominantly lipid production. A maximum and constant specific rate of lipid accumulation was observed. This was consistent with the hypothesis that a single enzyme controls the rate of lipid accumulation.

The batch and continuous fermentations were satisfactorily described by a kinetic model. The sets of parameters required to describe the batch and continuous fermentations were significantly different for some parameters. This may be because the accumulation of cellular nitrogen, nonlipid biomass, and lipid which were somewhat sequential in the batch fermentations were concurrent in the continuous fermentations. Parameters which should be independent of the fermentation system were not significantly different for the two systems.

This model demonstrates a means by which lipid-accumulating fermentations can be described. The success of this model indicates that for fermentations in which changes in the ratio of cellular nitrogen to nonlipid biomass are significant, expressing specific rates with respect to the cellular nitrogen concentration is

a useful way of expressing the fermentation kinetics.

From the kinetic model three conclusions were drawn:

1. A single-stage continuous fermentation requires a shorter average residence time than a batch fermentation for utilization of lactose and reduction in biological oxygen demand.
2. Lipid accumulation has the slowest reaction rate in the fermentation. The time required for lipid accumulation might be shortened by optimizing the composition and state of the fermentation broth for lipid accumulation, isolating different yeast strains, or accepting a lower percentage of the biomass as lipid.
3. A two-stage continuous fermentation system probably will not significantly decrease the overall average residence time as compared to a single-stage continuous fermentation system.

BIBLIOGRAPHY

A.O.A.C. 1980. Official Methods of Analysis. 13th ed. Association of Official Analytical Chemists, Washington, D.C.

Aiyar, A. S., and R. Luedeking. 1966. A kinetic study of the alcoholic fermentation of glucose by Saccharomyces cerevisiae. Bioengineering and Food Processing, Chem. Eng. Progr. Symp. Ser. 62(69):55-59.

Allen, L. A., N. H. Barnard, M. Fleming, and B. Hollis. 1964. Factors affecting the growth and fat formation of Rhodotorula gracilis. J. Appl. Bacteriol. 27:27-40.

Almazan, O., M. Klibansky, and M. A. Otero. 1981. Microbial fat synthesis by Rhodotorula glutinis from blackstrap molasses in continuous culture. Biotechnol. Lett. 3:663-666.

Ayres, G. H. 1968. Quantitative Chemical Analysis. 2nd ed. Harper and Row, Publ., New York, New York. 710 pp.

Bailey, J. E., and D. F. Ollis. 1977. Biochemical Engineering Fundamentals. McGraw-Hill Book Company, New York, New York. 753 pp.

Bajpai, R. K., and M. Reuß. 1980. A mechanistic model for penicillin production. J. Chem. Tech. Biotechnol. 30:332-344.

Barford, J. P., and R. J. Hall. 1978. An evaluation of the approaches to the mathematical modeling of microbial growth. Process Biochem. 13(8):22-24, 26, 29.

Barford, J. P., and R. J. Hall. 1981. A mathematical model for the aerobic growth of Saccharomyces cerevisiae with a saturated respiratory capacity. Biotechnol. Bioeng. 23:1735-1762.

Bellgardt, K.-H., W. Kuhlmann, and H.-D. Meyer. 1982. Deterministic growth model of Saccharomyces cerevisiae, parameter identification and simulation. Pages 67-74 in A. Halme, ed. Modelling and Control at Biotechnical Processes, Proceedings of the First IFAC Workshop, Helsinki, Finland, August 17-19, 1982. Pergamon Press, New York, New York.

Bergmeyer, H.-U., and E. Bernt. 1974. 2-Oxoglutarate UV spectrophotometric determination. Pages 1577-1580 in H.-U. Bergmeyer, ed. Methods of Enzymatic Analysis. Vol. 3, 2nd English Ed. Academic Press, New York, New York.

Bijkerk, A. H. E., and R. J. Hall. 1977. A mechanistic model of the aerobic growth of Saccharomyces cerevisiae. Biotechnol. Bioeng. 19:267-296.

Blackman, F. F. 1905. Optima and limiting factors. Ann. Bot. (London) 19:281-295.

Botham, P. A., and C. Ratledge. 1978. Metabolic studies related to lipid accumulation in yeast. Pages 383-385 in Biochem. Soc. Transactions, 53rd Meeting, Hull, England.

Botham, P. A., and C. Ratledge, 1979. A biochemical explanation for lipid accumulation in Candida 107 and other oleaginous micro-organism. J. Gen. Microbiol. 114:361-375.

Boulton, C. A., and C. Ratledge. 1980. Regulatory studies on citrate synthase in Candida 107, an oleaginous yeast. J. Gen. Microbiol. 121:441-447.

Boulton, C. A., and C. Ratledge. 1981. Correlation of lipid accumulation in yeasts with possession of ATP:citrate lyase. J. Gen. Microbiol. 127:169-176.

Brown, B. D., and K. H. Hsu. 1982. Kinetic modeling of lipid accumulation in Candida curvata R. Pages 1-8 in L. E. Erickson and L. T. Fan, eds. Proceedings of the Twelfth Annual Biochemical Engineering Symposium, Kansas State University, Manhattan, Kansas.

Calam, C. T., S. H. Ellis, and M. J. McCann. 1971. Mathematical models of fermentations and a simulation of griseofulvin fermentation. J. Appl. Chem. Biotechnol. 21:181-189.

Carpenter, B. H., and H. C. Sweeney. 1965. Process improvement with simplex self-directing evolutionary operation. Chem. Eng. 72(14):117-124, 126.

Chahal, D. S., M. Singla, and R. P. Gupta. 1979. Comparison of lipid production by unicellular and filamentous fungi. Proc. Indian Natl. Sci. Acad., Part B, 45:18-26.

Chiu, S. Y., L. E. Erickson, L. T. Fan, and I. C. Kao. 1972. Kinetic model identification in mixed populations using continuous culture data. Biotechnol. Bioeng. 14:207-231.

Choi, S. Y., D. D. Y. Ryu, and J. S. Rhee. 1982. Production of microbial lipid: effects of growth rate and oxygen on lipid synthesis and fatty acid composition of Rhodotorula gracilis. Biotechnol. Bioeng. 24:1165-1172.

Condrey, R. E. 1982. The chemostat and Blackman kinetics. Biotechnol. Bioeng. 24:1705-1709.

Constantinides, A., J. L. Spencer, and E. L. Gaden, Jr. 1970. Optimization of batch fermentation processes. I. Development of mathematical models for batch penicillin fermentations. Biotechnol. Bioeng. 12:803-830.

Contois, D. E. 1959. Kinetics of bacterial growth: relationship between population density and specific growth rate of continuous cultures. J. Gen. Microbiol. 21:40-50.

Dabes, J. N., R. K. Finn, and C. R. Wilke. 1973. Equations of substrate limited growth: the case for Blackman kinetics. Biotechnol. Bioeng. 15:1159-1177.

Dagley, S. 1974. Citrate UV spectrophotometric determination. Pages 1446-1451 in H.-U. Bergmeyer, ed. Methods of Enzymatic Analysis. Vol. 3, 2nd English ed. Academic Press, New York, New York.

Davies, R., E. A. Falkiner, J. F. Wilkinson, and J. L. Peel. 1951. Ester formation by yeasts. I. Ethyl acetate formation by Hansenula species. Biochem. J. 49:58-61.

Deindoerfer, F. H. 1960. Fermentation kinetics and model processes. Adv. Appl. Microbiol. 2:321-334.

Drew, S. W. 1981. Liquid culture. Pages 151-178 in P. Gerhardt, R. G. E. Murray, R. N. Lostilow, E. W. Nester, W. A. Wood, N. R. Krieg and G. B. Phillips, eds. Manual of Methods for General Bacteriology. American Society for Microbiology, Washington, D.C.

Duncan, B. 1973. Nutrition and fat production in submerged cultures of a strain of Penicillum lilacinum. Mycologia 65:211-214.

Enebo, L., L. G. Anderson, and H. Lundin. 1946. Microbiological fat synthesis by means of Rhodotorula yeast. Arch. Biochem. 11:383-395.

Evans, C. T., and C. Ratledge. 1983a. A comparison of the oleaginous yeast, Candida curvata, grown on different carbon sources in continuous and batch culture. Lipids 18:623-629.

Evans, C. T., and C. Ratledge. 1983b. Biochemical activities during lipid accumulation in Candida curvata. Lipids 18:630-635.

Evans, C. T., A. H. Scragg, and C. Ratledge. 1983a. A comparative study of citrate efflux from mitochondria of oleaginous and non-oleaginous yeasts. Eur. J. Biochem. 130:195-204.

Evans, C. T., A. H. Scragg, and C. Ratledge. 1983b. Regulation of citrate efflux from mitochondria of oleaginous and nonoleaginous yeasts by adenine nucleotides. Eur. J. Biochem. 132:609-615.

Evans, C. T., A. H. Scragg, and C. Ratledge. 1983c. Regulation of citrate efflux from mitochondria of oleaginous and nonoleaginous yeasts by long-chain fatty acyl-CoA esters. Eur. J. Biochem. 132:617-622.

Fahmy, T. K., J. W. Hopton, and M. Woodbine. 1962. The mineral nutrition of Hansenula spp. of yeast in relation to fat production. J. Appl. Bacteriol. 25:202-212.

Fan, L. T., C. L. Hwang, and F. A. Tillman. 1969. A sequential simplex pattern search solution to production planning problems. AIIE Transactions 1:267-273.

Floetenmeyer, M. D. 1983. Oil accumulation by yeasts grown on simple and complex carbohydrates under various fermentation conditions. M.S. Thesis. Iowa State University. 86 pp.

Fredrickson, A. G., D. Ramkrishna, and H. M. Tsuchiya. 1971. The necessity of including structure in mathematical models of unbalanced microbial growth. Food and Bioengineering, Fundamental and Industrial Aspects, Chem. Eng. Progr. Symp. Ser. 67(108):53-59.

Gaden, Jr., E. L. 1955. Fermentation kinetics and productivity. Chem. Ind. 33(7):154-159.

Gaden, Jr., E. L. 1956. Chemical technology of fermentation. Chem. Eng. 63(4):159-174.

Gaden, Jr., E. L. 1959. Fermentation process kinetics. J. Biochem. Microbiol. Tech. Eng. 1:413-429.

Gill, C. O., M. J. Hall, and C. Ratledge. 1977. Lipid accumulation in an oleaginous yeast (Candida 107) growing on glucose in single-stage continuous culture. Appl. Environ. Microbiol. 33:231-239.

Gondo, S., K. Venkatasubramanian, W. R. Vieth, and A. Constantinides. 1978. Modeling the role of cyclic AMP in catabolite repression of inducible enzyme biosynthesis in microbial cells. Biotechnol. Bioeng. 20:1797-1815.

Guthke, R., and W. A. Knorre. 1982. Efficiency of the cyclic batch antibiotic fermentation. Biotechnol. Bioeng. 24:2129-2136.

Hall, M. J., and C. Ratledge. 1977. Lipid accumulation in an oleaginous yeast (Candida 107) growing on glucose under various conditions in a one- and two-stage continuous culture. Appl. Environ. Microbiol. 33:577-584.

Hammond, E. G., B. A. Glatz, Y. Choi, and M. T. Teasdale. 1981. Oil production by Candida curvata and extraction, composition, and properties of the oil. Pages 171-187 in E. H. Pryde, L. H. Princen and K. D. Mukherjee, eds. New Sources of Fats and Oils, AOCS Monograph No. 9. American Oil Chemists Society, Champaign, Illinois.

Harrison, D. E. F., and P. K. Maitra. 1969. Control of respiration and metabolism in growing Klebsiella aerogenes. The role of adenine nucleotides. Biochem. J. 112:647-656.

Henri, V. 1903. Lois Générales de L'Action des Diastases. Librairie Scientifique A. Hermann, Paris, France. 129 pp.

Hettinga, D. H., A. H. Miah, E. G. Hammond, and G. W. Reinbold. 1970. Sensitive enzymatic method for determination of glucose, galactose, and lactose in cheddar cheese. J. Dairy Sci. 53:1377-1380.

Hong, B., N. H. Choi, and L. T. Fan. 1983. Sequential utilization of mixed sugars by Clostridium acetabutylicum. Pages 1-10 in P. J. Reilly, ed. Proceedings of the Thirteenth Biochemical Engineering Symposium, Iowa State University, Ames, Iowa.

Hopton, J. W., and M. Woodbine. 1960. Fat synthesis by yeasts. I. A comparative assessment of Hansenula species. J. Appl. Bacteriol. 23:283-290.

I.M.S.L. 1982. Library Reference Manual. 9th ed. International Mathematical and Statistical Libraries, Inc., Houston, Texas.

Imanaka, T., T. Kaieda, K. Sato, and H. Taguchi. 1972. Optimization of α-galactosidase production by mold. (1) α-Galactosidase production in batch and continuous culture and a kinetic model for enzyme production. J. Ferment. Technol. 50:633-646.

Kendall, D. G. 1949. Stochastic processes and population growth. J. Roy. Statist. Soc., Series B, 11:230-264.

Kessel, R. H. J. 1968. Fatty acids of Rhodotorula gracilis: Fat production in submerged culture and the particular effect of pH value. J. Appl. Bacteriol. 31:220-230.

Koch, A. L. 1981. Growth measurements. Pages 197-207 in P. Gerhardt, R. G. E. Murray, R. N. Lostilow, E. W. Nestor, W. A. Wood, N. R. Krieg and G. B. Phillips, eds. Manual of Methods for General Bacteriology. American Society for Microbiology, Washington, D.C.

Kurz, G., and K. Wallenfels. 1974. Lactose and other beta-D-galactosides. Pages 1180-1184 in H.-U. Bergmeyer, ed. Methods of Enzymatic Analysis. Vol. 3, 2nd English ed. Academic Press, New York, New York.

Levenspiel, O. 1980. The Monod equation: a revisit and a generalization to product inhibition situations. Biotechnol. Bioeng. 22:1671-1687.

Luedeking, R., and E. L. Piret. 1959. A kinetic study of the lactic acid fermentation. Batch process at controlled pH. J. Biochem. Microbiol. Tech. Eng. 1:393-412.

Lundin, H. 1950. Fat synthesis by micro-organisms and its possible applications in industry. J. Inst. Brew. 56:17-28.

Michaelis, L., and M. L. Menten. 1913. Die kinetik der invertinwirkung. Biochem. Z. 49:333-369.

Misra, S., A. Ghosh, and J. Dutta. 1984. Production and composition of microbial fat from Rhodotorula glutinis. J. Sci. Food Agric. 35:59-65.

Monod, J. 1942. Recherches sur la Croissance des Cultures Bactériennes. Herman et Cie, Paris, France. 210 pp.

Moon, N. J., E. G. Hammond, and B. A. Glatz. 1978. Conversion of cheese whey and whey permeate to oil and single-cell protein. J. Dairy Sci. 61:1537-1547.

Moser, H. 1958. The Dynamics of Bacterial Populations Maintained in the Chemostat. Carnegie Institution of Washington, Publication 614, Washington, D.C. 136 pp.

Nestaas, E., and D. I. C. Wang, 1983. Computer control of the penicillin fermentation using the filtration probe in conjunction with a structured process model. Biotechnol. Bioeng. 25:781-796.

Nord, F. F. 1939. Enzymatische umsetaungen durch Fusarien: beitrag zum mechanismus der alkoholischen gärung. Ergeb. Enzymforsch. 8:149-184.

Pamment, N. B., R. J. Hall, and J. P. Barford. 1978. Mathematical modeling of lag phases in microbial growth. Biotechnol. Bioeng. 20:349-381.

Panikov, N. 1979. Steady state growth kinetics of Chlorella vulgaris under double substrate (urea and phosphate) limitation. J. Chem. Tech. Biotechnol. 29:442-450.

Panikov, N., and S. J. Pirt. 1978. The effects of cooperativity and growth yield variation on the kinetics of nitrogen or phosphate limited growth of Chlorella in a chemostat culture. J. Gen. Microbiol. 108:295-303.

Pedersen, T. A. 1961. Lipid formation in Crytococcus terricola. I. Nitrogen nutrition and lipid formation. Acta Chem. Scand. 15:651-662.

Ratledge, C. 1978. Lipids and fatty acids. Pages 263-302 in A. H. Rose, ed. Economic Microbiology. Vol. 2. Academic Press, New York, New York.

Ratledge, C., and P. A. Botham. 1977. Pathways of glucose metabolism in Candida 107, a lipid-accumulating yeast. J. Gen. Microbiol. 102:391-395.

Ratledge, C., and M. J. Hall. 1979. Accumulation of lipid by Rhodotorula glutinis in continuous culture. Biotechnol. Lett. 1:115-120.

Reiner, J. M. 1959. Behavior of Enzyme Systems. Burgess Publishing Co., Minneapolis, Minnesota. 329 pp.

Roehr, M., O. Zehentgruber, and C. P. Kubicek. 1981. Kinetics of biomass formation and citric acid production by Aspergillus niger on pilot plant scale. Biotechnol. Bioeng. 23:2433-2445.

Roy, M. K., K. Vadalkar, B. Baruah, U. Misra, S. D. Bhagat, and J. N. Baruah. 1978. Production of intracellular fat by the yeast Lipomyces starkeyi. Indian J. Exp. Biol. 16:511-512.

Schultz, J. S., J. D. Goddard, and S. R. Suchdeo. 1974. Facilitated transport via carrier mediated diffusion in membranes. Part 1. Mechanistic aspects, experimental systems, and characteristic regimes. AIChE J. 20:417-445.

Shu, P. 1961. Mathematical models for the product accumulation in microbial processes. J. Biochem. Microbiol. Tech. Eng. 3:95-109.

Sigma Chemical Co. 1982. Glucose in whole blood, plasma or serum at 425-475 nm. Sigma Technical Bulletin No. 510. Sigma Chemical Company, St. Louis, Missouri. 12 pp.

Sigma Chemical Co. 1983. Prod. No. L-7004, Colorimetric Assay Procedure, using lactose as substrate. Sigma Chemical Co., St. Louis, Missouri. 2 pp.

Smith, E. L., R. L. Hill, I. R. Lehman, R. J. Lefkowitz, P. Handler, and A. White. 1983. Principles of Biochemistry. 7th ed. McGraw-Hill Book Co., New York, New York. 886 pp.

Sprössler, B., and H. Plainer. 1983. Immobilized lactase for processing whey. Food Technol. 37(10)93-95.

Steinberg, M. P., and Z. J. Ordal. 1954. Effect of fermentation variables on rate of fat formation by Rhodotorula gracilis. Agric. Food Chem. 2:873-877.

Toda, K., T. Takeuchi, and H. Sano. 1979. Growth rate dependence of enzyme synthesis in chemostat cultures: α-amylase, β-galactosidase, acid phosphatase, and β-fructosidase. J. Chem. Tech. Biotechol. 29:747-755.

Toda, K., and I. Yabe. 1979. Mathematical model of cell growth and phosphatase biosynthesis in Saccharomyces carlsbergensis under phosphate limitation. Biotechnol. Bioeng. 21:487-502.

Tomita, T., R. Hasegawa, and E. Hayashi. 1979. Neutral lipid accumulation in yeast due to inositol deficiency. J. Nutr. Sci. Vitaminol. 25:59-66.

Tseng, M. M.-C., and C. R. Phillips. 1982. The kinetics of yeast growth and nicotinic acid production. Biotechnol. Bioeng. 24:1319-1325.

Tsuchiya, K., and T. Kimura. 1982. Kinetics of substrate utilization in adenine-limited chemostat cultures of Bacillus substilis KYA 741. Appl. Environ. Microbiol. 43:794-799.

Tsuchiya, K., T. Kimura, M. Okazaki, and Y. Miura. 1980. Growth kinetics under adenine-limiting conditions of Bacillus substilis KYA 741, an adenine-requiring strain. Biotechnol. Bioeng. 22:401-410.

Weast, R. C., ed. 1974. CRC Handbook of Chemistry and Physics. 57th ed. CRC Press, Inc., Cleveland, Ohio. I58 pp.

Williams, F. M. 1967. A model of cell growth dynamics. J. Theor. Biol. 15:190-207.

Yamauchi, H., H. Mori, T. Kobayashi, and S. Shimizu. 1983. Mass production of lipids of Lipomyces starkeyi in microcomputer-aided fed-batch culture. J. Ferment. Technol. 61:275-280.

Yoon, S. H., and J. A. Rhee. 1983. Quantitative physiology of Rhodotorula glutinis for microbial lipid production. Process Biochem. 18(5):2-4.

Yoon, S. H., J. W. Rhim, S. Y. Choi, D. D. Y. Ryu, and J. S. Rhee. 1982. Effect of carbon and nitrogen sources on lipid production of Rhodotorula gracilis. J. Ferment. Technol. 60:243-246.

Zabriskie, D. W., W. B. Armiger, D. H. Phillips, and P. A. Albano. 1980. Traders' Guide to Fermentation Media Formulation. Traders' Protein Division of Traders' Oil Mill, Fort Worth, Texas. 57 pp.

ACKNOWLEDGMENTS

I would like to sincerely thank Dr. Kenneth Hsu for his guidance and patient assistance during the research for and preparation of this dissertation. I also want to thank Dr. Earl Hammond for his helpful suggestions throughout this investigation. My appreciation is extended to the members of my committee, Dr. P. Reilly, Dr. B. Glatz and Dr. C. Glatz, for their interest and help in this dissertation.

I am sincerely grateful to Dr. Peter Reilly for allowing me access to his labs during the course of this investigation.

I would especially like to extend my deepest gratitude to my wife, Judy, for her encouragement and support throughout this investigation and for the typing of this dissertation.